ABSTRACT

TO ERR IS HUMAN: THE EFFECT OF MISTAKES IN SOCIAL SIMULATIONS

by Jack T. Beerman

In Modeling & Simulation, a model must be fit for purpose. In the case of models for social simulations, it means that we must adequately capture the mechanisms of human behaviors. We focus on Agent-Based Models for human behavior and improve their realism by integrating human errors in an agent's decision-making routine via Machine Learning. Our framework allows experts to analyze the impact of different types of errors: superficial observations, biases, limited ability to comprehend a situation, and inaccurate perceptions. We illustrate this framework through simulation cases and provide a detailed case-study on COVID-19 which suggests that errors are essential to a model in order to replicate real-world vaccination rates. While our work focuses on realism of simulation models, realism can come at the expense of computational costs. To counter-balance these rising costs, we develop an innovative scheme that groups similar-thinking agents. We demonstrate that simple metrics can effectively capture similarities between agents and we create simplified simulations with average outcomes that are aligned with the results of the original model. Ultimately, we are able to decrease the computational cost at the expense of the confidence margin.

TO ERR IS HUMAN:
THE EFFECT OF MISTAKES IN SOCIAL SIMULATIONS

A Thesis

Submitted to the
Faculty of Miami University
in partial fulfillment of
the requirements for the degree of
Master of Science
by
Jack T. Beerman
Miami University
Oxford, Ohio
2023

Advisor: Philippe J. Giabbanelli
Reader: Dhananjai M. Rao
Reader: Daniela Inclezan

This Thesis titled

TO ERR IS HUMAN:
THE EFFECT OF MISTAKES IN SOCIAL SIMULATIONS

by

Jack T. Beerman

has been approved for publication by

The College of Engineering and Computing

and

The Department of Computer Science & Software Engineering

Philippe J. Giabbanelli

Dhananjai M. Rao

Daniela Inclezan

Table of Contents

List of Tables

List of Figures

Dedication

My family always supports my dreams and inspires me to approach everything I do with 100% effort. They have motivated me to constantly be curious, and always aim for excellence. I am on my own journey, but in every path I take, I strive to represent and honor the impact they have had on my life. I dedicate this work to my dad Charles, mom Ellen, sister Taylor Grace, and brother Benjamin. Thank you for making me the person I am today.

Acknowledgments

First and foremost, I am pleased to describe my appreciation and gratitude for Dr. Philippe J. Giabbanelli not only serving as my advisor but also as a mentor for my academic future. He has continually challenged me to perform to the utmost of my ability and has guided me throughout the entire graduate program. He has poured countless time and energy into my work and has served as my instructor for numerous courses. His guidance and leadership are the main principal causes that have led me to continue my academic career at the University of Virginia.

I also wish to thank Dr. Dhananjai M. Rao and Dr. Daniela Inclezan for supporting my thesis and serving as my course instructors throughout the years. They have served a vital role in my success as both an undergraduate and graduate student. I have been able to flourish in my classes due to their instruction and guidance.

My Air Force cadre have continually supported my growth as a leader and as a student. They have prepared me to lead with a passion and support all of my wing-men. Without funding from Detachment 640, I would have not been able to accomplish my academic goals or attend Miami University. Detachment 640 has provided a plethora of opportunities for me to lead and learn in Air Force ROTC and most recently I had the honor to serve as the Cadet Wing Commander with an outstanding Command Staff. I am thankful for the entire Cadet Wing's support and service throughout my entire position.

I would like to thank the following for our discussions regarding perceptual errors in ABMs: Drs Piper Jackson (Thompson Rivers University, Canada), Ashkan Nagahban (The Pennsylvania State, USA), Andrew Crooks (University at Buffalo, USA), Nicolas Verstaevel (University of Toulouse, France), William Kennedy and Hamdi Kavak (George Mason University, USA).

Ashley Perone, thank you for always supporting my work and teaching me your knowledge in Tableau. I continually value your professional advice and business world experience. You always inspire me to go above and beyond.

Finally, I am thankful for my fellow classmates and friends who have supported my work. Whether it has been tackling logic problems together, working on projects, or supporting each other to accomplish our goals, these people have played a major role: Gwendal Beaumont, Kareem Ghumrawi, Jacob Krzciok, Tim Finucan, Brian Bergem, Blake Edmunds, Daniel Canter, Dillon Canter, Sam Pearl, David Berent, Jake Bemis, Jenna Sayle, and Will Shuppert. My time at Miami would not have been the same if you all were not a part of the journey.

Quote

“I hope that in this year to come, you make mistakes. Because if you are making mistakes, then you are making new things, trying new things, learning, living, pushing yourself, changing yourself, changing your world. You’re doing things you’ve never done before, and more importantly, you’re Doing Something.

So that’s my wish for you, and all of us, and my wish for myself. Make New Mistakes. Make glorious, amazing mistakes. Make mistakes nobody’s ever made before. Don’t freeze, don’t stop, don’t worry that it isn’t good enough, or it isn’t perfect, whatever it is: art, or love, or work or family or life.

Whatever it is you’re scared of doing, Do it. Make your mistakes, next year and forever.”
- Neil Gaiman. *My New Year Wish.* 2011.

Chapter 1

Introduction

Agent Based Models (ABMs) depict the behaviors and interactions of entities within an environment. This modeling approach is useful in domains where individual differences exist, as it becomes possible to track heterogeneous perspectives across virtual agents. Most commonly, the model and its entities pertain to humans in a society [2]; however, these entities can also represent a variety of organisms within their respective domain such as fish in a water-system [3]. Over several decades, these models have been developed significantly to aid in studying social phenomena for concepts in social theory and have been introduced into numerous disciplines such as Psychology, Marketing, Transportation, and Healthcare [4]. As an example, one of the earliest, most influential ABMs (i.e., in Modeling & Simulation) is the Schelling Model [5]. In 1971, this model was designed to replicate humans moving in a neighborhood and measure the likelihood of agents self segregating in the social dimension. These results illustrated the emergent behavior of like-minded individuals in society. Since then, these models have continued to advance and have recently exploded in use in systems science from fields such as public health to sustainability [6, 7, 8].

1.1 Motivation

In *Modeling & Simulation* (M&S) with Agent Based Models, modelers represent how (virtual) agents behave, as a proxy to their real-world human counterpart. It is not assumed that agents make perfect decisions, because the data used to build models is imperfect, theories are incomplete, and computing power does not allow for every agent to look at all possible decisions. Consequently, agents are bounded in their rationality and appear more humane [9]. However, one may design agents to be perfect in other aspects, which makes them more mechanical than humans. In particular, agents are generally assumed to make perfect observations about other agents they interact with and about the environment in which they act [10]. For example, an agent can tell with 100% accuracy whether another agent is engaging in a desirable or undesirable behavior [11]. As a representation of humans, this accuracy is not realistic. In reality, humans make mistakes because they have partial observations (e.g., you see a fit person eating burgers so you think it's good for your health without knowing that they exercise a lot) or because they are forced to make decisions with limited time resources [12]. Human decisions are also affected by personal beliefs, values, and cognitive biases (e.g., an individual may be biased towards a specific race/ethnicity while having a friend from that group [13]) which may differ from one person to the next and these differences are not homogeneous across agents [14].

There have been ongoing and recent attempts at making virtual agents more 'human-like', in particular due to the growing use of machine learning in conjunction with M&S. Intuitively, one illustration is the idea of increasing the intelligence of an agent by growing their virtual brain (i.e., their ruleset) from data rather than manually coding a small number of set behavioral templates [15, 16]. As machine learning models often include estimates for errors (e.g., accuracy, precision, recall), there is an opportunity to create agents who have a certain likeliness to make mistakes, thus potentially acting more humanely.

1.2 Contributions

My objective is to enable computational models of social systems to resemble real-world individuals more closely by accounting for individual heterogeneity (e.g., in traits and decision-making) and changes over time. This will be achieved through three specific aims detailed below.

1.2.1 Aim 1: Develop a Framework that Utilizes Machine Learning to Analyze the Effect of Agents Mistakes on Model Trajectory

Humans make mistakes for numerous reasons. People may over-generalize based on a few anecdotes, that is, they learn from *insufficient* data. A human may struggle to draw generalizations in complex environments, which depicts their *limited ability* to infer a model from data. Another person may discard new knowledge as it conflicts with their deeply held beliefs and values; this exemplifies the *integration* of a model depending on a pre-existing one. In ABMS, these types of errors and those similar regarding the decision making of agents are handled inconsistently across models [17]. However, by focusing on integrating these types of errors into ABMS, modelers are able to model human error and replicate real-world behavior [18].

In order to examine all three of these causes of error, machine learning can be utilized to provide a controlled environment [19]. For example, we can control the data that is given to an agent (human) and examine how the percentage of observations and/or the selection of these observations change the agents' decisions and ultimately affects the collective of agents [18]. Similarly, we can control the ability of each agent in forming a model. An example would be equipping each agent with a decision tree and limiting its depth. Lastly, one can examine how a new model competes with existing ones through the notion of ensembles of models. Based on these techniques, I have (i) created a simulation testbed in which these three sources of errors will be configured and their effects observed over the

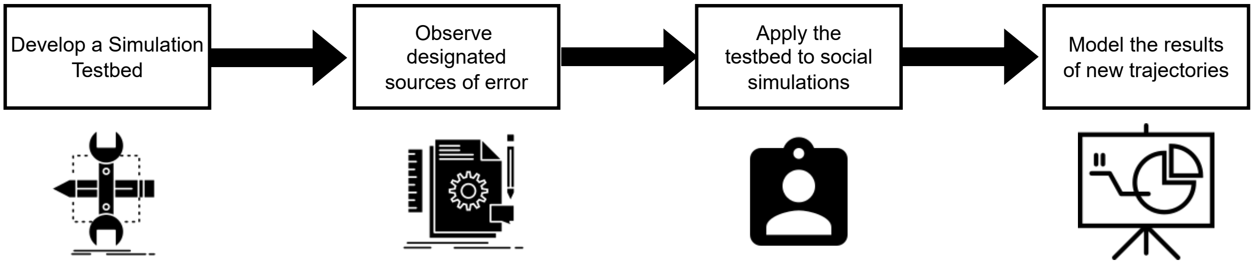

Figure 1.1: Flow Chart for Aim 1

simulated population; and (ii) applied the testbed to classical social simulations to examine how certain mistakes (i.e. a greater fidelity to human decision making) may set the model on a new trajectory (**Figure 1.1**). This aim is accomplished in Chapter 3.

1.2.2 Aim 2: Assess Whether Errors are a Necessary Component to Model Social Systems

The previous aim creates a framework that *can* include errors in a social simulation. The second aim pivots to a key related question: are human decision-making errors *necessary* to create accurate models? To answer this question, my work takes two consecutive steps. First, I perform a comprehensive review of errors in simulation models of COVID-19, with particular attention devoted to the types of human errors. The review is provided in Chapter 4. Then, building on this review, I operationalize errors through my framework and apply it to replicate the real-world vaccination rates of COVID-19 in the USA. As shown by my findings in Chapter 5, errors are necessary to achieve the expected rates.

1.2.3 Aim 3: Lower Computational Costs by Clustering Like-Minded Agents

The beliefs and values of an agent can be represented using a modeling approach such as a Fuzzy Cognitive Map (FCM), which leads into hybrid ABM/FCM systems that have greater fidelity to human behaviors and allow for the transparent integration of different behaviors [20]; this approach is explained in detail in **Section 6.1**. On one hand, simulating a very large population as individual agents can become computationally prohibitive. On the other hand, arbitrarily down-sizing the population with a set resolution (e.g., 1 virtual agent represents 500 people) may lose track of their individual behaviors [21, 22]. A trade-off is thus necessary to perform simulations given limited computational sources while retaining the ability to represent key differences in individual behaviors [22]. This research analyzes this trade-off (**Figure 1.2**) by creating a population of individual agents, each with their FCM, and then grouping agents into clusters based on similarities between their FCMs. These similarities are measured by creating a distance metric for how different the 'thoughts' of two or more agents might be. Results related to this aim can be found in Chapter 6.

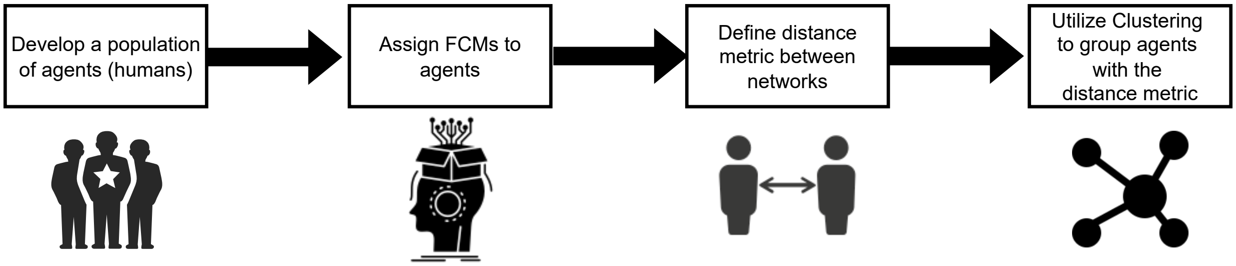

Figure 1.2: Flow Chart for Aim 3

Chapter 2

Background & Related Work

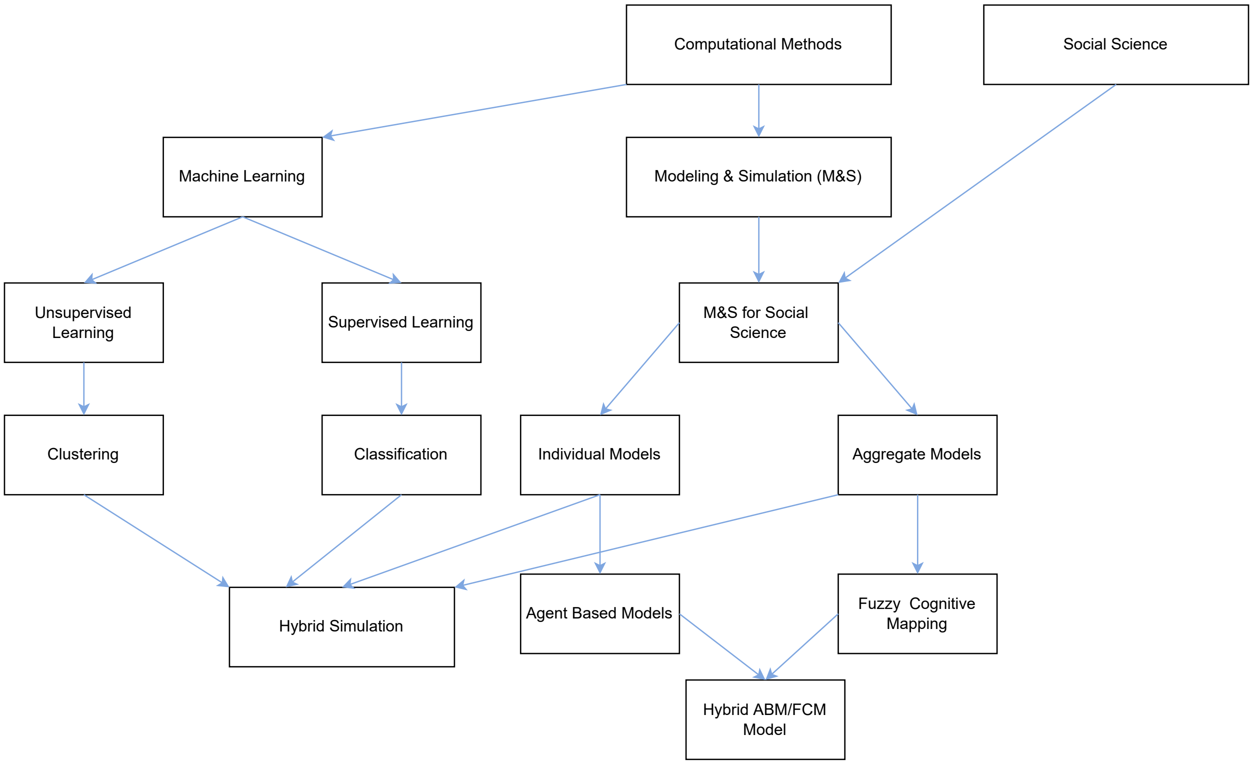

Figure 2.1: Background Overview

2.1 Modeling & Simulation

In 1955, John Von Neumann stated, ‘The sciences do not try to explain, they hardly ever try to interpret, they mainly make models.’ [23]. Six years later, Jay W. Forrester expanded on his work of *Systems dynamics* and began producing models powered by computer simulations to predict industrial, urban, and world dynamics [24, 25, 26]. As time progressed, the study of System dynamics was revolutionary in its methods which aggregated a system by disregarding individual characteristics and recording aggregate variables over time [27, p. 14]. Furthermore, this methodology is continued in practice today and is formally known as *Aggregate Modeling*. Around the same period of time (1957), *Microsimulation* was built upon a methodology that contrasted System Dynamics. Now known as *Individual Modeling*, this approach kept track of all members in a system and detailed the activity of each entity in its environment. Famous examples of these types of simulations emerged in the following years such as the fluoridation referendum campaign model in 1963 [28](an early predecessor of modern day Agent Based Models) and Thomas Schelling's Cellular Automata model of segregation in 1971 [29]. Since then, both technology and computational resources have advanced as well as the methods utilized in Individual and Aggregate Modeling. These advancements have established a robust field known as Modeling & Simulation, which is illustrated alongside Machine Learning in **Figure 2.1**.

Currently, models are utilized that allow researchers to examine data and test hypotheses in simulations that are either too dangerous, expensive, or impossible to physically construct [30, 31]. This process is the backbone of Modeling & Simulation and employs the use of aggregate, individual, and hybrid models that are centered on the principal constituent of obtaining, replicating, and manipulating data to provide real-world insights by formulating predictions and detailing observations. The variety of these models may range greatly; however, Tolk defines the six epistemological elements of any model as task-driven, purposeful, simplification, abstraction, perception, and reality [32]. At the bare minimum, a valid model is designed for a task (task-driven) that handles researchers' perceived problems (perception) and creatively innovates solutions and activities based on empirical data, observations, or theories (purposeful, reality). In addition, simplification and abstraction are necessary to ensure models are constructed in a concise manner and at various levels (e.g., macro, micro) [32]. Even with these outlined elements, it is important to note that some models themselves are theories undergoing development and in order to build a robust model, one must maintain a balance between exploration and consolidation [33]. Once the model has been developed, researchers transition their conceptualizations into executable simulations to test hypotheses via computer programming. These actions are simplified in **Figure 2.2** and illustrate the transitions between Conceptual Models, Mathematical Models, Computational Models and the cycle of the Validation Process.

A simulation is the action of computing the results of a mathematical model, which captures key dynamics of a real-world phenomenon. In Modeling & Simulation, the type of simulation constructed serves specific purposes such as user prediction and may be associated with the observational category [34]. The observational category is comprised of four primary purposes that encompass different systems and incorporate various models [34]: Management of a System, Engineering of a System, Evaluation & Verification, and Comprehension. When managing a system, a simulation serves as the contributing factor of operational or strategic decisions as seen in environmental management [35]. These types of systems are primarily human-centered and/or socio-technical which regard entity interaction commonly found in

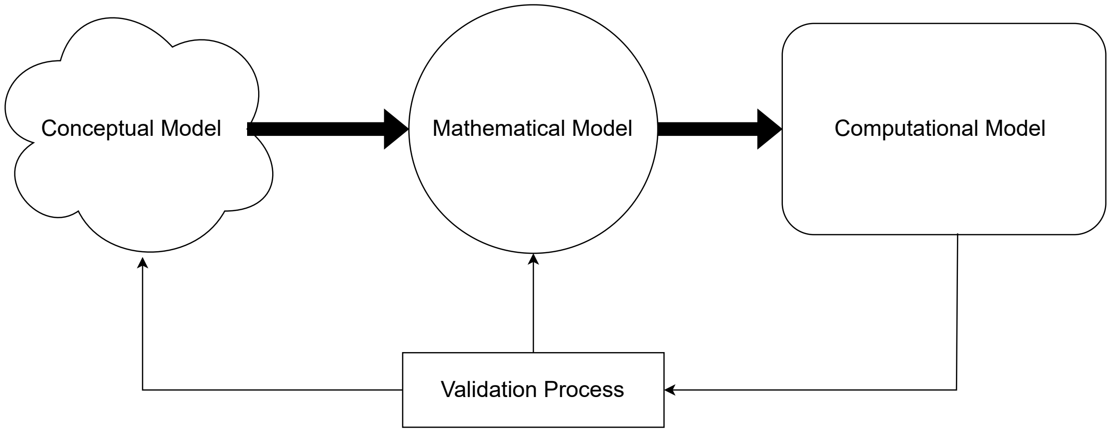

Figure 2.2: Flow Chart of the Modeling Process

Section 2.2. The second purpose of observational simulations is the replication of systems and the advanced development of these structures, thus being categorized as Engineering a System. The two final purposes of simulations, evaluation & verification and comprehension, provide means to test, compare, and possibly refine hypotheses [36].

Whether it is the variety of modeling methodologies, or simulation purposes, Modeling & Simulation is prevalent in a plethora of disciplines and is only increasing in popularity [37, p. 14]. Previously unfathomable to confine and control real-world systems and scenarios, now real-life entities are continually replicated as virtual counterparts and manipulated in simulations to provide observations, generate predictions, and broaden our understanding of the world we reside. Furthermore, types of these simulations may be continuously informed by changes in physical systems and have lead to new frontiers of digital twins.

2.2 Computational Social Science

With the increase and introduction of massive amounts of human-driven data (Big Data), due to the dependency on information and communications technology (ICT), Modeling & Simulation has emerged as one of several computational techniques used within Computational Social Science and is an advanced frontier that captures various objectives and knowledge pertaining to societal phenomena and behavior [38, 39]. Currently, scholars regard Computational Social Science as one of three pillars of modern science [40] and define it as the study of virtual, complex, socio-economic systems that replicate and analyze humans, their interactions, and behavior. These behaviors pertain to countless categories such as reciprocity of humans, terrorism [14], and institutional norms [41]. They are studied in a variety of disciplines that range from health systems to government policy [40].

Human behaviors and interactions have been studied in social and behavioral science through mathematics and computations since the mid 20th century [42]; however, the recent evolution of computational resources and advanced technological capabilities have enabled researchers to simulate large-scale populations while simultaneously recording and analyzing the behavior and interaction of every entity. These observations are achieved through computational models that provide quantitative and qualitative information of societal patterns [38].

Because humans rely on interactions to form beliefs and values and these interactions additionally shape human behavior, humans are labeled as Complex Adaptive Systems (CAS) [14]. An example of human process that underpins CAS is *Cognitive Dissonance Theory*, which explains how humans adapt their perspectives based on whether their beliefs, desires, and emotions agree (congruent) or not (dissonant) with the views of their peers [43]. The Social Influence Network (SIN) Theory (i.e., the theory of how individuals assess their own attitudes and the attitudes of others) depicts the formation of these congruent and dissonant concepts and defines how they evolve in a CAS [43]. Furthermore, the SIN Theory describes changes of human behavior in relation to direct social interaction and details actions that can be pursued to minimize cognitive dissonance [43].

2.3 Individual Models: Agent Based Models

One technique that serves to measure social phenomena by tracking humans and calculating results for each person is using *Individual Models* [44]. Individual Models are capable of distinguishing characteristics centered on the behavior of the entity or the state of an entity and are assembled through a *bottom-up* approach. Furthermore, these models often exhibit several features, succinctly explained as follows. An individual model could fixate on the actions of a goose to illustrate the *emergent* behavior of a flock of geese, such as the V-shaped flight formation that they display as a group. Emergence is the concept that the behavior pattern of an entity may create a high level pattern behavior when aggregated as a group. The initial behavior may be individualized or uniform across a collective of entities or result in an entire new behavior. In addition, each entity may behave dynamically (i.e., adapting through interactions) or statically (i.e., unchanging behavior). Lastly, the conduct of a (virtual) individual may be constrained by programmed rigid rules or allowed freedom through random probability [34], resulting in a *stochastic* model. Even more so, the state of an individual may be divided between a physical and mental state where the physical state represents attributes such as wealth, status, and intelligence, and the mental state, especially in humans, represents complex decision making [34] – Complex decision making and the mental state will be discussed further in **Section 2.5.1**. Because the complexity of individuals' actions and dispositions vary, there are numerous applications and types of individual models within Computational Social Science. In this thesis, we focus on Agent Based Models (ABM) [35].

From determining segregation [29], to developing public policy [45], Agent Based Models are prevalent across numerous domains and are utilized in modeling environments such as `MESA`, `NetLogo`, `MASON`, `REPAST`, `GAMA`, and `Swarm`. For example, we may design an ABM in NetLogo to illustrate the spread of Covid in a classroom (**Figure 2.4**). At a high level, an ABM tracks the actions of agents in a space. More specifically, an ABM is comprised of agents

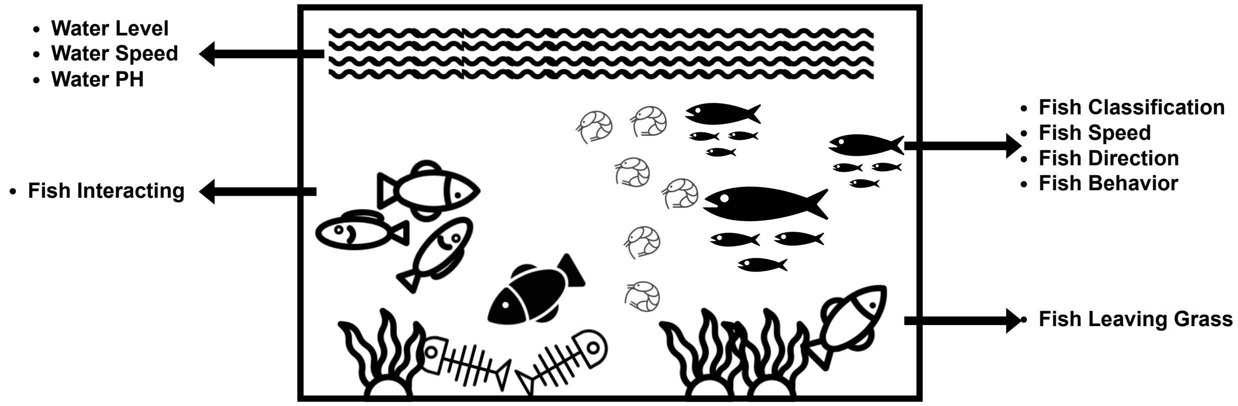

Figure 2.3: Example of Agent Based Model

that represent entities in the real world, a replicated environment and its possible states, the interactions of agents with each other and with the environment [2, 3, 7, 8, 46, 47, 48]. These components are governed by the initial configuration of the system and it various rules to capture key dynamics of real-world phenomenon such as fish in an ecosystem (**Figure 2.3**).

2.4 Aggregate Models: Fuzzy Cognitive Maps

2.4.1 Definition and Model Building Process

Unlike Individual Models, *Aggregate Models* are assembled through a *top down* approach that implements causal rules to create and shape social systems. In addition, Aggregate Models do not operate on heterogeneous data defined by individuals, since they focus on homogeneous groups to provide insight on systems (e.g. social systems) as a whole [30]. This was originally demonstrated through mathematical equations by treating social systems as physical systems and was derived by the Lanchester equations [30]. In 1916, Frederick Lanchester developed an aggregate model pertaining to modern warfare and the elimination of soldiers on the battlefield. This was constructed by aggregating all soldiers in the system (battlefield) and determining the collective feedback and interactions attributable to specific equations [49]. The Lanchester equations were fairly simple, revolutionary, and an example of *Quantitative Aggregate Models*.

In Modeling & Simulation, Aggregate Models can be divided into two primary categories: *quantitative* and *qualitative*. Quantitative Aggregate Models characterize systems and components of the system through sets of equations and mathematical expressions. For example, Function Fitting, Regression, Bayesian Nets, Differential Equations, and System Dynamics, are commonly employed in this top down approach [44]. Another type of approach is the use of Qualitative Aggregate Models, which tend to focus on social issues. Among many types of qualitative aggregate models [50], this thesis focuses on *Fuzzy Cognitive Maps* (FCMs).

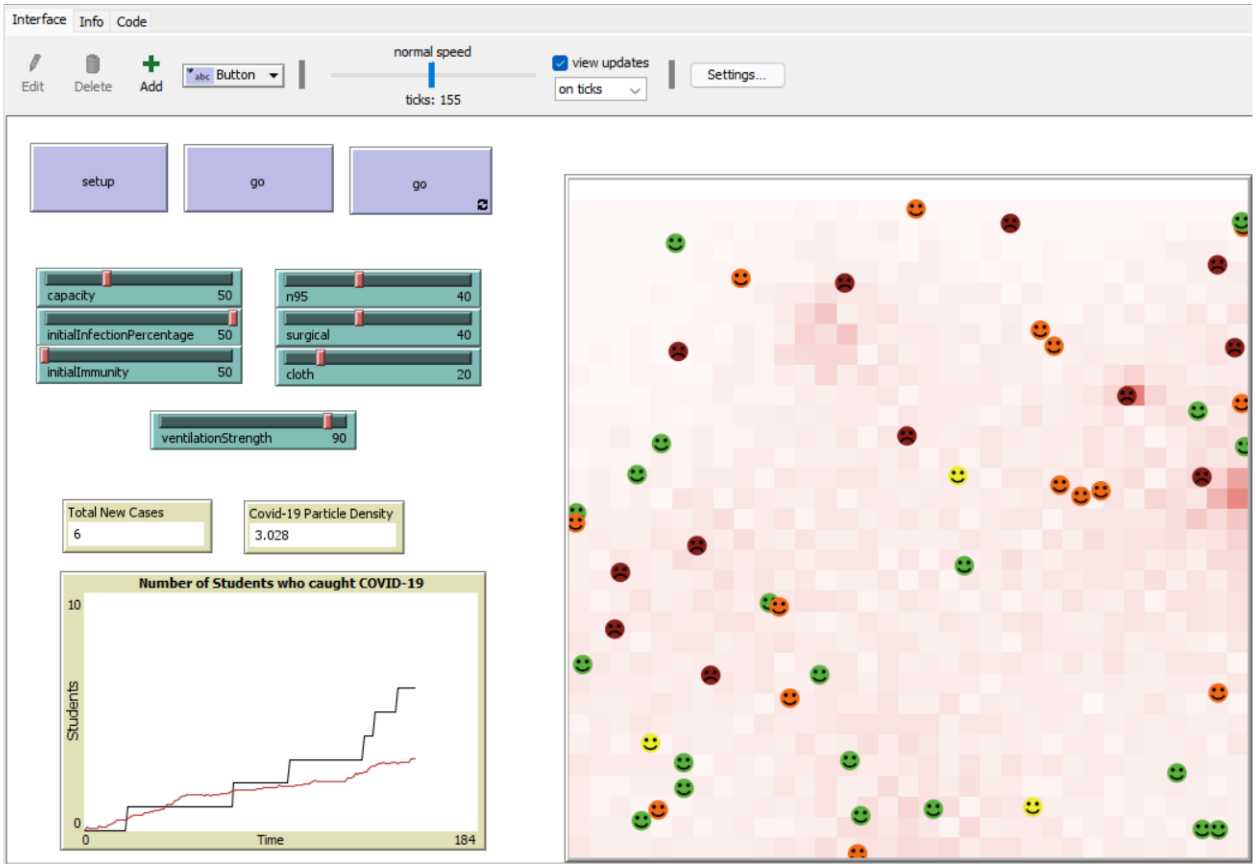

ticks: 155

capacity 50

initialInfectionPercentage 50

initialImmunity 50

n95 40

surgical 40

cloth 20

ventilationStrength 90

Total New Cases 6

Covid-19 Particle Density 3.028

Figure 2.4: Example of Agent Based Model in the `NetLogo` environment. *This high resolution image can be zoomed in for details.*

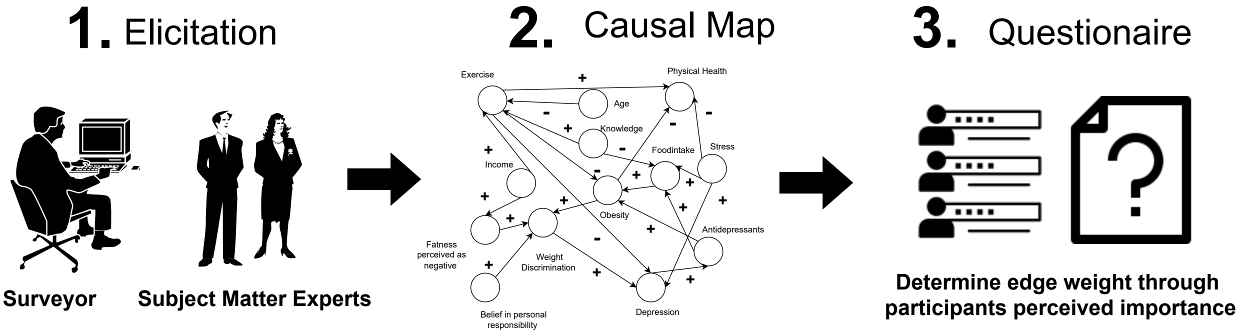

Figure 2.5: Simplified Process of Creating an FCM

Fuzzy Cognitive Maps are networks that illustrate causality during decision making. An FCM is a *digraph* that is comprised of nodes (a.k.a vertices, representing concepts of the system) that represent specific concepts and directed edges that state whether there is a causal increase ("+") or decrease ("-") in a concept of a target node from the source node [51]. Node weights change between [0, 1] where 0 is the absence of a concept, and 1 is the concept's full presence. In addition, edge weights vary between [-1, 1] where positive weights represent an increase and negative weights specify a decrease. The primary purpose of these aggregate models is to produce solutions that answer and characterize "what if" predictions [52]. For example, these models can answer what would happen if a policy was implemented in a institution or what may unfold after an individual joins a terrorist organization [53].

In order to generate these predictions and analyze specific events, FCMs utilize *fuzzy logic* (i.e., a degree of causality) which is obtain through elicitation of subject matter experts (SME). Through elicitation, surveyors are able to access the semantic memory of humans and produce a conceptual model of their thought process known as a *causal map* [54, p. 48]. Once a causal map is created, participants of the study are typically given a questionnaire to associate a level of causal strength (e.g. high, low, medium) for each edge in the network [55]. These three steps are found in Figure 2.5. After the results are collected, the causal strength is mathematically computed and assigned to each associated edge [56]. At this point, an FCM is formed and is depicted in Figure 6.1. Lastly, the model is applied to a case until designated concepts stabilize or stabilization is determined improbable [57]. Stabilization is assessed at the end of each update of the model (i.e., iteration); specifically, iterations stop once a threshold value or threshold values are met for a specific concept/concepts. If the threshold value is not met, a max number of iterations should terminate the update. The update and termination of a FCM (Figure 2.7) are detailed in the equations below respectively [58].

$$V_i^{t+1} = f(V_i^t + \sum_{j=1,j\neq i} V_j^t \times A_{j,i}) \tag{2.1}$$

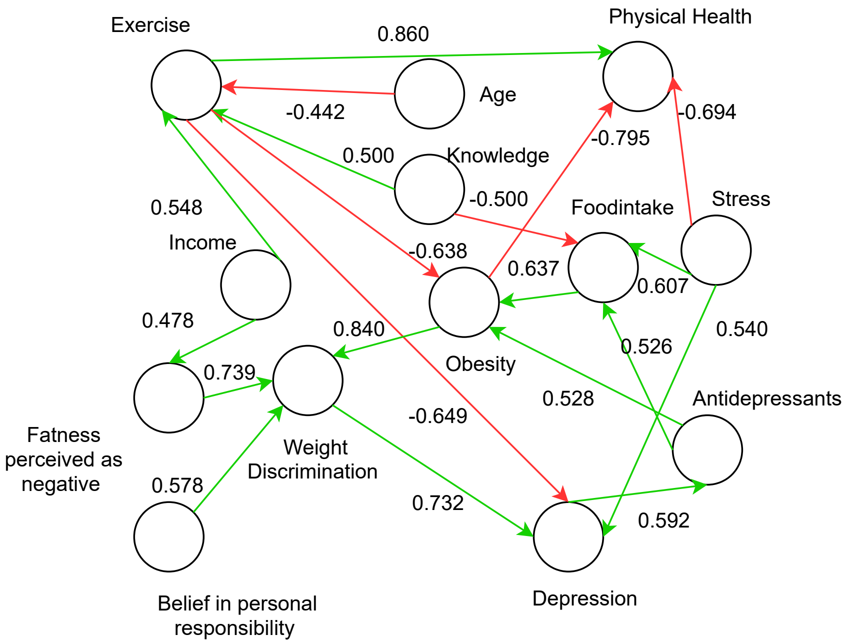

Figure 2.6: Example of Fuzzy Cognitive Map where positive and negative causation are shown as green and red arrows, respectively.

$$while \begin{cases} \exists i \in S \text{ such that} |V_i(t+1) - V_i(t)| > \varepsilon \ and \\ t < t_{max} \end{cases} , \qquad (2.2)$$

where V_i^t is the value of a concept node i at iteration t, f is a clipping function that serves to keep the new value within the desired range (e.g., via a sigmoid), $A_{j,i}$ is the weight of the link from node j to node i in the adjacency matrix A, and ϵ is set to a very small positive value [59].

2.4.2 Measuring similarities between FCMs

Once FCMs are developed on a particular subject matter, the comparison of these models may provide insight to support policy coherence or depict shared goals of a group [60]. Furthermore, these comparisons can highlight significant differences between cognitive and identity diversity and aid in sustainable management of common-pool resources [61]. In order to compare FCMs, a variety of methodologies can be used and the selected methodology will reflect different notions of similarity between graphs or variances between graphs. This thesis focuses on methodologies that are concentrated on two properties of graphs at two levels: *centrality* at the level of individual nodes, and *distance* at the graph-level.

In network analysis (i.e., applied graph theory), measuring centrality establishes a ranking system by assigning an individual value to each node in a graph. This value can then be utilized to establish importance or priority of one node over the others. However, the values

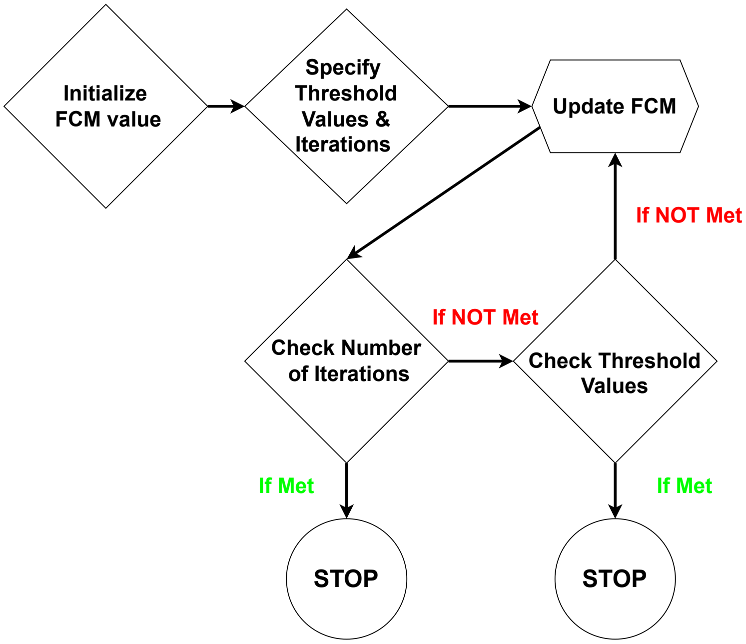

Figure 2.7: Process of updating an FCM

and importance of each node may fluctuate depending on the type of centrality methodology implemented. This is a result of the lack of agreement on the definition of centrality and the creation of abundant centrality measures [62]. Researchers will have various goals in mind when analyzing networks such as determining the best placement for a hospital, finding which celebrity is most popular, or selecting whom to quarantine in a pandemic. In addition, each scenario would require different centralities to measure and rank the data. This thesis will utilize both *degree centrality* and *betweeness centrality*.

One of the most simple centralities to implement is degree centrality [63, 64, 65]. This centrality is often used in many studies on FCMS [66, 67, 68] and can serve various means such as analyzing urban resilience and transformation [67] or modeling solar energy usage [68]. Degree centrality functions by calculating a node's degree (i.e., the amount of connections a node possesses) and either divides the degree by the total number of nodes to convert the number to between 0-1 or leaves the degree as it is. The higher the computed value, the more important or central the node is in the network [69] (**Figure 2.8**). The average degree of a given graph can be defined by $d(u)$ for all $u \epsilon V$ as the degree of each node u divided by the total nodes of the graph as n:

$$d = \frac{\sum_{u \varepsilon V} d(u)}{n}, \tag{2.3}$$

Although the degree centrality index is considered an important measure in determining the centrality of a node in an FCM, it is not sufficient and has significant shortcomings [70]. As an alternative, betweeness centrality has become a popular measure to determine the cognitive similarities between agents [71, 72, 73]. Betweenness centrality totals the number

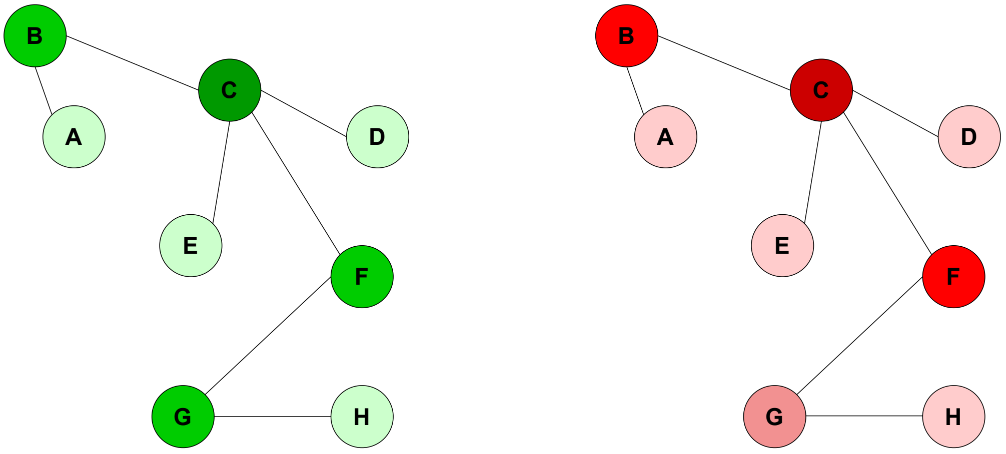

Degree Centrality **Betweenness Centrality**

Figure 2.8: Degree & Betweenness Centrality

of shortest paths that pass through a given node [74] (**Figure 2.8**) and is calculated for a node n by:

$$g(n) = \sum\nolimits_{x \neq n \neq y} \frac{\sigma_{xy}(n)}{\sigma_{xy}}, \tag{2.4}$$

where $g(n)$ is the betweenness centrality, $\sigma_{xy}(n)$ is the total number of shortest paths from x to y that goes through n, and σ_{xy} is the total number of shortest paths from x to y.

Lastly, to determine the similarity or distance between two inexact graphs (i.e., inexact graph matching), *Graph edit distance* (GED) can be applied [75]. GED operates by transforming a source graph into a target graph by executing a sequence of operations on nodes and/or edges [76]. At one step at a time, these operations either delete or insert an edge or node or relabel a node of the source graph while finding the optimal path to the target graph **(Figure 2.9)**. The search for the optimal path is most important because it is possible to perform unlimited operations to reach a target graph [76]. In order to determine the best path, the operations are assigned a value of importance that are of either equal or various magnitudes. Once the best path is determine, the cost of operations is totaled and the value can be used to compare the distance and similarities between one graph and another.

2.5 Hybrid Simulations: ABM/FCM Models

2.5.1 ABM/FCM Model

A hybrid technique that has emerged in Computational Social Science is the pairing of an Agent Based Model with a Fuzzy Cognitive Map [77]. This combination serves various purposes such as regulating the interactions of agents [58] or establishing decision making processes in an agent's environment [51]. As a general overview, agents of a system are

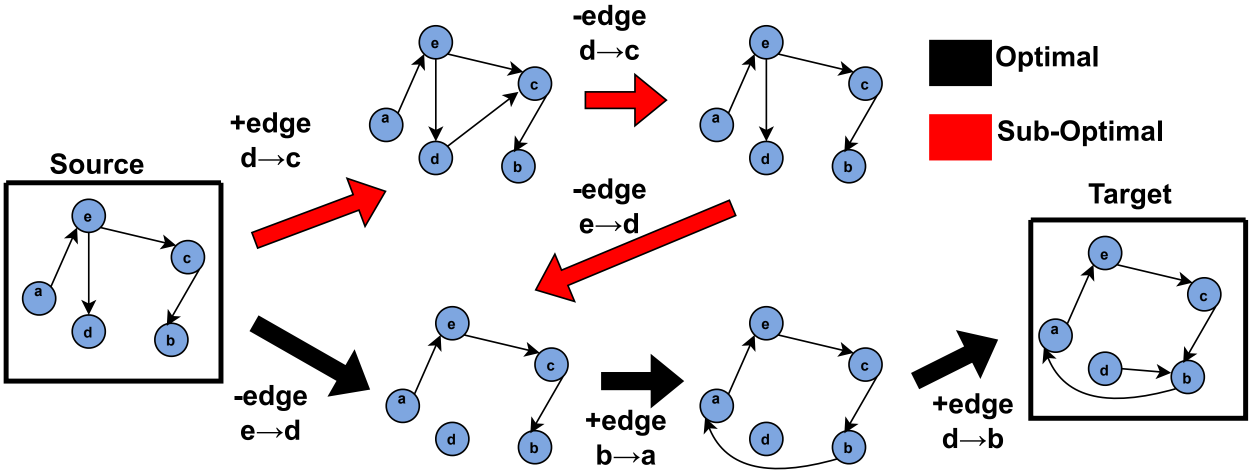

Figure 2.9: Graph Edit Distance Operations of Equal Value

assigned an FCM that serve as a “brain” individually or collectively. More specifically, ABM/FCM hybrid models (i) embed each agent with an FCM that shifts during agent-to-agent interaction (**Figure 2.10**) or (ii) use a single FCM to describe the system and expand selected concepts into agents when greater accuracy is required [78]. For example, researchers are able to simulate the spread of social influences through the hybrid coupling of ABM/FCMs [51]. In this example, ABMs were paired with a variety of FCMs to replicate the many rules and behaviors an agent may have. As time steps increased, agents interacted with the environment and each other while their attached FCM was updated. This application represented the social phenomena of humans shaping societal norms and transforming their views over time.

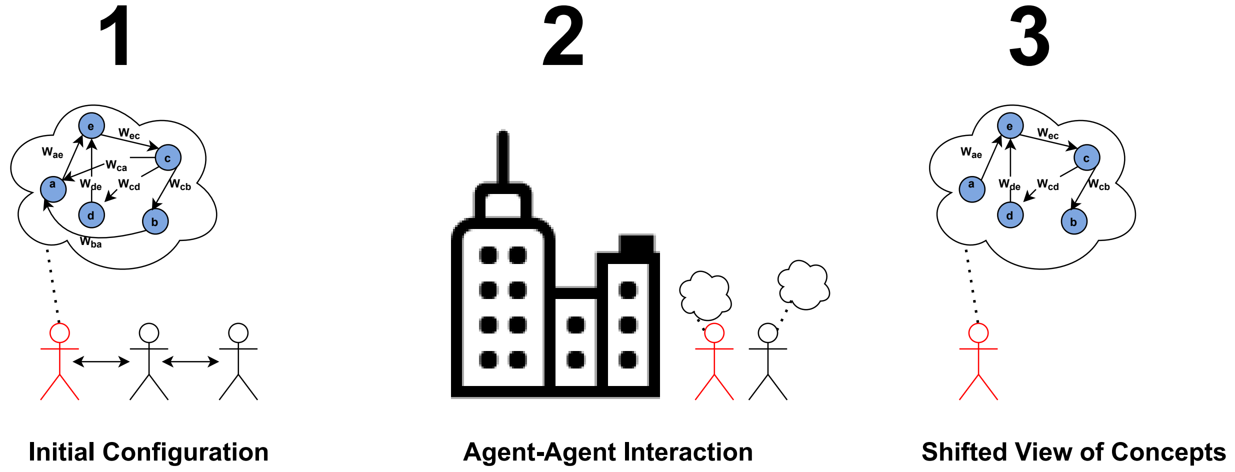

Figure 2.10: Hybrid ABM/FCM

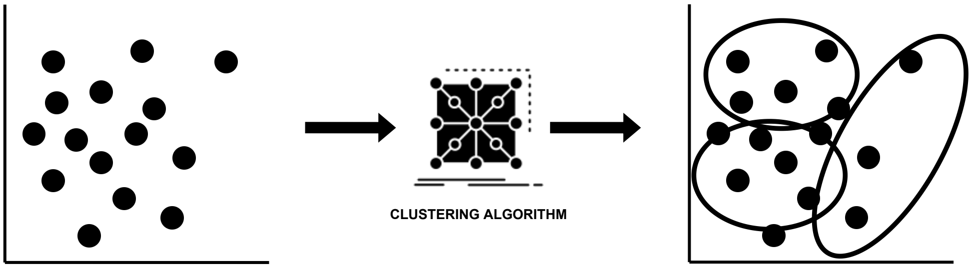

Figure 2.11: Example of Clustering (i.e., dividing segments)

2.6 Machine Learning

In 1997, Tom Mitchell defined *Machine Learning* (ML) as follows: "A computer program is said to learn from experience E with respect to some task T and some performance measure P, if its performance on T, as measured by P, improves with experience E" [79]. Simply put, Machine Learning is the act of computers learning (training) on data rather than being given a fixed set of rules. In fact, this act of training can be divided into four categories: supervised, unsupervised, semi-supervised, and reinforcement [80]. In this thesis, the focus is on supervised and unsupervised learning for Simulations. During supervised learning, the selected algorithm operates with the information of the desired output for the input data [81]. Some of the most common algorithms utilized are Decision trees, K Nearest Neighbors, and Random Forest [81]. On the other hand, unsupervised learning, implements algorithms that operate on information without any context and labels. The algorithm then labels the data without any regulation [81]. The algorithms that are most commonly implemented in this approach are known as Apriori, Hierarchical clustering, and DBSCAN [28].

2.6.1 Clustering

One common algorithm category (i.e., *unsupervised learning*) of ML implements methods of data learning through pattern recognition. This occurs by feeding the model variable inputs that are not labeled [82] then utilizing a clustering algorithm to group and assign labels to the inputted data (i.e., cluster analysis determines similarities between groups) [83, p. 332]. For example, clustering can be used with social networks to recognize communities of people, implemented in biology to generate artificial phylogenetic trees, or divide a population into marketing segments. A simplified version of these processes can be seen in **Figure 2.11**. Lastly, there are various methods that accomplish cluster analysis such as Partitioning, Hierarchical-based, and Density-based methods [80]. From these methods, a variety of clustering algorithms are utilized. For example, partitioning methods most commonly use algorithms known as K-means, CLARA, DBSCAN, and K-Mediods [80, 83].

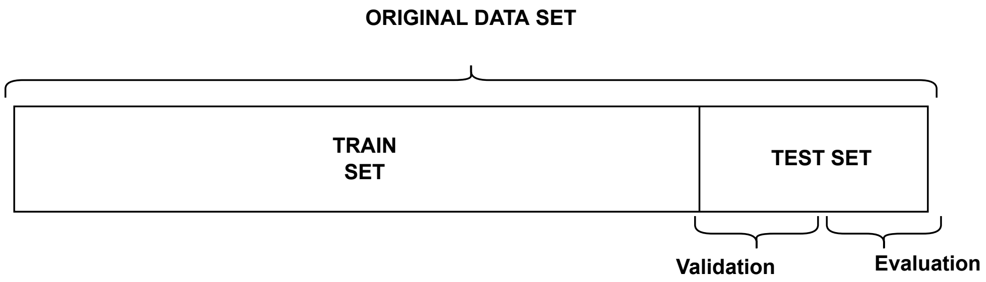

Figure 2.12: Division of Data

2.6.2 Classification

Another prominent task in ML is a methodology of supervised learning: *classification*. Supervised learning encompasses the process of forecasting data from previous data sets [84] and can be applied to numerous topics such as demographics, social predictors, and mental health [84]. In order to predict categorical outcomes, classification can be broken into three main processes: training, validation, evaluation. First, both training, validation, and evaluation operate on the same original data set; however, this data is initially divided into a training and testing subset (**Figure 2.12**). Next, training occurs as the model learns via the training data set which contains attributes and a class outcome. These attributes are mapped with the class to ultimately build a trained classifier such as a decision tree. (provide example, illustration, reference) Next, the classifier is then validated with the test data set which only contains data attributes. This process utilizes the classifier to label the class outcome. Finally, this process is evaluated to measure the accuracy of the trained model.

2.6.3 Using Machine Learning for Simulations

Even though Machine Learning has been around for over 60 years, only recently, the field has exploded with advanced research and has been regarded as one of the most disruptive innovations of modern technology [85]. As Machine Learning has been leading cutting-edge research and development, many have viewed the field independently from Modeling & Simulation. However, in recent years, researchers have provided evidence that illustrates Machine Learning's ability to solve critical problems in Big Data Simulations [15]. For example, Machine Learning can be utilized with Agent Based Models, Fuzzy Cognitive Maps, and Hybrid ABM/FCM models to navigate social phenomena in relation to uncertainty [15]. This was demonstrated by Papageorgiou by refining the values of rules in a FCM to deal with uncertainty [86] (**Figure 2.13**).

In order to have *adaptive agents*, Machine Learning can be utilized to provide agents the ability to learn from consequences, and guide their own individual experiences [87]. This can be achieved through combining the two separate cycles of ABMs and Machine Learning. First, the ABM cycle is defined by (i) initializing the environment and its agents, (ii) the agents observing the world and (iii) updating their internal model , and (iv) agents taking

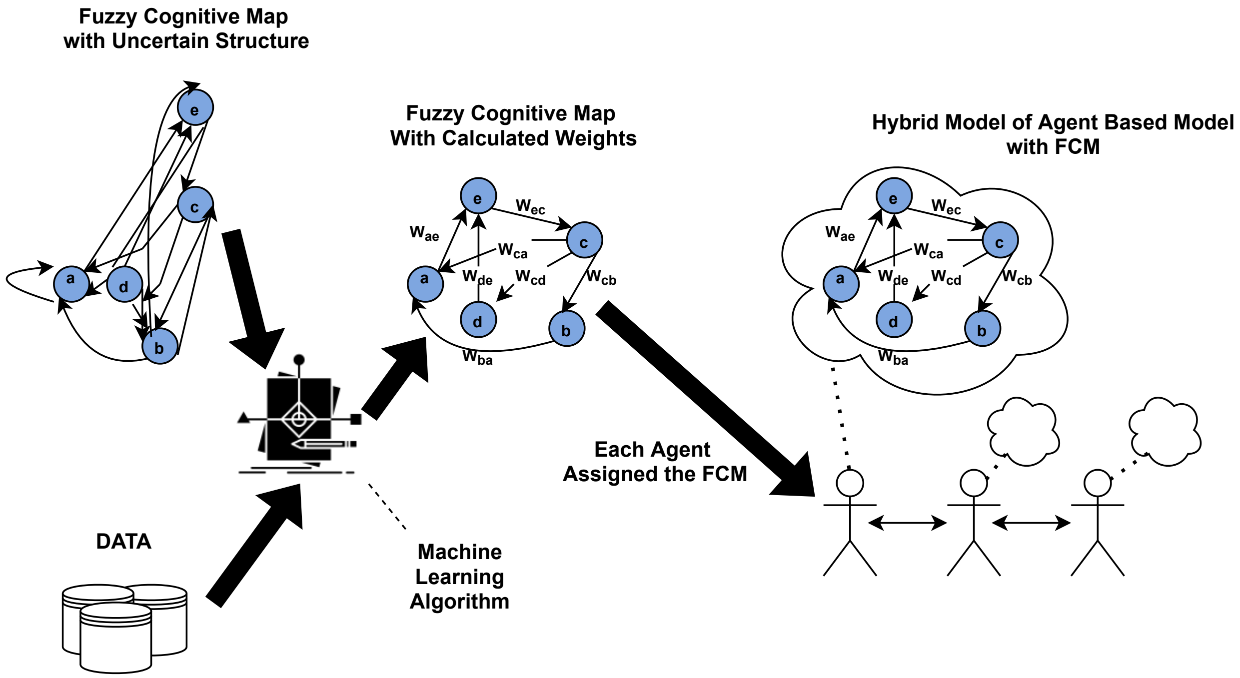

Figure 2.13: Machine Learning

action (**Figure 2.14-A.**). A ML cycle is similar in its approach; the cycle (i) creates an internal model, (ii) trains on data, (iii) updates the internal model, and (iv) takes actions while recording [88] (**Figure 2.14-B.**). Through minor manipulation, the two processes can be integrated (**Figure 2.14-C.**) to produce adaptive agents. The hybrid cycle would then be composed of 7 primary steps: (i) initialize the environment and agents of the ABM, (ii) allow agents to interact and observe their environment, (iii) provide the observations to the ML model to train the model, (iv) update the internal ML model, (v) send the updates and adaptive actions to the ABM, (vi) update the agents internal model, (vii) agents move, interact, react.

Integrating ML processes with Modeling & Simulation to equip agents with learning algorithms potentially improves the quality of their decision-making module, thus changing their interactions with the environment and/or other agents [89]. Yet, there are multiple decisions to be considered while integrating the two. Both supervised and unsupervised learning techniques may be chosen for a ML algorithm; however, the selected methodology should depend on researchers' desired actions of agents. For example, we may want an agent to decide whether it should wear a mask or not (which is a binary *classification*) based on its observations of disease severity or symptoms in other agents. Alternatively, an agent may decide what is a sufficient level of social distancing (e.g., 2 ft, 3 ft, 6 ft) with nearby agents, thus performing a *regression* task [88].

Other important aspects of using ML for simulations is the type of data implemented in the model or the amount of available data for learning [90, 91]. For example, the data utilized during an integrated ABM and ML process will have major implications on the

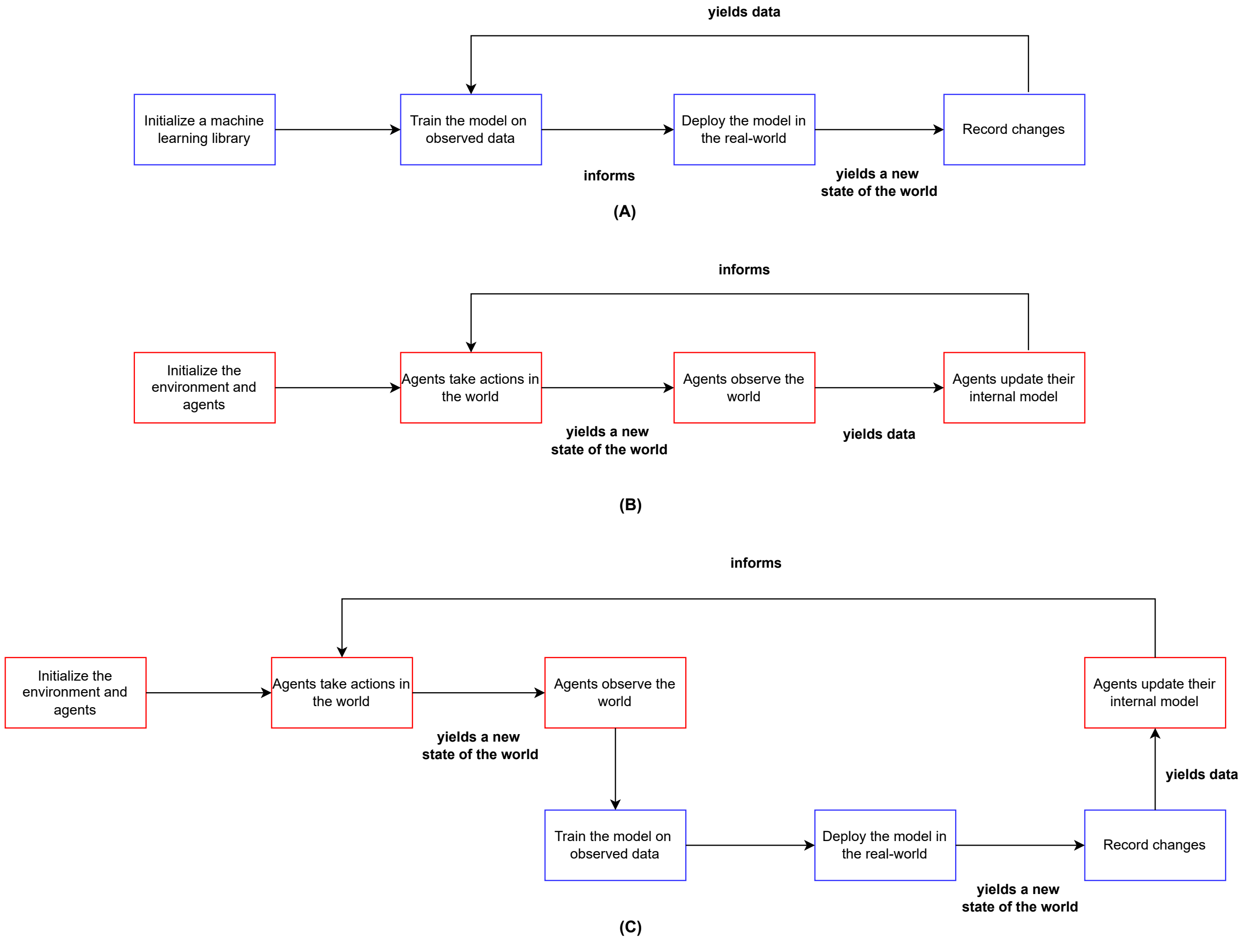

Figure 2.14: Integrated Cycle

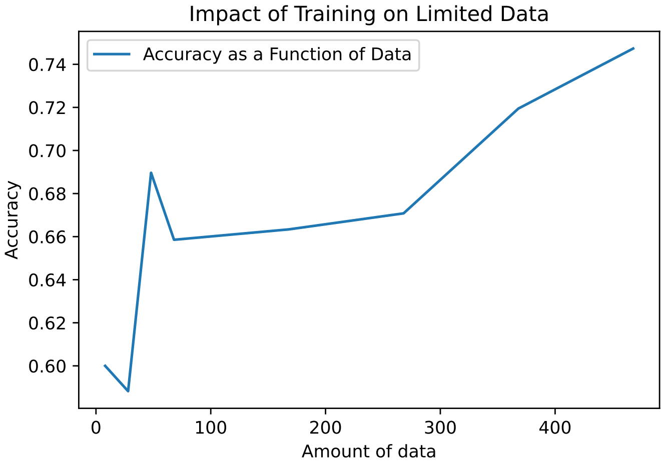

Figure 2.15: Accuracy from Limited Data

model and simulation [92]. These implications can be categorized as initialization, structure modifications, and structure generation. When designing or updating the initial setup of an ABM (i.e., the initialization process) the data applied can modify the initial attributes of agents or the environment. Furthermore, if new processes or partial model components are constructed through ML methods, these additions can be hidden or trouble researchers in tracking the components during structure generation. However, these additions and impacts of data can be illustrated during structure modification.

The amount of available data will also impact the trajectory of a hybrid model. This can be illustrated by manipulating a data-frame created using the Python library Pandas and decision trees. For example, a file of information can be randomly divided from the original data set into data frames that ascend in the amounts of data. These ascending data sets can then be sequentially split into separate training and testing data sets that each build a decision tree classifier. This decision tree classifier would then predict the target variable and output the accuracy of predicting that response. After the results are recorded, accuracy can be plotted as a function of the amount of data used to build the classifier (**Figure 2.15**). The results of this example illustrate that as the amount of available data increases the accuracy of ML algorithms increases as a result. Furthermore the validity of this relationship is detailed in work that demonstrates modeling the spread of COVID-19 with strong interventions must be done with large amounts of data to achieve stable accuracy [91].

Chapter 3

A Framework for the Comparison of Errors in Agent-Based Models using Machine Learning

Across common ABM frameworks (e.g., BDI, SOAR, ACT-R) errors in human perceptions are inconsistently handled through implementation or lack thereof. Without the proper integration or absence of key human behaviors, researchers in cognitive social simulations may overlook various features that would have affected the overall model trajectory. We address this concern by developing a framework that illustrates the value of agents possessing internal models[93] that are driven by Machine Learning. We illustrate the impact of this framework on two well-known models (Schelling and Axelrod) and on a COVID-19 simulation. Our work employs various Machine Learning models (e.g., Decision Tree Classifier, Logistic Regressor) to depict how the inclusion of human errors alters the overall model trajectory and may justify the integration of imperfections and heterogeneity into individual decision-making processes. Our open source framework can be integrated into existing and future models and utilized to examine the consequences of an agent making a decision without the appropriate amount of information (insufficient observation), by ignoring specific information (superficial observation), when inaccurately recording information (inaccurate perception), or due to a gap between environmental complexity and individual capacity (limited ability).

All of this chapter is currently under revision.

3.1 Introduction

Agent-Based Models (ABMs) are a simplification of reality in which a system is decomposed into a set of (potentially heterogeneous) agents that interact with each other and with their environment. In many instances, simplifications that may at first sound odd can be tolerated because the model is sufficiently *fit for purpose* [94]. For example, in a classic prey-predator model, sheep may jump with blissful unawareness into a location occupied by a wolf, who will simply eat them. While real sheep are less suicidal, the perception error does not prevent the model from being adequate in its ability to reflect population level dynamics over the course of a simulation. Errors may even be a necessary *feature* for application domains such as gaming, where the unpleasant prospect of an all-powerful computer opponent is addressed by using different decision making algorithms that force an opponent's agents to make errors (e.g., greedy algorithms instead of optimization). A similar need arises in several scientific applications, as a purposeful inclusion of errors in a model can preserve accuracy vis-à-vis real social systems. For instance, a model of gentrification purposely limited an agent to finding a house by only looking at a cluster (the 'microscale') rather than optimizing over an entire city. Although results could be sub-optimal for the agents (e.g., a better deal may only be a few blocks away), the simulation accurately generated patterns of human relocation within submarkets [95].

Despite such examples, there is a broader tendency to create ABMs where agents are very homogeneous and rational [96]. Indeed, "most AI researchers have little interest in replicating the all too human errors [...] observed in nature." [97] In an application domain such as agricultural policy, most ABMs use optimization and only 20% employ behavioral heuristics [98]. In human health behavior research, models have assumed that virtual agents are perfectly accurate in sensing the state of other agents [99], and that they make informed decisions after performing a thorough inventory of their surroundings [100]. But in reality, humans only take in a small portion of the information available in their environment [101], potentially make errors in memory encoding or retrieval, interpret the world through their own heterogeneous sets of beliefs [102], and react based on their emotions [103]. Filtering out information is one of the key skills that characterize human decision making, which allows us to focus on specific tasks amidst a busy environment [93]. Although emotions used to be considered as a disruptive and irrational behavior from a modeling standpoint, they are now seen as essential to generate "a more human-like behavior thus having deeper and more meaningful human-machine relationship" [103]. The growing recognition that virtual agents ought to make errors echoes popularized notions such as Pope's "To Err is Human", or established concepts such as bounded rationality [104] and its illustration above in the gentrification model. In this paper, we focus on including errors in ABMs, thus contributing to the study of cognitive social simulations by covering errors in the individual mental processes of agents and in their social processes [105].

The impact of such judgment errors on model outcomes has been inconsistently addressed in ABMs [17]. Our previous work showed that errors could be introduced into ABMs and helped to identify problematic assumptions in some of the models, as simulation outcomes would be either highly sensitive to a small level of errors or (to the other extreme) would remain unchanged regardless of how erratic an agent may become [18]. However, the ad-hoc introduction of errors into various implementations of ABMs leads to multiple challenges. First, tempering with various codes is a laborious process as errors have to be introduced in different ways, which raises the potential for bugs. Second, comparing the effect of errors on various ABMs (e.g., to select one that is appropriately robust) becomes a very timeconsuming enterprise, since each ABM could be written in its own ways. Third, there is a vast array of phenomena that qualify as 'errors', and programmers may only implement some based on their own awareness and the convenience of modifying existing codes. These shortcomings point to the need for a framework that facilitates the systematic inclusion of human errors into ABMs, thus echoing calls for frameworks that let us rigorously handle key aspects of ABMs [106] and for building blocks that facilitate the inclusion of core features into ABMs [107].

The growing interest in combining Machine Learning (ML) with ABM offers an opportunity to support the systematic specification and implementation of errors. Although the general notion of using ML to set the behaviors of agents has long been discussed [108], a recent review of 51 ABMs employing ML techniques allows for a more precise definition [109]. The authors suggest that ML can "replace, augment, or optimize the agent's internal behavioral rules" in two ways: either the ML component is already developed and each agent uses it as such during the simulation, or the ML component is used to learn and improve agent decisions at runtime. In this paper, we use the latter approach by equipping each agent with an ML algorithm (e.g., a decision tree) that receives observations and combines them to arrive at a decision. The ML algorithm acts as a key conduit to systematically handle various types of errors, either in observations (e.g., insufficient data, inaccurate measurements) or in inferences (e.g., when an agent's capacity cannot cope with the complexity of its environment).

Hybrid ML/ABM models by nature include many ways that lead agents to make suboptimal decisions, but these errors were not the main focus of the associated studies. For instance, agents have previously been equipped with a neural network, and their decisions were inherently affected by limitations in training data, lack of perfect knowledge about their peers' true preferences, and the accuracy of their neural network predictions [16, 110]. In contrast, this paper focuses on the systematic treatment of errors. Our contributions are threefold:

- We unify the treatment of errors in the decision-making processes of Agent-Based Models by using Machine Learning as a filter for observations and inferences. In previous studies, the mechanisms underlying social learning between agents were treated as a blackbox [111, 112]. Our framework is thus a first step towards operationalizing the errors that shape human behaviors.

- We implement our framework in Python and release it open source for the research community on the Open Science Framework at `https://osf.io/n6pja/`.

- We instantiate our framework on classic models (Schelling for segregation, Axelrod for culture) and a sample COVID-19 application, thus illustrating the supported error types and exemplifying how researchers can assess the effect of errors onto simulation outcomes.

The remainder of this paper is structured as follows. In section 3.2, we provide an overview of how previous frameworks have covered the notion of errors in ABMs in order to enhance their realism. Rather than detailing every agent architecture as this has been covered in many studies [113, 114, 115], we utilize a sample of well-known frameworks from formal logic (e.g., belief-desire-intention) and cognitive science (e.g., appraisal theories) to illustrate which errors could be incorporated in future work and how these errors would be implemented. Then, our background covers the inclusion of data in ABMs, to provide the foundations for our approach at the intersection of ML and ABM. Our framework is introduced in section 3.3 and exemplified via three case studies in section 3.4, with a continued emphasis on identifying which errors can be included in a model and how. Results are provided in section 3.5, while noting that they illustrate how modelers can analyze the impact of errors onto their output, hence the focus is on the ability to perform analyses rather than on a specific model (e.g., we do not seek to generate new insight into the Schelling model). Limitations and future works are summarized in section 3.6 and concluding remarks are offered in section 3.7.

3.2 Background

3.2.1 Integrating Errors into Agent-Based Models

The errors that characterize human behaviors are handled inconsistently among empirical ABM studies [17]. A variety of works tend to include certain errors (e.g., uncertainty, assumptions) [18, 116, 117, 98] through differing methodologies or exempts human errors from their ABMs altogether [97] (**Table 3.1**). In order to develop models which demonstrate sufficiently realistic human behavior, it is vital to integrate common human errors [18] into existing ABM frameworks. The *Enhancing Realism of Simulations* (EROS) [118] approach seeks to integrate psychological realism into agent-based models. The concept of EROS has been advocated for over twenty years, yet the theoretical discussion and actual implementation has only proceeded in recent years [119, 118]. A variety of existing frameworks (e.g., *SOAR*, *ACT-R*, *CLARION*, *EMA*, *DETT*, *eBDI*) attempt to capture psychological realism, although they may focus on only a subset of aspects and can have drawbacks. For example, frameworks such as SOAR and ACT-R include complex psychology reasoning by integrating long and short term memory, but they require an extreme computational cost [120, 121, 119].

One of the most popular ABM frameworks is the *Belief-Desire-Intention* (BDI) which was founded on ideas expressed by philosophers [2, 124]. The BDI framework is based on the idea that it is possible to represent human behavior by defining an individual's beliefs, desires and intentions [97]. An agent's beliefs account for their personal information about their environment. This is the perception of the world, as seen per the agent, which may be subject to uncertainty and errors. The agent's desires are all the possible states of affairs that the agent wishes to accomplish, and the agent's intentions are commitments to a particular course of actions for achieving a particular goal [2, 124, 97]. A variety of languages and programming environments support the BDI framework, often by using `Java` and formerly via interprets of the logic-based language `AgentSpeak` [125]. Emerging solutions are leveraging cross-language development platforms such that the socio-psychological module for the BDI

Table 3.1: Different errors and how they were handled in the literature

Type of Error	**Example Study**
Uncertainty	Probability for agents to make mistakes during perception of their environment [18]
	Used attitudinal models to calculate the values of uncertainty arising from agent-to-agent interactions [116].
Assumptions	Rule-sets of logic to contrast outcomes of agents' decisions from making assumptions [117]
Emotions	The OCC theory accounts for emotions and social relations in ABMs [122], for instance by specifying that emotions are positive/negative reactions due to events, actions of agents, or aspects of objects [103]
	The reasoning module of the agents is directly related to emotions [123]

agents can be written in any language and accessed by a simulator [126].

Behavior with Emotions and Norms (BEN) is a framework that has comprehensively implemented the principles of EROS [119, p. 148]. For instance, BEN is comprised of predicates, cognitive mental states, emotions, social relations, norms, personalities, and obligations [127]. BEN thus provides a high-level overview of an agent's behavior at any moment during the simulation in efficient computational time [119].

Numerous other extensions to the BDI framework have been proposed but remain at a theoretical stage [2]. For example, *Belief-Obligation-Intention-Desire (BOID)* [2, 124, 128] accounts for normative concepts such as social norms and obligations [129]. In BOID, agents can choose to follow social rules and contribute to the collective interest of agents. The decision making of the agents is similar to BDI; however, agents take social norms and obligations into consideration while interacting in simulation [2, 124]. Similarly, the *Belief-Response-Intention-Desire-Goals-Ego* (BRIDGE) framework accounts for social awareness, 'own' awareness and reasoning based on the BDI modules [2, 128]. This framework introduces three new modules called *ego*, *response*, and *goals* while also refining some of the original modules present in BDI. In addition, BRIDGE differs from BDI by allowing all components to work in parallel to provide continuous processing of the environment. The BEN ego component helps specify different types of agents and their emotional responses to various stimuli [2], which adheres to EROS.

Unlike the previous frameworks, *CLARION* uses a hybrid neural network system to simulate tasks in cognitive and social psychology for artificial intelligence applications [130]. This framework emphasizes the difference between explicit and implicit (i.e., learned via neural networks or reinforcement learning [124]) representation of knowledge. CLARION integrates routines, generic rules, decision making, and has one of the most complex learning methodologies across frameworks [2].

As shown in **Table 3.2**, most of the frameworks aforementioned do not handle emotions.

Table 3.2: Frameworks, references and some key features of popular ABMs

Framework	**References**	**Reasoning**	**Emotions**	**Social norms**	**Learning**	**Communication**	**Uncertainty**
PRS	[97, 2, 124, 122, 128]	×	×	×	×	×	×
BDI	[97, 2, 124, 122, 128, 136]	✓	×	×	×	×	×
eBDI	[2, 124, 122, 128]	✓	✓	×	×	×	×
BOID	[2, 124, 128]	✓	×	✓	×	×	×
BRIDGE	[2, 128]	✓	≈	≈	×	×	×
EMIL-A	[2, 124, 128]	✓	×	✓	✓	×	≈ (considered)
Consumat	[2, 128]	✓	≈ (values and money)	×	✓	×	✓
CLARION	[2, 124]	✓	×	×	✓	×	×
BEN	[119, 127]	✓	✓	✓	✓	×	≈ (considered)

'×' means that the feature is **not accounted** in the framework, '≈' means that the feature is **partially** accounted, and '✓' means that the feature is **part** of the framework.

Although emotions are not typically included under the umbrella of 'errors', they participate to increasing the realism of agents (particularly for crisis models) and the diversity of their reactions. Extrapolating from the example in [103], when an agent sees its house burn, it may express fear and sadness because the house is gone, or joy because the insurance will build a better house. Advances in neuropsychology suggest that "cognitive information-processing models and emotion information-processing models work in tandem" [131], hence a different line of architectures handles emotions by combining these two models in the decision-making module of an agent. Such architectures may be mathematical grounded using decision field theory [132] or rooted in less formal approaches such as appraisal theories. For instance, the *emotional Biologically Inspired Cognitive Architecture* (eBICA) has been used in several studies to explain or predict human behavior [133]. This framework integrates two systems [134]: one is the 'rational' system with specified goals, constraints or utility functions, and a planner; the other is the socio-emotional system, where moral schema and a representation of the world (i.e. cognitive map) will bias the agent towards certain actions. To integrate the two systems, the authors note that the purely rational piece only sets high-level goals and leaves some freedom of choice; instead of being made uniformly at random, probabilities are biased by what is emotionally preferable [135].

3.2.2 Data-Driven Agents and Data-Driven ABMs

The extracted rule-sets and information from psychological theories that agents utilize and collect to update their internal model during simulation serve a crucial role in producing *data-driven* or *adaptive agents*. In addition, the data used to compose the entire ABM defines whether an ABM is data-driven or not. Data-driven ABMs emerged in the 2000's (c.f., the first theoretical study in [137]) and researchers have differing definitions of what comprises a data-driven agent or ABM. Some works consider that a data-driven ABM has the initial environment constructed at the very start from the available big data [138, 139] (**Figure 3.11-a**). This is a *static* definition, as the agents and their environment derive rules and attributes during initialization from a variety of analytic methods and/or *Machine Learning* (ML). In contrast, others view data-driven agents more *dynamically* (**Figure 3.11-b**), as entities continually learn from their observations of their surroundings (e.g., other

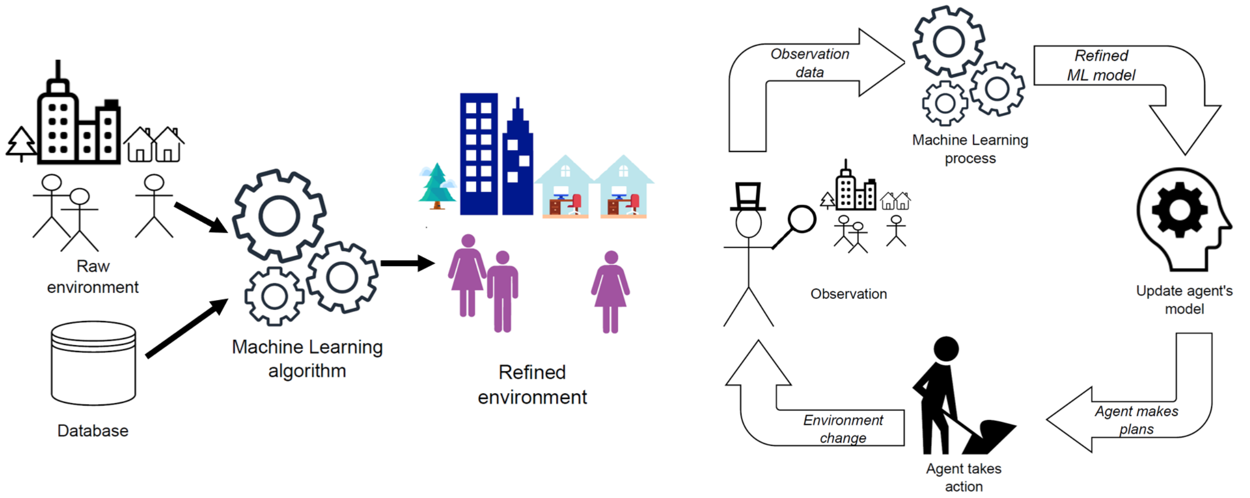

(a) Static ML model: ML runs once, to *initialize* from data **(b)** Dynamic ML model: model runs at every *update* step

Figure 3.1: Difference between initializing a model from *Machine Learning* (a; static) and having agents adapt through a simulation by ML (b; dynamic)

Table 3.3: Different data-driven agents found in the literature

Data-driven approach	**Example studies**
Agents with Big-Data	Created a new agent-based modeling approach that incorporates big data at the individual-level to generate agent behavior rules and initialize agent attributes [92].
Agents with Reinforcement Learning	Agents are implemented with no knowledge and learn iteratively while observing their surroundings while using reinforcement learning [140].
Agents with Policy Trees	Agents are integrated with interactive dynamic influence diagrams to construct decision making processes with clustering methods and policy trees [141].

agents, the environment) with the use of Machine Learning [92] (**Table 3.3**). Our paper is rooted in this dynamic view.

In a dynamic process, the agents start by making observations through their *initial* ruleset. The observations are used as training data for the ML model, which aids in updating the decisions of each *adaptive* agent [142, 143]. Consequently, the initial ruleset can shift as it is updated by ML at each step [142, 143], which allows each agent to gradually differentiate its behavior based on its local physical and social environment. Note that 'adapting' is used loosely since it can lead an agent to make a decision from which it does not fully benefit (i.e., a 'wrong' decision). For example, obesity is occasionally presented as 'maladaptation to a

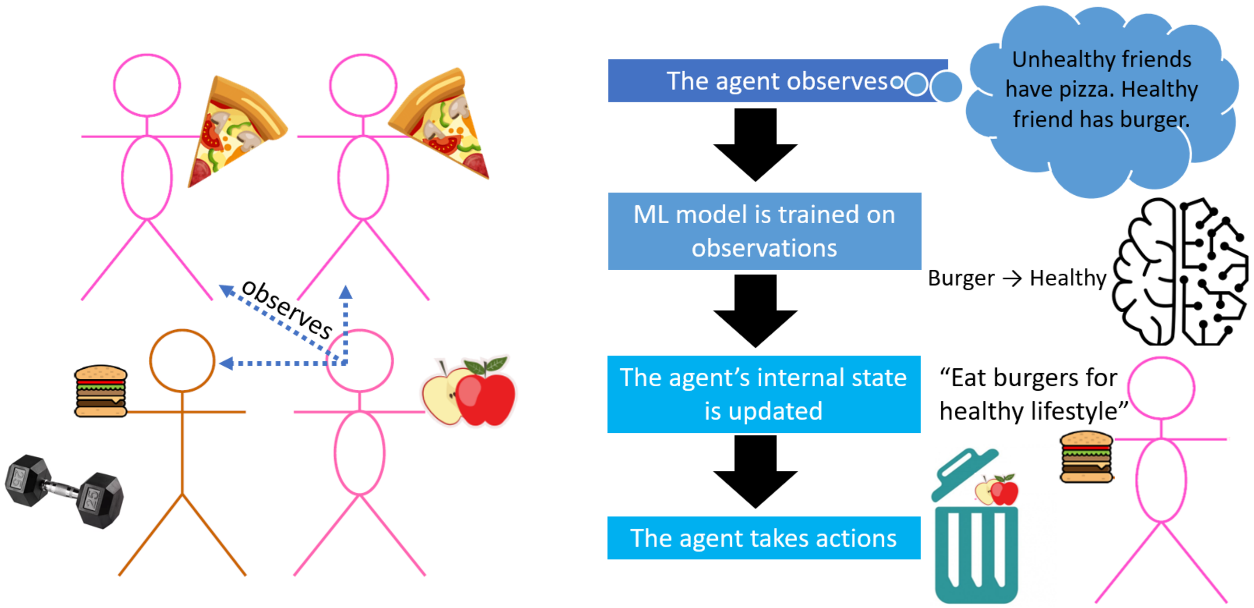

Figure 3.2: A data-driven agent observes its surroundings and, between two equally likely discriminating factors, makes an error in the choice of feature.

modern world', but agents can become obese (and may make a simulation more realistic) if they adapt to an obesogenic environment where peers have unhealthy habits (**Figure 3.2**); they are socially adapted, at the detriment of their own health. The integration of ML and evidence based rule-sets in ABMs has demonstrated higher performance compared to ABMs that exclusively use expert-driven rulesets, or only derive rules from data [144]. However, this integrated approach is an emerging area of research, so its benefits and drawbacks continue to be assessed [109].

3.3 Framework

3.3.1 Errors represented

Our framework was developed by integrating four particular human errors. These errors are motivated by the growing evidence that humans use social information sub-optimally despite the vast expected benefits, such as obtaining an accurate representation of the world without incurring costly individual explorations [112] or reusing solutions that have been honed by peers. We account for over-generalization, which happens when a person forms a conclusion from insufficient observations. To operationalize over-generalization, we represent the observations made by an agent in the form of a table where each observation is a row and its characteristics (or features) are tracked by columns; for example, in **Figure 3.2**, the table would have at most three rows (since three peers are observed) and two columns (what they eat, whether they exercise). One error happens when an agent has *insufficient samples* of information, which means there are too few rows of data. In **Figure 3.2**, the agent may only be observing the two neighbors above, who only eat pizza, and hence never learn about the virtues of exercising. Another error happens when an agent makes *superficial observations* and transpires when a human has access to enough samples, but pointedly determines a position from only a portion of the characteristics. In **Figure 3.2**, the agent may look at all three neighbors, but only pay attention to what they eat (i.e., account for only one of two features). In short, the data received by the agent is either limited in number of rows (insufficient samples) or in number of columns (superficial observations). The third error is *inaccurate perception*, which happens when an agent does not perfectly make an observation. From a tabular viewpoint, the error is applied on a cell. For instance, an agent may observe what others eat, but would not be able to perfectly determine the amount of calories. This covers distortions due to measurement errors and uncertainty in human perceptions. We stress that this error is about observations, rather than attitudes or expectations (e.g., an agent incorrectly evaluating flooding risks or acceptable insurance premiums [145]).

Finally, humans cannot necessarily form accurate models even when they are provided with complete and flawless observations. We represent this as *limited ability* to capture that the capacity of the agent cannot match the complexity of its observations, hence a simplification occurs. Consider the following example: an agent walks into a restaurant with friends and must order at the counter from dozens of potential items, while other customers are waiting in line behind. The agent does not have the mental capacity to quickly review all options and pick the optimal one, hence the agent may just have the same as its peers or opt for the 'special of the day'. In fact, obesity research has repeatedly emphasized that "to promote healthier eating, the healthiest option could be set as the default option" since individuals are overwhelmed with choices and simplify significantly [146, 147].

The presence of errors do not necessarily mean that the decisions will be worst for the agents. For example, forced simplifications due to limited ability mean that an agent will generate a model that does not follow the data too closely; the model is thus less likely to over-fit, hence it may be more generalizable and the agent can reuse it in a variety of settings. Further note that despite our presentation of the four errors as separate, they can happen *jointly* in a given model; illustrative examples are provided in the next section. Accumulating several errors does not necessarily imply poorer decisions. For instance, if measurements are noisy, then a limited ability can be an asset by avoiding an overfit to noise [148]. Conversely, if there are insufficient samples and, in addition, superficial observations, then the errors may have a cumulative negative effect.

3.3.2 Operationalization via Machine Learning

The foundation of our framework builds upon data-driven agents which are incorporated in every case study. We implement data-driven agents that dynamically update their rulesets and change their actions after observing the attributes and actions of agents in their environment and sending these observations to a variety of ML models. All agents start by collecting data in a perfect manner (i.e., no missing rows or columns, no errors in the cells). For the first three errors given in section 3.3.1, the data table is altered as follows.

First, *insufficient samples* consist of taking a random percentage of the observed data (e.g., 5%, 15%) and discarding the rest, as in previous studies [91]. Although *superficial observations* could be operationalized through a random subset, the literature does not usually eliminate features randomly. Indeed, a subset of features is identified either based on perceived value [149] (e.g., via feature selection algorithms) or from model-specific questions (e.g., 'how would population weight change if individuals tried to match their peers' weight based on nutrition only'). Our framework thus allows the user to select specific features to disregard when agents observe their peers. *Inaccurate perceptions* are operationalized by applying noise to the data. We use a Gaussian distribution (i.e., 'white noise'), in line with previous works [150, 151]. By setting the parameters of the distribution, users can include common phenomena such as systematically overestimating calories [152] or systematically underestimating the weight status of overweight and obese peers [153]. For flexibility, we allow users to select the features onto which noise will be applied [150, 151]. This reflects that humans do not make the same amount of mistakes depending on what they attempt to quantify; for example, weight may be vastly underestimated but height could be accurate.

Once the three errors have been applied to the data, the table can be processed by a machine learning algorithm. The choice and parameters of the algorithm reflect the *limited ability* of the agents. For example, a decision tree with an insufficient depth would coerce agents into making simplifications. Simplifications could also be caused by certain parameter values in a penalized regression, or by having too few (or small) layers in a neural network. Our framework thus allows the user to pass an ML model of their choice and to set limits on its parameters (e.g., depth of the tree, number of layers).

3.3.3 Implementation

A *core network* is used to position the agents. Each *node* of the core network can contain a set of agents, which can be empty when no agent occupies this position. An *edge* signifies that an agent can either reach a node (if a model requires mobility) and/or observe the behaviors of agents residing in the other node. The core network is a flexible representation as it can be used to capture two common scenarios:

(a) A *physical* network (**Figure 3.3**-a). Each node serves as a physical location, which is occupied by agents. Connecting edges represent pathways an agent must travel to traverse from one location to another and a modeler can restrict the edges to only support mobility. This restriction limits an agent to only observe its peers who are in the same physical location (i.e., the same node).

(b) A *social* network (**Figure 3.3**-b). By creating a one-to-one mapping between nodes and agents, each node represents an agent and edges capture social tie. In this case, social ties may specify observable peers rather than mobility.

Although none of our case studies need it, our framework supports a *secondary network* to enable applications that require both a mobility network (where individuals see each other

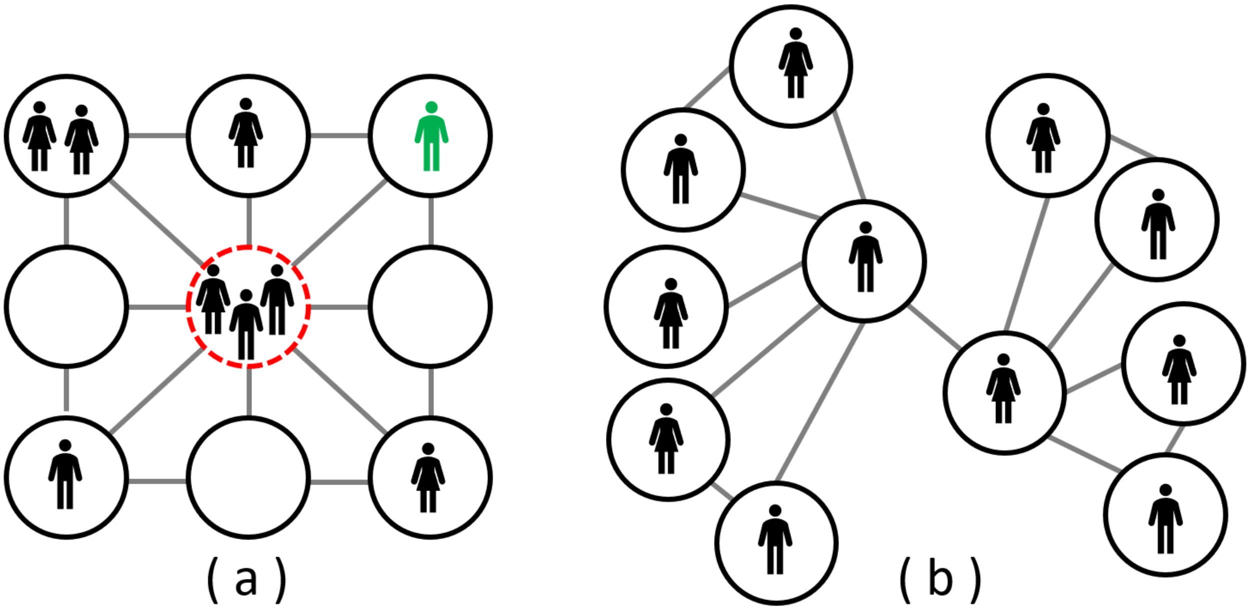

Figure 3.3: In the core network, each node can contain a (possibly empty) set of agents. When any number of agents can be in a node, it can be used to represent a physical environment (a). In (a), the central location (dashed/red) contains three agents, who can see each other. The top-right location (green agent) has a single agent, who is able to directly move into three locations. When each node contains exactly one agent, it serves as a social network (b).

if they share a physical location) and a social network (where individuals are in contact regardless of physical locations).

Our framework is built in `Python` 3.10. This choice is driven by the growth of ABM packages built on the `Python` programming language [154, 155, 156, 157], thus indicating familiarity with this language from our intended user base. Similarly to the Python `Mesa` package, our framework "seamlessly integrates with popular data science tools such as Jupyter notebooks and Pandas for ease of analysis of data" and we also use `NumPy` arrays to accelerate computations [154]. Specifically, at each simulation tick, an agent adds the new observation of its peers to a growing record in the form of a `NumPy` array. After synchronous observations have taken place, each agent independently runs a machine learning model on its array, via `scikit-learn`. Actions are then decided accordingly and the new states of the agents are computed. These states may be stored in a `Pandas` dataframe (e.g., to accumulate the number of agents who are happy/unhappy at each step) to visualize simulation results at the end. Users are expected to provide custom code to encapsulate the logic of their model, in line with recent frameworks [126].

3.4 Case Studies

We use three models to exemplify (i) which errors are applicable to a given simulation model and (ii) how they work within our framework. The models cover Schelling's model of segregation [158], the Axelrod model of culture [159], and a Covid case. In the same way as Chattoe-Brown, we used classic models because they are "widely known in the ABM community and simple enough to demonstrate relevant issues clearly without 'bogging down' in potentially divisive modeling detail" [160]; the Covid model is more complex but captures an application area that has recently brought ABMs to attention in a wider scientific community. Each model is provided on our repository as a dedicated Jupyter Notebook.

3.4.1 Schelling Model of Segregation

The *purpose* of the well-known Schelling model is to illustrate how agents in society can become highly segregated based on a seemingly mild preference towards being surrounded by similar neighbors. As the model has been covered abundantly elsewhere [161, 158, 162], our succinct description allows us to focus on the nature and inclusion of errors. In short, the core logic is that each agent belongs to one of two groups (abstracted as colors such as blue and red) and wants the fraction of at least τ nearby peers to be in the same group. The use of colors helps to visualize the emergence of segregation patterns. We implement it by structuring the environment as a 25×25 grid, where each node represents an agent location at each time step. The nodes are empty (black; 12% of nodes) or occupied with an agent (blue or red). At *initialization*, agents are assigned one of the two colors equally at random (i.e., 88% of the grid is occupied by agents who are 50% blue and 50% red) and then given an initial location on the grid. This visualization allows users to ensure the total population is segregating over time.

During an *update*, agents synchronously observe their neighbors. We use Moore's definition of a neighborhood, whereby each agent is surrounded by eight neighbors; the network topology is thus created as in **Figure 3.3**-a, where the central node (red/dashed) is connected to eight neighbors. Since we use closed boundaries, nodes on the edges and corners have fewer neighbors. For each agent, the observation consists of counting the share of its neighbors that have the same color. If that fraction is above a user-defined threshold (known as 'Preferred Proportion' and set to $\frac{1}{3}$ in our example), then the agent is seen as happy and stays in its current location. Conversely, unhappy agents will move to an empty location at the next round; we handle their relocation by creating a queue of agents who seek to move and matching them with a shuffled queue of available locations. At each step, we record the amount of happy agents. The simulation stops when this number stabilizes and agents no longer relocate or 100 steps are reached, whichever comes first.

Each agent uses a decision tree classifier, where the only feature is the number of neighbors with the same color, and the prediction is a binary outcome of (un)happiness. Since there is a single feature, this model is not eligible to a perceptual error of superficial observations. We thus focus our example on the impact of insufficient observations, limited ability, and the combination of insufficient observations and limited abilities on model trajectory. For insufficient observations, each agents' decision tree was given access to a random percentage of data observed during the simulation (set to 5%, 10%, 20%, 40%, 60%, 80%, 100%). To represent the baseline (i.e., simulation outcomes without errors), 100% percent of the data was utilized to update the agents' internal models. For limited ability, every agent's decision tree was constrained by a maximum depth (set to 1, 2, 3, 4). Note that in this application scenario, an agent does *not* need to surpass a depth of 2, so we *expect* depths of 3 and 4 to have no impact; visualizations should reveal this effect. Finally, we combined both insufficient and limited ability by limiting the decision tree depth in each simulated run at specific percentages of observation. (e.g., 5% with depths 1, 2, 3, 4). Note that since each agent runs its own ML model, the decision process is no longer the same for everyone, so the inclusion of errors contributes to addressing the issue of heterogeneity discussed in previous works [160].

3.4.2 Axelrod model of culture

The *purpose* of the Axelrod model is to reflect the dissemination of culture in a population; the model can also be interpreted as spreading opinions. Each node of the network represents a village, characterized by an array of cultural features, each of which has several possible values (known as 'traits'). These cultural features can abstract a variety of properties (e.g., index 0 can be language, index 1 stand for religion) and their numerical values represent various states of each property (e.g., language could be comprised of English, French, Chinese). Nearby villages (i.e., adjacent nodes) interact with a rate proportional to the number of shared feature values, and they become more similar as a result. Said otherwise, *homophily* governs the selection of dyadic interactions, and one agent adopts a trait value from the other agent as a result of *social influence*. In the *initialization*, we create a 2D grid (set to 8×8 in this example) and equip each node with 5 feature categories, each with 10 possible values.

During an *update*, an agent is selected at random and we measure the ratio of cultural features shared with each neighbor. To measure this ratio, each feature value must match exactly: for example, if an agent has the array [3, 5, $\underline{6}$, $\underline{7}$, 0] and a neighbor has [1, 3, $\underline{6}$, $\underline{7}$, 1] then they share two features out of five, hence a ratio of $\frac{2}{5}$. A neighbor is then selected with a probability weighted based on the ratio of shared features. The agent randomly picks from one of the features with a mismatch and aligns its value with the neighbor; in the example, the first feature would be replaced from its value of 3 (mismatch) into 1 (**Figure 3.4**). In a similar vein to the Schelling model, the Axelrod model runs until cultural regions are established, or for at most 100 steps.

Because of the numerical distance between features, each agent learns by performing a logistic regression with stochastic gradient descent. Each observation consists of the agent-neighbor pair, the time step, the absolute differences between features of the pair (e.g., in the example above we would have [2, 2, 0, 0, 1]), the ratio of shared features (40% in this example), and whether the neighbor was selected. Note that neither the pair nor the time step would be used in decision-making; they are only included in order to guarantee that observations are unique. The ML model learns whether to select a neighbor based on the

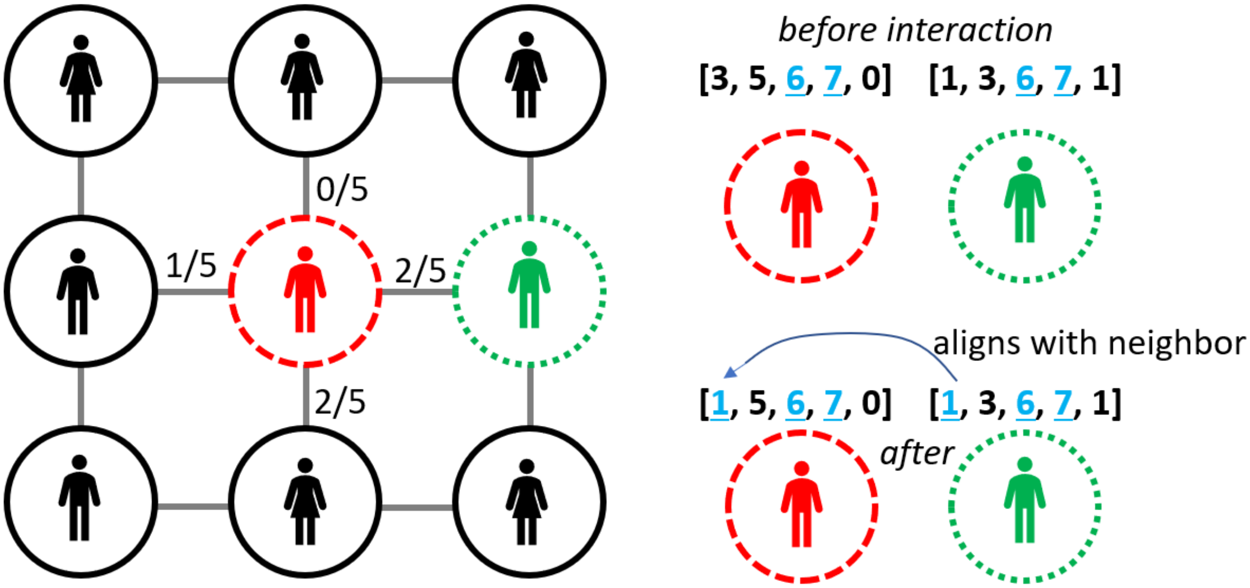

Figure 3.4: Given a randomly picked agent (long dashes / red), a neighbor is selected (short dashes / green) with a probability proportional to the ratio of shared features. One feature with a different value is selected at a random and the difference is solved.

absolute differences between features and the ratio. For instance, when agents have five characteristics, the ML model is given $5 + 1 = 6$ features. Since ML needs *some* observations to start learning, we run the first step of the simulation based on the standard Axelrod rules and then start applying the ML process.

This application allowed us to test all four errors: insufficient and superficial observations, inaccurate perception, and limited ability. Insufficient observations were produced by only allowing the machine learning model to have access to a random sample of data, in the same way as the Schelling model. For superficial observations, agents could drop 1, 2, 3, or 4 of the features at random when computing the cultural similarity. Inaccurate perception consisted of adding a Gaussian noise (5%, 10%, 20%, 40%, 80%, 100%) to the perceived values of some features in a neighbor; values were then rounded up, since they had to be integers. Limited ability was generated in the same manner as the Schelling Model where we limited the depth of the decision tree. Errors were combined by pairing each random sample of observations to a specific amount of dropped features, added percentage of noise, and various depths.

3.4.3 COVID case study

Agent-based modeling emerged as one of the main computational techniques to study the COVID-19 pandemic [163], which has resulted in an abundance of new ABMs [164]. As a result, core concepts of ABM have now reached new research communities [165], who may not have been familiarized with the Schelling or Axelrod models through traditional training. We address this audience by exemplifying errors in a COVID model whose *purpose*

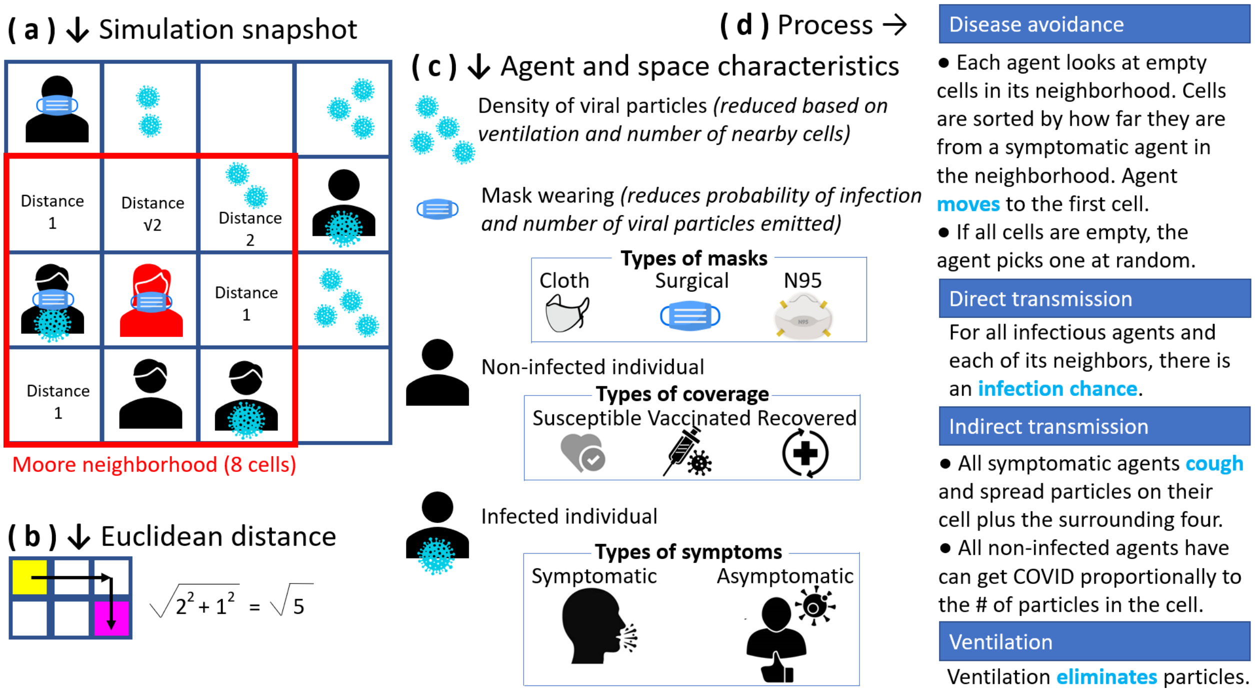

Density of viral particles *(reduced based on ventilation and number of nearby cells)*

Mask wearing *(reduces probability of infection and number of viral particles emitted)*

Disease avoidance

- Each agent looks at empty cells in its neighborhood. Cells are sorted by how far they are from a symptomatic agent in the neighborhood. Agent **moves** to the first cell.
- If all cells are empty, the agent picks one at random.

Direct transmission

For all infectious agents and each of its neighbors, there is an **infection chance**.

Indirect transmission

- All symptomatic agents **cough** and spread particles on their cell plus the surrounding four.
- All non-infected agents have can get COVID proportionally to the # of particles in the cell.

Ventilation

Ventilation **eliminates** particles.

Figure 3.5: Each agent moves in its Moore neighborhood (a) into an empty cell that offers a safe distance (b) to visibly ill peers. Agents have different masks, immune status, and symptoms (c). The process accounts for disease avoidance, direct and indirect transmissions, and ventilation (d).

is to track the spread of infections in a room. In a similar manner to previous COVID-19 ABMs dedicated to indoor transmission, the space is modeled as a large square (without walls) [166]. Agents can contaminate each other through direct contact or indirectly via aerosols, which are affected by ventilation systems [167]. Spatially explicit mechanisms for disease avoidance steer agents away from peers with symptoms [168], while individual attributes such as wearing certain types of masks or having acquired immunity mediate the level of aerosols expelled and the risk of infection [169].

In the initialization, 250 agents are randomly assigned positions in a 50 × 50 closed grid (**Figure 3.5-a**) with Moore neighborhood (**Figure 3.3-a**), as used in the Schelling model. The agents initially wear masks of different types (cloth, surgical, N95), have acquired immunity either by recovering from infection or from vaccines, and infected agents may present symptoms or not (**Figure 3.5-c**); initial percentages are listed in Table 3.4. During an *update*, each agent scans moves in a nearby empty location that puts a safe distance with any visibly ill agent. Specifically, available cells are sorted by their Euclidean distance (**Figure 3.5-b**) to the nearest symptomatic agent in the neighborhood. Note that it allows an agent to move (unknowingly) next to a person who is infected but asymptomatic, or into a location with a high density of aerosols. The process continues (**Figure 3.5-d**) with direct transmission of infection, then indirect transmission as infected agents cough (thus dispersing droplets in nearby cells depending on their masks) and susceptible agents have

Description of the variable	**Default value**	**Source**
Size of the grid	2500	User-defined
N (Number of agents)	250	User-defined
Fraction of initial agents with immunity	0.62	[170]
Vaccine compliance (fully vaccinated)	0.67	[171]
Fraction of initial agents with infection	0.5	User-defined
Strength of ventilation in the closed area	0.8	[172]
Chance of infecting of other agents	0.04	[173]
Chance of coughing	0.05	User-defined
Infection chance for immune agents	0.3	[174]
Chance of being asymptomatic	0.6	[175]
Reduction factor for cloth mask	0.2	[176]
Reduction factor for surgical mask	0.1	[177]
Reduction factor for N95 mask	0.09	[177]
Distribution of cloth masks	0.2	User-defined
Distribution of surgical masks	0.4	User-defined
Distribution of N95 masks	0.4	User-defined
Number of prerun steps	5	User-defined

Table 3.4: Variables used in the COVID-19 model

a risk proportional to the density of aerosols; in both cases, transmission risk is impacted immune status and mask wearing. Finally, the full outdoor air supply rates provided by optimal ventilation systems remove aerosols containing viral particles. Each simulation ticks represents one minute, and the simulation stops after two hours.

The decision tree of each agent governs its steering behavior. That is, each agent decides whether to move into a particular cell based on the perceived distance to an infectious agent. In order to store unique observations in the agent's array, we also record the agent's ID and the simulation step, but this information is not used for decision making. Three errors can be present: insufficient samples, inaccurate perceptions, and limited ability; they are handled in the same manner as in the previous two models. In the same way as the Axelrod model, the model runs initially with the baseline ruleset (for five steps) so that agents have made observations, then they start differentiating via ML.

3.5 Results

By definition of the *Schelling model*, when agents only look at *some* of their neighbors, the condition of 'moving only if neighbors are too dissimilar' is no longer applied exactly. This is akin to introducing uncertainty in the decision to move, as has been studied by Sahasranaman and Jensen, who found that it affects dynamics by making it harder to produce segregated clusters [178]. **Figure 3.6** confirms this effect, as the amount of time to stabilize is inversely proportional to the percentage of samples. To understand the effect of limited abilities, we measured the depth of the decision tree in the baseline simulation, where it was 0.95 ± 0.25 over 50 simulation runs. Hence we expected a difference between limiting the depth of the tree to 1 and 2, but no effect beyond this. The heatmap in **Figure 3.7** shows the joint consequence of limited abilities and insufficient samples: there is mostly a gradient along the x-axis (percentage of samples) and very little effect along the y-axis (limited abilities), which confirms that outcomes are primarily affected by insufficient samples rather than by limited abilities.

In the *Axelrod model*, the concept of noise has often been studied but it was operationalized in diverse ways. Several studies of the Axelrod model [179, 180] and related opinion spread models [181] consider noise as the probability that an agent spontaneously changes its own values (known as 'cultural drift'), which is different from the notion of noise in observing a neighbor's values. When models include noise in the interactions (e.g., destroying and recreating links, hesitating), they often find that a homogeneous state is reached after a much longer time than in the initial Axelrod model [182, 183], and it may even become impossible to stabilize [184]. Our results on insufficient samples confirm these previous findings, as the number of changes before stabilization is inversely proportional to the sampling rate (**Figure 3.8c–d**). The model is visibly robust to small inaccuracies in measurement (**Figure 3.8e**), but deviations are observed from an error of 40% and onward (**Figure 3.8f**). Superficial observations have a noticeable impact (**Figure 3.8b**).

The impact of errors on a *COVID model* is more mixed in the nascent literature. For example, meta-modeling studies have shown that in *some* cases, a small sample of observations from an entire simulation sufficed to characterize it, but in other cases a much higher sampling rate was necessary [91]. While other studies have examined errors in several models, they were concerned with *software* errors (i.e., bugs), which are not our focus [185]. Given the lack of referential, our observations are based solely on results in **Figure 3.9**. Of all three models, the COVID case is the only one where trends are preserved regardless of the nature or intensity of the errors. This suggests that, despite its relative sophistication in several aspects (e.g., various masks, direct and indirect transmissions), the decision-making component for each agent is ultimately so rudimentary that it is hardly swayed by errors. Results may be different if the mobility of agents was more extensively data-driven [186].

3.6 Discussion

As people, we only pay attention to some of our surroundings and make mistakes when we record this information [101, 102]. These errors are profoundly human traits, hence cognitive social simulations may be more adequate when they account for such perceptual errors. However, ABMs do not systematically account for these errors [17]. In this paper, we used Machine Learning as a conduit to systematically represent four types of errors for social learning in ABMs (i.e., how agents learn from information acquired via social ties): insufficient number of observations, superficial observations that ignore certain features, mistakes in recording the observations, and a limited ability to process complex information

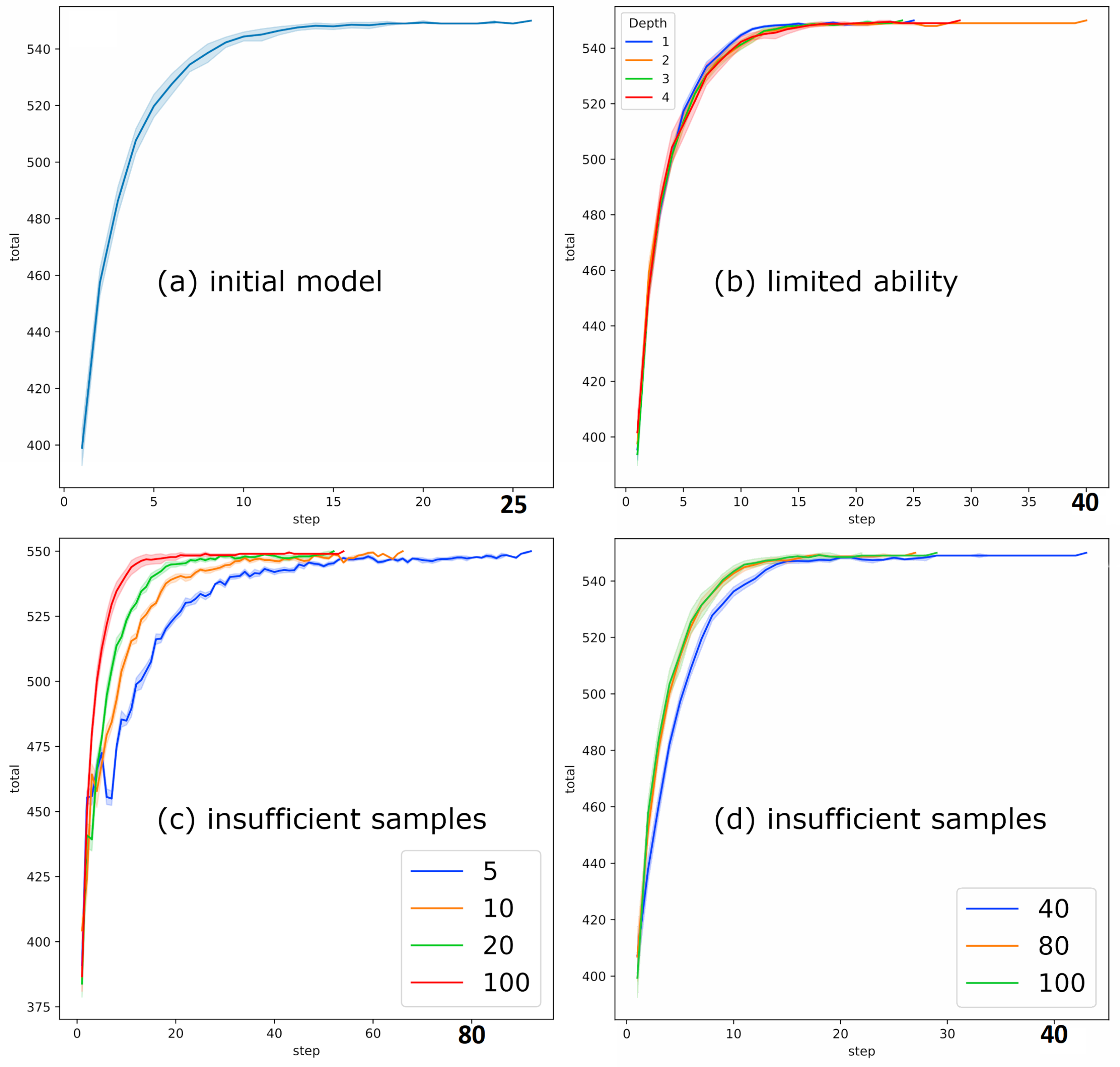

Figure 3.6: baseline (a); limited abilities as constrained by the depth of the decision tree(b); observations using all (100%) or part (5, 10, 20%) of the data (c); and observations using all or part (40, 80, 100%) of the data(d).

from the world. The errors were exemplified on three ABMs, thus showing which errors are applicable to a given model and which consequences we may expect. Although our focus is on the perceptual errors of individual agents, we have repeatedly emphasized that such individual errors do not necessarily lead to erroneous simulation results for the population. Indeed, at the level of the collective, perceptual errors may lead to more diversity in decision-making, ultimately contributing to a population that is more adaptable; this hypothesis has been confirmed on several occasions, such as in biological and socio-ecological systems [187].

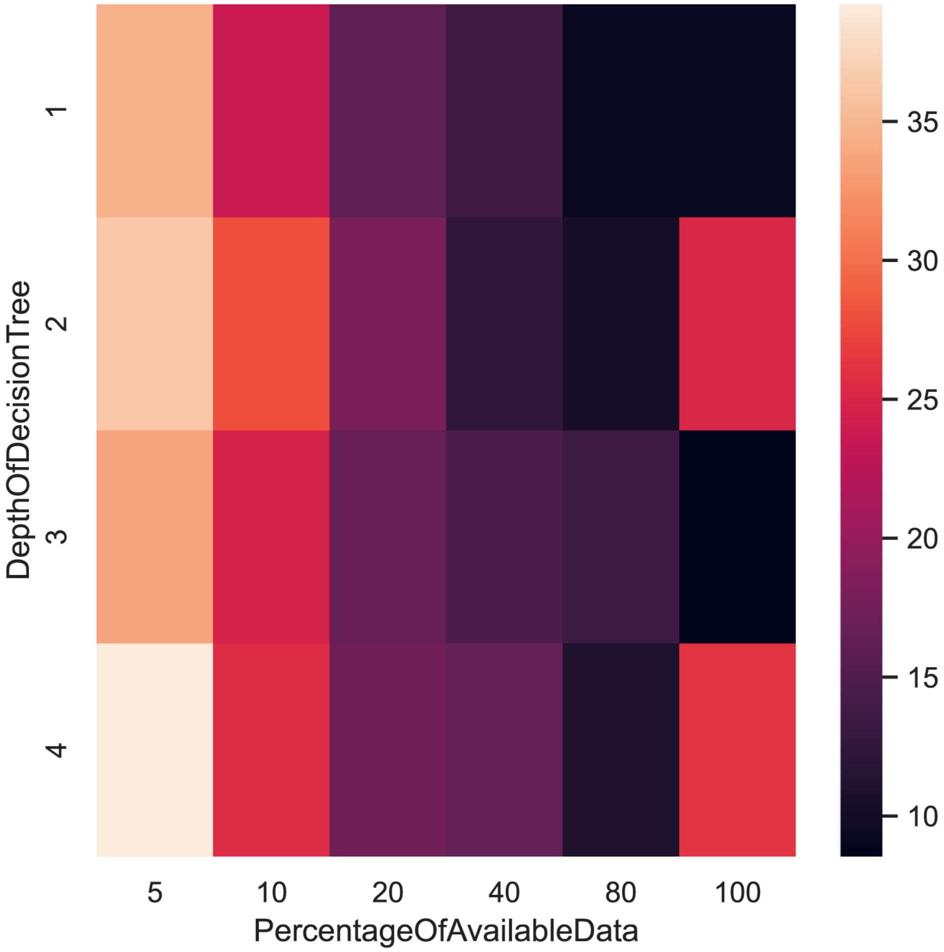

Figure 3.7: Heatmap of the average number of steps for 10 runs on different percentages of data available (insufficient samples) and different depths of tree (limited ability) for the Schelling model. The number of steps displayed is the steps required to reach the end of the simulation.

From a computational standpoint, users of our open source framework would need to write all model-specific code in Python. While this language is now well-understood in the ABM community as evidenced by a growing set of libraries, there are software solutions to avoid being language-specific. For instance, Bhattacharya and colleagues used Apache Arrow so that users could write the decision making module in any language and link it with the framework [126]. Most interestingly for simulationists, extensions of the the framework may be used to pinpoint *where* an agent made errors, if modelers wish to investigate why some agents erred. For example, we could record when an agent took the 'wrong branch' in a decision tree, enabling the model to later flag where the error occurred.

The variety of errors that could be represented in human perceptions is almost boundless, hence our framework does not claim to be all-encompassing. For instance, real-world individuals may not be relocating as frequently as agents in the Schelling model, and cognition

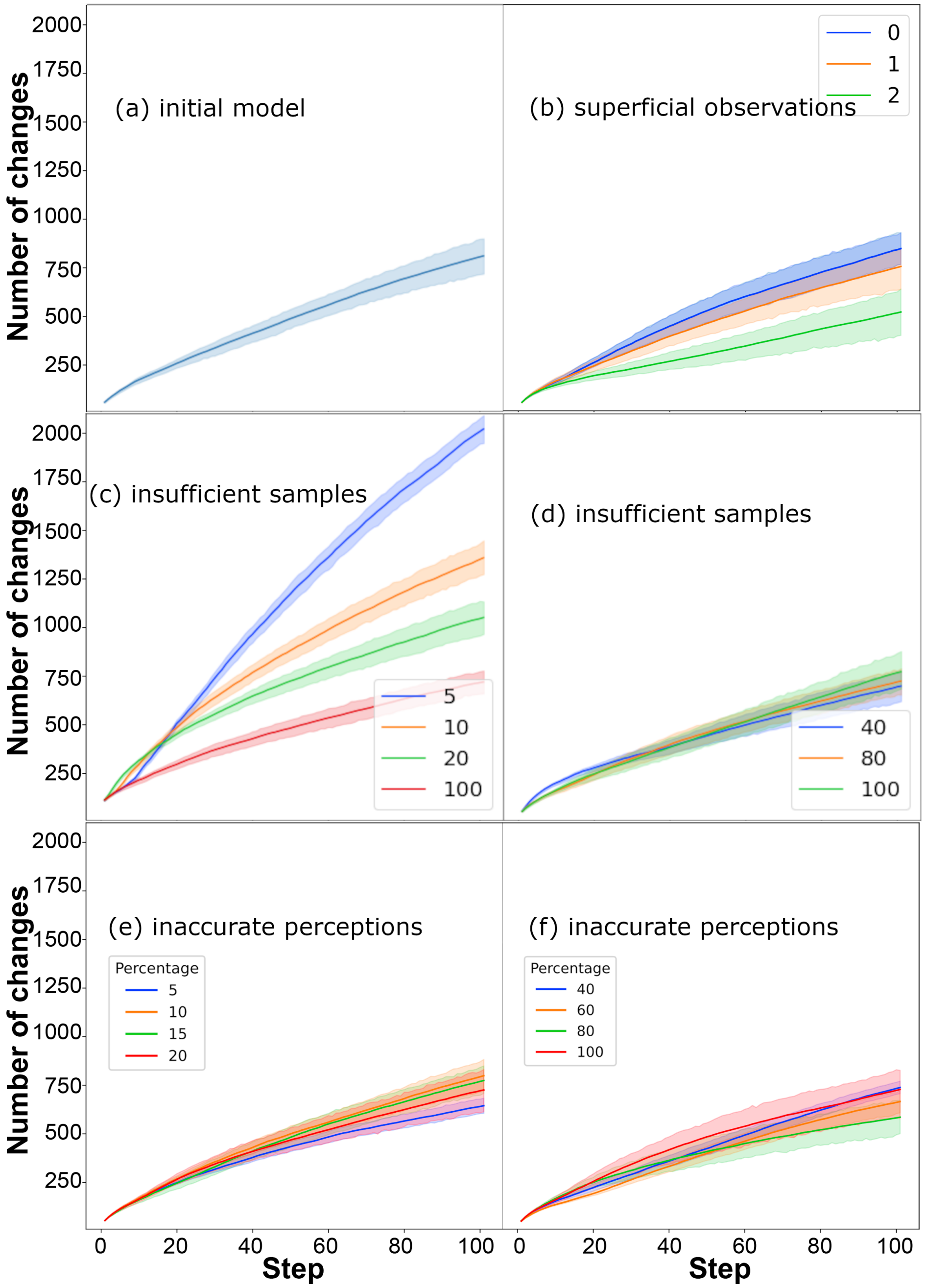

Figure 3.8: Impact of various errors on the number of changes achieved to stabilize the Axelrod model. Note that superficial observations (b) report the number of features *ignored*, hence zero is equivalent to baseline (no feature ignored).

may be affected by other attributes such as age. Future work can reuse and extend our framework based to account for specific cognitive theories, for example in the representation of emotions. When it comes to the transmission of information, two broad mechanisms are

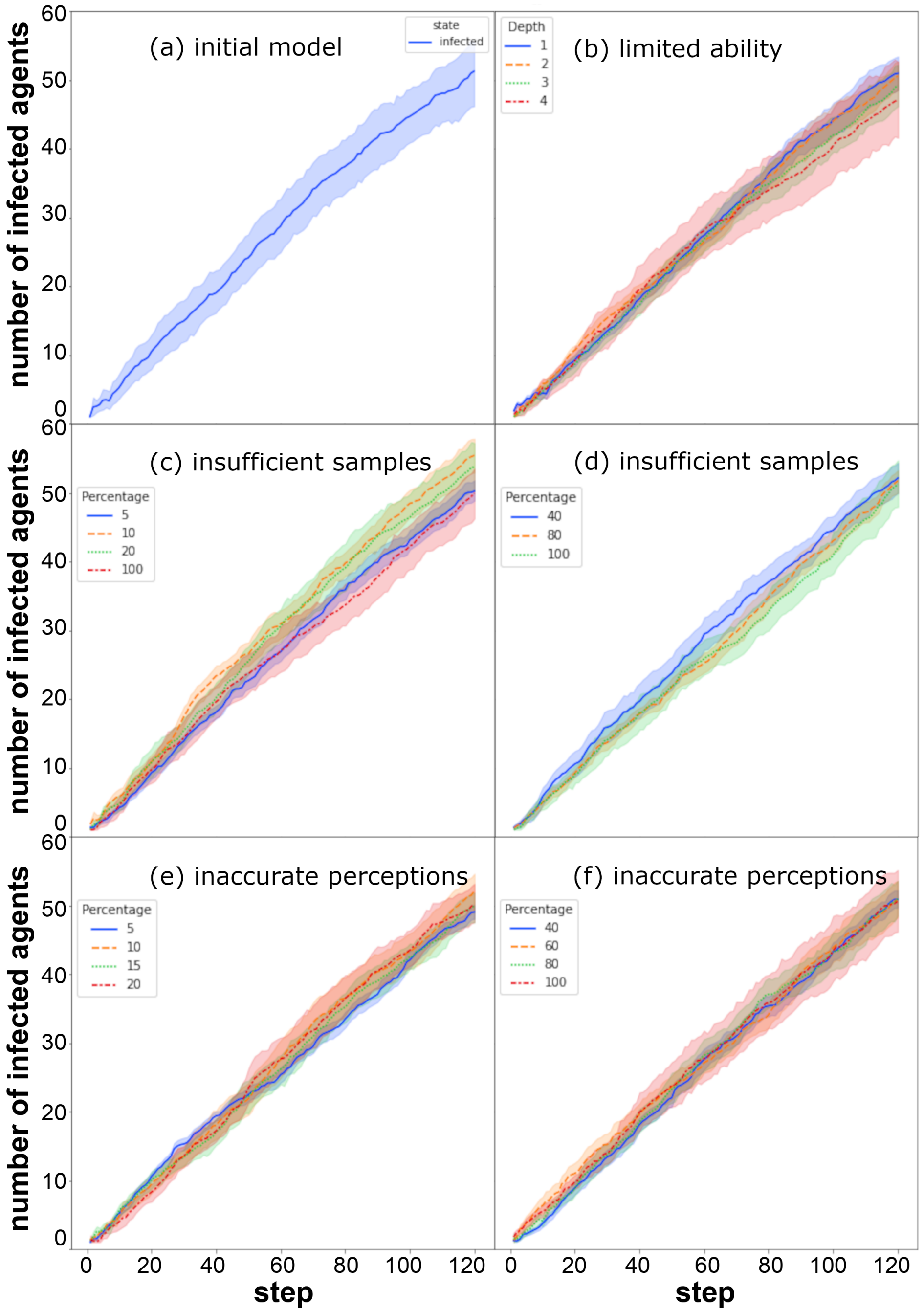

Figure 3.9: Behavior of the COVID model at baseline (a), under limited abilities as constrained by the depth of the decision tree (c), by using a few (c) or most (d) of the observations (including the baseline of 100%), with (e) small or (f) large inaccuracies in perception.

involved and can be detailed: *cognitive biases* and *status asymmetries* [188]. Indeed, one of the reasons for which we do not pay attention to all peers or all of their attributes is because social learning is *selective*. As explained through the notion of 'selective filters' and the handling of conflicts (e.g., via balance theory), this selection depends in part on what an individual deems compatible with existing knowledge [189]. The inclusion of cognitive biases in our framework would require extending how the cognition of an agent is represented. Status asymmetries explains why individuals do not pay equal attention to all of their peers; that is, the likeliness that some peers make an impact is not uniform, unlike in the current framework. Social ties are different in nature and frequency, as some peers may be close friends who are often seen, some may be acquaintances with whom we seldom interact, and we may even include celebrities whose interactions may be rare and distant yet impact decision-making [190]. However, accurately capturing the structure and function of social ties is a research domain in itself, which goes beyond our framework.

3.7 Conclusion

To enhance the realism of a cognitive social simulation, modelers may account for imperfections in individual decision-making processes. Our framework combines four types of errors and allows to analyze the change in model trajectory once 'perfect' agents become more error-prone, like their real-world counterparts. By illustrating the practicality of data-driven ABMs and the importance of including human errors in practice, our study seeks to motivate researchers to further the development of more realistic models and expand upon the framework we created.

Chapter 4

Reviewing three dimensions of COVID-19 vaccination models

The virus that causes COVID-19 changes over time, occasionally leading to Variants of Interest (VOIs) and Variants of Concern (VOCs) that can behave differently with respect to detection kits, treatments, or vaccines. As previous vaccines become less effective, new ones will be released to target specific variants and the whole process of vaccinating the population will restart. While previous models have detailed logistical aspects and disease progression, there are three additional key elements to model COVID-19 vaccination coverage in the long term. First, the willingness of the population to participate in regular vaccination campaigns is essential for long-term effective COVID-19 vaccination coverage. Previous research has shown that several categories of variables drive vaccination status: sociodemographic, health-related, psychological, and information-related constructs. However, the inclusion of these categories in future models raise questions about the identification of specific factors (e.g., which sociodemographic aspects?) and their operationalization (e.g., how to initialize agents with a plausible combination of factors?). While previous models separately accounted for natural- and vaccine-induced immunity, the reality is that a significant fraction of individuals will be both vaccinated and infected over the coming years. Modeling the decay in immunity with respect to new VOCs will thus need to account for hybrid immunity. Finally, models rarely assume that individuals make mistakes, even though this over-reliance on perfectly rational individuals can miss essential dynamics. Using the U.S. as a guiding example, our scoping review summarizes these aspects (vaccinal choice, immunity, and errors) through ten recommendations to support the modeling community in developing long-term COVID-19 vaccination models.

All of this chapter was published in the following article:
Beerman, J. T., Beaumont, G. G., & Giabbanelli, P. J. (2022). A Scoping Review of Three Dimensions for Long-Term COVID-19 Vaccination Models: Hybrid Immunity, Individual Drivers of Vaccinal Choice, and Human Errors. *Vaccines*, 10(10), 1716.

4.1 Introduction

Most Americans have come to agree that “we will never be rid of COVID-19 in our lifetime” [191]. Although vaccines and the ongoing development of antiviral drugs are great achievements [192, 193], COVID-19 has continued to wreak havoc in several ways. During the first half of 2022, more than 170,000 individuals died from COVID-19 in the U.S., amounting to over a million deaths since the emergence of the virus [194]. In addition, COVID-19 continues to exert a significant toll on the economy through disruptions in the workforce. As COVID-19 has exacerbated existing systemic challenges, the temporary matter of sickness-related absences in the early days of COVID-19 [195] is now amplified by broader issues manifested through waves of resignation. For example, many nurses or teachers are leaving the profession‘[196, 197], with departures being even more pronounced in places that already experienced staffing shortages before COVID-19 [197]. This phenomenon, ”The Great Resignation”, is not limited to healthcare or academia, and is the theme of dozens of articles that document labor shortage across occupations [198, 199, 200]. As a result, several efforts are underway to transition to a post-pandemic future, such as shifting work arrangements with a growing part of remote work [201].

Despite our logistical preparedness, there are reasons to be concerned when we ac-count for two phenomena. First, and most importantly, the effectiveness of our vaccines is decreasing against new strains, which leads to (re)infections. Indeed, many Americans have already had COVID-19 multiple times [191] and the spread of immune-evasive sub-variants is fueling the growth of reinfections. For instance, California went from 1 in 20 reinfections cases at the beginning of 2022 to 1 in 7 by July [202]. Currently available COVID-19 vaccines were developed for a prototype strain, but variants such as Omicron have more than 30 mutations in the spike protein of the prototype strain, which is essential for infection as it initiates the host cell entry [203]. Consequently, “available FDA-approved and -authorized COVID-19 vaccines are less effective against currently circulating virus variants than against previously circulating strains of virus”. [204] This effect is demonstrated since most infections in the U.S. as of June 2022 are attributed to two Omicron sublineages (BA.4 and BA.5) [204]. Second, the problem is compounded by our shifting responses and attitudes to the pandemic. A survey in June 2022 reported that half of U.S. adults wear a face mask “when away from home, the lowest since the start of the pandemic” [205]. Another survey showed that the proportion of people bothered when others do not mask in public fell to an all-time low, at 18% among Republicans and 52% among Democrats [206]. On the one hand, we see a diminishing use of face masks, lower vaccine effectiveness, and a lower intended receipt of COVID boosters [207]. On the other hand, we likely need annual vaccine composition updates [208]. Surveys in Jordan shows that less than 1 in 5 persons would take an annual booster [209], while about 2 in 3 Canadians [210] and more than 4 in 5 German-speaking adults would be willing [211]. Results in the U.S. are mixed, as surveys were conducted across sub-populations with different pro-files [212].

The Modeling & Simulation (M&S) approach of Agent-Based Modeling (ABM) has been used to model COVID-19 since the second half of 2020, because of the approach’s ability to track individual agents who can have different attributes, different decision-making processes, and be exposed to different environments [213]. This ability to implement heterogeneity is indeed essential for COVID-19 since it is found in individual risk factors (e.g., age, hypertension, diabetes), contact patterns (e.g., social networks in the community or work settings), behaviors (e.g., willingness to be vaccinated), and spatial aspects (e.g., access to healthcare) [214, 215, 216]. Although ABMs for COVID-19 have been extremely varied in purpose and design [164], their design broadly followed three stages in the pandemic [165]: ABMs started with a handful of stages (e.g., susceptible, exposed, infected, recovered) and examined which non-pharmaceutical interventions would have the strongest effect [217, 218, 219], then ABMs were created to support vaccine-related studies (e.g., who should be vaccinated, where to place the centers and how to staff them) [220, 169, 221]and lastly, the current wave of studies where repeated boosters account for waning immunity [222, 223].

Truszkowska and colleagues provided one of the first models in which immunity was totally and gradually lost over the course of six months [222]. This approach included vaccine hesitancy, which was captured by assuming that only a percentage of the population would get vaccinated [222]. More recently, Kelly et al. proposed a comprehensive model that accounts for the waning vaccine induced immunity and naturally acquired immunity, as well as seasonal patterns in infection, and the emergence of annual or biannual variants [223]. Again, vaccine hesitancy was modeled population-wide by assuming either a high booster intake (85% to 98%) of individuals 50 years of age or higher with comorbidities, or modeled with a reduced intake of 50%. These models concluded that a high ad-herence to frequent booster doses is necessary to avoid future outbreaks and prevent a burden on the healthcare system – a conclusion shared by studies using differential equations [224, 225]. Since adherence to frequent boosters is the key but it was only modeled by assuming a percentage across wide sub-populations, it is important for future ABMs to address this research gap by detailing how individuals decide to get vaccinated as a function of sociodemographic, health, psychological, and information-related variables.

Several open-source COVID-19 ABMs can be reused and extended by the research community, including COVASIM [226], OpenABM-Covid19 [227], and COMOKIT [228]. These packages and other individual-based epidemiology simulation kits [229, 230] allow us to create a virtual population that reflects several demographic indicators (e.g., age, sex) and their impact on disease spread (e.g., age-linked disease progression and mortality). Packages such as COVASIM also embed each individual in several networks (home, community, work, school) based on age (e.g., children go to school, adults to work). Through revisions, the current version (3.1.2 from January 16th 2022) also captures “co-circulating variants, imperfect immune memory, and multiple vaccines” [231], tracks the properties of variants (relative transmissibility compared to wild type, relative severity, relative immunity, variant-specific protection of vaccines), and allows users to add custom variants. The popularity and reuse of such packages is demonstrated by their applications to multiple settings such as Australia [232, 233, 234], the UK and/or US [235, 236, 237], Vietnam [238], or Italy [239], at both the country- and city-scale [240]. Our scoping review thus emphasizes elements that are commonly missing across these packages in order to have a broad representation of the current technical capabilities in the field.

The main contribution of our scoping review is to support the development of the next generation of ABMs by examining three aspects: vaccine hesitancy, joint occurrence of natural- and vaccine-induced immunity, and the inclusion of human errors in decision-making. Specifically, we synthesize the current evidence base and identify research gaps, leading to 10 recommendations on aspects to include in future models, alongside their operationalization. The recommendations are featured prominently (as R1, R2, etc.) throughout the sections.

The review is organized as follows. Section 2 starts with the concept of immunity and its representation in models. Then, section 3 summarizes the evidence base regarding strong drivers of vaccinal choice. We cover the last dimension in section 4 by explaining how individuals are not perfect and can engage in several types of errors during their decision-making processes. The last two aspects have received less attention in modeling packages, hence these two sections include detailed suggestions for inclusion in future models. Finally, section 4 discusses a list of limitations inherent to the modeling process and limited current knowledge of variants and individual choices.

4.2 Immunity: variants, waning effect, and hybrid cases

Early models of COVID-19 that included vaccines were developed to help plan ahead. For instance, models would determine the most effective locations to setup vaccination centers or prioritize certain sub-populations that should be first administered vaccinations. In the simulated time spans of these models, it was adequate to consider that individuals would have a constant level of immunity once recovered or vaccinated, and that the dominant strain at the time was the only one. As we transition into a more long-term perspective, we need to account for changes in the level of immunity, including the cumulative effect of vaccination and recovery (particularly since most Americans have had COVID-19 [91]), as well as the ongoing emergence of variants. As shown in **Table 4.1**, recent models have handled immunity differently. Most models use a gradual decay, with arguments in favor of a Gamma distribution rather than an exponential one (to reflect that the initial immunity remains at a high level for several weeks instead of declining immediately). This is represented either by the direct use of a fitted Gamma distribution, or by the 'linear chain trick' which consists of use a sequence of exponentially-distributed decays (e.g., agents go through stages V1, $\cdots$, V5 back-to-back).

The models either did not account for the synergistic effect of natural infections together with vaccinations, or created a dedicated stage without specifying the corresponding transitions. For example, a model considered that a vaccinated person who became infected lost the vaccine-induced immunity and only gained natural immunity upon recovery, hence making the two forms of immunity mutually exclusive [242]. However, the hybrid case resulting from natural infection and vaccination confers the most robust and durable immunity [246, 247, 248]. Studies on immunology on different variants and various countries have found that hybrid immunity was protective against reinfection and severe disease outcomes [249, 250, 251, 252]. As summarized by Bates and colleagues, "the additional antigen

Handling of Immunity				
Ref	**Variants**	**Natural**	**Vaccine**	**Hybrid**
[222]	Delta Variant Only	Lasts 180 days	Impact on 5 parameters (e.g., death, infection, hospitalization, transmission, asymptomatic) defined via piecewise linear functions. Peak reached 2 weeks after one shot, remains constant for 8 months, then linear decay for 6 months. The level of immunity for each linear segment depended on the vaccine used. Booster restores peak vaccination benefits in 1 day.	Exists but unspecified
[223]	Emerge ahead of the winter, every 6 or 12 months	Initial peak at 95% exponential decay to 20% in 600 days	Initial peak at 85% exponential decay to 15%, half-life 105 days. Higher peak after a booster, but same decay.	None
[241]	Randomly appear 4/6/10 months after past variant	2-part exponential decay, with half-life and duration parameters fit to data. Neutralization level depends on variant and vaccine.		None
[242]	Omicron variant only	Gamma distribution set either to 9 months (shape 7 and scale 39.11) or one year (shape 3.7 and 98.65)		None
[243]	Omicron variant only	Protection against same variant has exponential duration of mean 1/900, then no protection.	After an average of 6 months since the second dose or a booster, individuals transition into a ’waned vaccine effectiveness’ status.	Exists but unspecified
[244]	Unspecified (2021 data)	Delayed gamma-distributed temporary immunity with mean 350 (for vaccines) and 242 days (for recovery).		None
[245]	Delta variant only	Full immunity for entire duration of simulation (March 2020- Nov 2021).	10% of individuals do not lose immunity, 10% have little protection, the remaining 80% get temporary protection by moving through a series of compartments instead of a single one (which would cause an exponential decay) hence using a Gamma distribution with peak efficacy of 92% and decay to 35% over 6 months	None

Table 4.1: Handling of variants and (temporary) immunity in recent COVID-19 models.

exposure from natural infection substantially boosts the quantity, quality, and breadth of humoral immune response regardless of whether it occurs before or after vaccination” [253]. Newer models are starting to include this effect, for example by assuming that a prior infection counts as a single vaccination, hence the ‘actual’ vaccination has the effect of a booster [254]. A recent retrospective cohort study in Sweden [255] confirmed several of the numbers in the OpenCOVID model and sheds light on the effect of the synergistic effect of hybrid immunity. The study showed that natural immunity conferred a 95% lower risk of infection and 87% lower risk of hospitalization for up to 620 days, which closely aligns with OpenCOVID. The study further established that hybrid immunity provided an additional 58% (for one dose) or 66% (for two doses) reduction in infection compared to natural immunity, and lasted up to 9 months with mixed findings on attenuation. Although numerous knowledge gaps remain [256], findings are starting to emerge regarding mediating factors in the immune response created by receiving a vaccine after a natural infection. In particular, a study using the U.S. Military Health System further suggested that the timing between a prior infection and vaccination was highly predictive of immune response, while prior disease severity did not play a role [248]. The prevalence of hybrid immunity is rising quickly; a cross-sectional study of blood donors in the U.S. found an increase from 0.7% of blood samples with hybrid immunity in January 2021 to 18.9% by December [257]. A review by Bhiman and Moore listed several scenarios as potential consequences of this ongoing increase in the hybrid immune population [258]; the inclusion of such scenarios in future computational models may improve our ability at forecasting population-wide trends. Few models examined the continuous emergence of new variants. For example, in the OpenCOVID model [223], each new variant retained the same severity and was assumed to be 25% more infective as well as 25% more able to evade immunity than its predecessor. Another model considered that new variants would be 3.5-fold as virulent compared to the wild-type [244]. Although models assumed a regular emergence of new variants, illustrative examples [259] explain that the emergence depends on the number of circulating cases (I) and susceptible individuals (S) as well as the rate of infection (β) and the chance of each infection to create an escape variant by mutation (μ). Thus, the time until the first escape mutation appears is approximated as an exponential of mean

$$\frac{1}{SI\beta\mu} \tag{4.1}$$

Based on sensitivity analyses on the models, scholars determined that the primary effect of vaccines was to block infections (80%) and secondarily of avoiding severe disease outcomes (the remaining 5%) [223]. Simulation results from COVASIM [244] on vaccine design further suggest that, going forward, creating a broadly neutralizing vaccine would be more beneficial (40% reduction in death) than a more durable vaccine (10% reduction in death). However, the effect would be highly reliant on releasing the vaccine at the right time, hence the preferred solution would be a vaccine that is both durable and broadly neutralizing (65% reduction). Given the evidence base, we recommend that future models include:

- **(R1)** a gradual decay in immunity by using a Gamma distribution, for instance through the creation of intermediate states (i.e., the 'linear chain trick').
- **(R2)** hybrid immunity, which confers the most robust and durable immunity; this may be approximated by counting a prior infection as having the effect of a booster dose.
- **(R3)** the ongoing emergence of new variants that partially evade immunity, with a timing depending on circulating cases rather than at fixed time intervals.

4.3 Vaccinal Choice

4.3.1 Drivers of Vaccinal Choice

Numerous studies have been conducted to identify socio-demographic factors related to an increased or decreased willingness to take vaccines. Using the U.S. population as a guiding example, sample studies relevant to this context are listed in **Table 4.2**. Note that models of COVID-19 have not yet accounted for the many drivers of individual vaccination choices, instead opting to either use a population-wide percentage of vaccinated individuals [222] or account for age [169, 239]. This occurred even in highly configurable frameworks where agents execute detailed plans based on their health, demographic, and organizational roles [260]. Two models accounted for the level of caution (rising with case numbers), sense of safety (rising with vaccination), or perceived vaccination risk, but at the population-level rather than via individuals [261, 262]. Given **Table 4.2**, we recommend that future models include:

- **(R4** multiple soci-demographic factors (e.g., age, sex, race and ethnicity, annual income, college degree, key comorbidities, political party) that were found to strongly

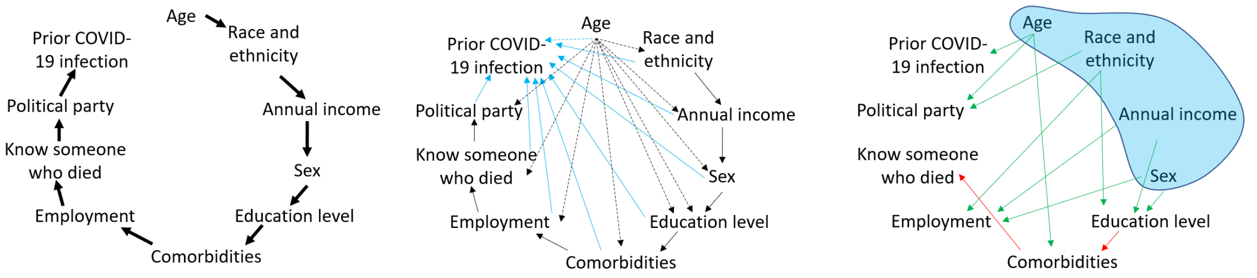

(a) *Simple* initialization scheme, 'one at a time'. Each dependency has the form p(X|Y).

(b) *Complete* initialization scheme. Each variable depends on all previous variables, using dependencies of the form p $(X_n|X_{n-1}X_{n-2}...X_1)$. For readability, we only show outgoing dependencies for age (dashes) and incoming dependencies for prior infection (blue).

(c) *Sequential* initialization scheme. A core subset of variables is initialized jointly (blue). Another subset is initialized based on them (green). The rest is then initialized (red), in a third 'wave'.

Figure 4.1: A simple initialization scheme (a) would ignore several important dependencies in the data, but capturing a large number of dependencies (b) may be infeasible given data limitations. A practical approach is thus to initialize the agents' attributes in consecutive waves (c).

predict vaccinal choices.

4.3.2 Capturing Drivers in a Model: The Role of Data and Sequential Agent Initialization

When agents possess multiple traits, the values may not be initialized independently, one at a time (**Figure 4.1-1a**). Indeed, values can be correlated: for instance, comorbidities tend to raise with age. Multiple correlations can exist, as is the case with the dependency of annual income both on employment and on educational attainments. Considering that every factor may depend on all other factors would be infeasible, as it leads to circular dependencies. Even a scheme where each factor depends on all those previously initialized can be practically infeasible since it would be arduous to find a nationally representative dataset that covers all factors (**Figure 4.1-1b**). Consequently, an initialization scheme will have to retain some of the dependencies based on the data available [269] (**Figure 4.1-1c**). In this subsection, we illustrate how these considerations can be addressed by using U.S. data.

Consider that we aim to create a virtual population of agents with multiple target socio-demographic factors. To start, we identify a data source that contains as many as possible of the important attributes together. In our case, the US Census Current Population Survey (CPS) 2019 [270] can serve to create a pool of agents who are jointly assigned an age, income, race and ethnicity, and sex. That is, all four attributes can be assigned simultaneously, thus capturing their interdependencies in the population. Then, additional data sources will need to be found to cover the remaining aspects. Note that these sources need to also include some of the previously initialized attributes, otherwise dependencies cannot be adequately reflected. For example, if a dataset contains the prevalence of prior COVID-19 infection based only on data per county, then there would be no way to link the data to individuals characterized by age, race and ethnicity, annual income, or sex. In the case of the U.S., several data sources can be used as shown in **Table 4.3**. Finally, there can be a gap between the factors used in studies on social determinants of health and the content of national surveillance systems. For example, studies reported that comorbidities were a strong determinant of vaccinal choice (**Table 4.2**), but different surveillance systems may track different types of specific comorbidities, hence there will be a need to translate a high-level concept into specific conditions and work across additional sources. A pitfall for modelers is to misunderstand the notion of comorbidities. Since comorbidities refer to other diseases present in a patient, death reporting systems may show pneumonia as a prevalent comorbidity, hence modelers could (erroneously) use pneumonia as an agent's attribute for comorbidity. However, pneumonia is a complication of COVID-19, rather than an underlying medical condition that increases the risk profile of a person if they get infected. It is thus important to carefully translate high-level constructs into specific ones given the context. In this example, comorbidities as risk factors may include hypertension and diabetes since they are commonly found in patients hospitalized with COVID-19 worldwide [271, 272], while noting that the evidence-base is weaker for hypertension once we control for other risk factors such as age [273]. Dependencies matter across comorbidities as well, since diabetic agents have an elevated risk for hypertension; **Table 4.3** thus initializes diabetes and then hypertension. In sum, a satisfactory initialization of several attributes in the agents will require:

- (R5) the identification of several data sources that share factors to allow data linkages.
- (R6) an initialization scheme that satisfies multiple core dependencies between factors by initializing them in a specific batch order.
- (R7) a careful contextual translation from high-level constructs onto specific variables offered in different surveillance systems and reports.

Note that a model is necessarily a simplification and data availability may govern some of these simplifications. For example, a modeling team may not have access to data for some of the strong drivers of vaccinal choice (**Table 4.2**), hence agents may not possess the corresponding attributes. For instance, sociodemographic information may not include occupations, hence a model may lack the notion that certain professions are at higher risk (e.g., medical professionals) or face specific obligations (e.g., annual vaccine).

4.3.3 Extending an Existing Package: Example in COVASIM

Although COVID-19 modeling packages are often open source, it may not be desirable to alter their initialization of agents by changing the code to add several factors and dependencies. Indeed, editing the source code of a package (known as 'forking') results in creating a new local version for a modeling team, which complicates the possibility of benefiting from updates in future package releases. Consequently, we recommend:

- (R8) to build on top of existing modeling packages whenever possible, so that future releases (e.g., an optimized COVASIM) can be conveniently used by the team

Expanding the characteristics of agents without altering a package's initialization process can be achieved by matching, illustrated in **Figure 4.2** for COVASIM. First, the modeling package would follow its normal procedure to initialize a set S of agents of the desired size. In parallel, modelers would create a larger pool P of agents with their required characteristics and dependencies (Section 3.2). Second, we augment the characteristics of each agent in S by finding a similar agent (i.e., a 'match') in P. This requires efficient data structures, as poor implementations could significantly slow down the process of agent creation. For example, an inefficient approach for an agent in S would be to scan the entire population P, each time computing the distance with an agent in P, then finally selecting the most similar one. Once a match in P has been found, it must be removed, which should also be done carefully to avoid triggering massive data movements. Research in discrete simulations has often used hierarchical data structures (e.g., two or three tiers) to optimize operations [282]. In this case, we need a structure that allows fast lookups to identify a match, hence the attributes offered by the package (e.g., age, sex) can be used as keys in a dictionary (**Figure 4.2**). We also need a structure that supports quick removals of an individual to move on to the next one, hence a queue.

4.4 Human Errors in Decision-Making

4.4.1 Limitations of Observations and Reflections

There is a broad tendency to create ABMs with highly rational agents [96], which is even more the case in COVID-19 research as models are often grounded in compartmental techniques designed for epidemiology. However, humans are neither mechanical objects nor omniscient, hence individuals neither form homogeneous responses to vaccines (e.g., with a set percentage of the entire population taking vaccines) nor engage in a comprehensive inventory of all relevant parameters to achieve an optimum (e.g., by maximizing a utility pay-off). Reusing the analogy of Giubilini and Savulescu, refusing vaccination is similar to refusing the use of seat belts when driving [283]: given the balance of extremely rare side effects and the cost of delayed or absent vaccination [284], this decision would not happen if individuals used the evidence-base to maximize their own benefits. Indeed, cognitive sciences show that humans only capture a small portion of the available information [101], sometimes making errors in storing this information, and ultimately interpreting it based on their own heterogeneous beliefs [102]. Prior works in modeling COVID-19 [165, 217, 169] and perceptual uncertainties in ABMs [18] have already accounted for some of these aspects when creating cognitive social simulations [105] that reflect the imperfect, heterogeneous decisions that individuals make on vaccination. While some works introduce the notion of imperfect decisions in COVID-19 by accounting for uncertainty about individual health states [285], research shows that there are at least three sources of individual errors to reflect that individuals use social information sub-optimally [112] when observing their peers (with respect to infection, vaccine choices, or

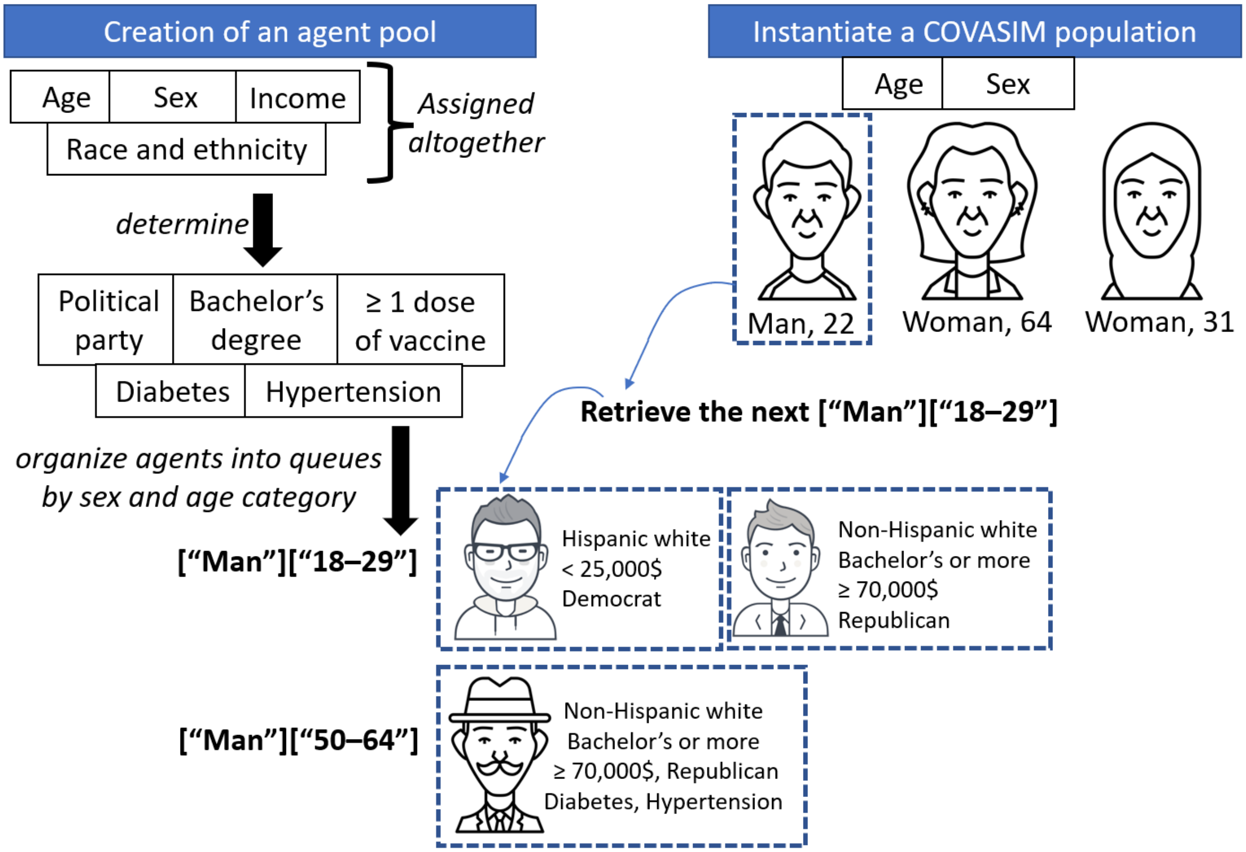

Figure 4.2: The attributes of COVASIM agents can be expanded by matching them with virtual individuals from a large pool generated from nationally representative U.S. datasets (**Table 4.3**). The pool should be larger than the COVASIM population to ensure that each retrieval request for a matching profile can be satisfied. Icons from User Insights and Domp Icon at icon-icons.com, CC Attribution license (CC BY 4.0).

death). That is, an agent may only observe some of its peers (insufficient samples) and/or pay attention to only some of their information (superficial observations) and/or does not sufficiently reflect on the evidence collected (limited ability). Consequently, we recommend to:

- (R9) shift from purely rationale/mechanistic COVID-19 models of human decision-making onto cognitive social simulations that account for imperfection in information capture, its storage, and its use for behavior change.

4.4.2 Operationalizing Human Errors in a Model: The Role of Machine Learning as a Filter

At each simulation tick, each agent can observe the behavior of its peers (e.g., whether to wear a mask, engage in social distancing, wash hands, vaccinate) along with their characteristics. Conceptually, the set of observations can simply be reduced to account for insufficient samples and superficial observations, as shown in **Figure 4.3**. However, the main technical difficulty is to ensure that an agent can change based on these observations. The development of such adaptive skills requires a learning mechanism. As we recently discussed [16], hybrid agent-based models can deal with adoption behavior in different ways, such as by giving their observations as input to a machine learning model. That is, an agent observes by gathering a data table, reflects by deriving a machine learning model (e.g., why do my friends wear masks?), and acts by applying the model to its own characteristics (e.g., my friends with comorbidities wear a mask and I have comorbidities hence I will wear masks). We thus recommend to:

- (R10) enable agents to change behavior not only in response to policies (e.g., lockdown) or instincts (e.g., disease avoidance), but also by learning from their individual contexts.

4.5 Discussion

4.5.1 Overview

In the absence of global vaccination, simulation experts have predicted continuous waves of COVID-19 infections [286]. This is now a reality, and most Americans understand that COVID-19 is here to stay [191]. As mutations and natural selection continue to occur, new variants emerge and vaccines need to be continuously redeveloped [204] and adopted by the population [207, 208, 209, 210, 211, 212]. In the U.S., the federal government has purchased 66 million doses of bivalent boosters that target BA.4 and BA.5 Omicron subvariants [287]. Although the Omicron subvariant BA.5 has been called 'the worst version', Bruce Y. Lee explained in a popular piece that "it's the worst version of what's been getting progressively worse, and you never know when another even worse version will emerge" (emphasis added) [288].Since COVID-19 precautions are going away [205, 206], the virus will continue

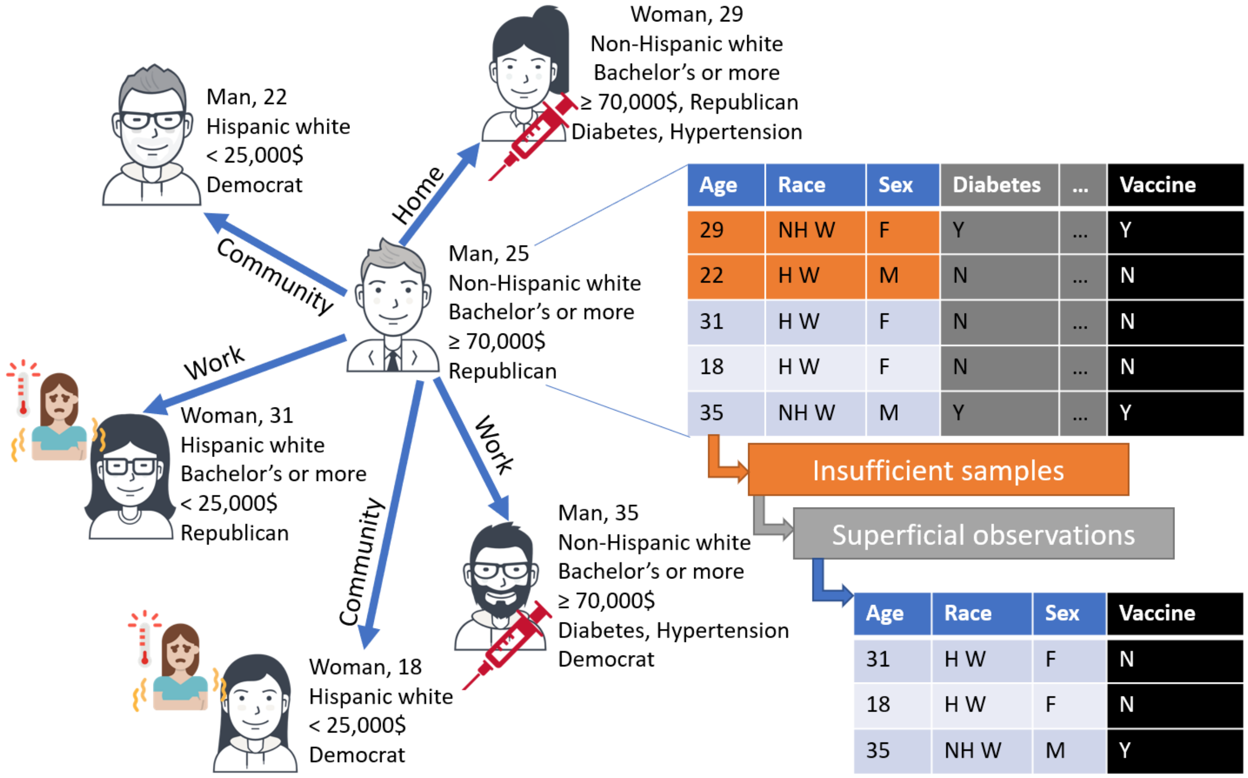

Age	Race	Sex	Diabetes	...	Vaccine
29	NH W	F	Y	...	Y
22	H W	M	N	...	N
31	H W	F	N	...	N
18	H W	F	N	...	N
35	NH W	M	Y	...	Y

Age	Race	Sex	Vaccine
31	H W	F	N
18	H W	F	N
35	NH W	M	Y

Figure 4.3: Each agent observes the vaccination decision and attributes of its peers. The initially perfect observations are altered by perceptual limitations and errors, thus producing an observation set with fewer peers and/or fewer attributes. Icons from User Insights and Coronavirus at icon-icons.com, CC Attribution license (CC BY 4.0).

to spread and subvariants will emerge. Expecting the problem to just disappear by believing variants will get gradually weaker may amount to wishful thinking, "like expecting different animal and plant species to get weaker over time." [287] Since Agent-Based Modeling has been the dominating approach for COVID-19 in recent times [289], our scoping review sought to guide the development of future ABMs by examining three dimensions that are essential to effectively pivot into a long-term view. We covered emerging considerations on immunity (e.g., decays, hybrid cases), the growing evidence base on determinants of vaccinal choice and the ability to use them in simulation, and the possibility of shifting towards cognitive social simulations to better capture human decision-making. While recent reviews and recommendations have targeted national health systems and governments [290, 291], our ten recommendations are directed at the community on modeling and simulation. However, ongoing discussions in the scientific community and changes in the evidence base may lead to additional considerations, as discussed below.

4.5.2 Limitations

Our scoping review stressed the importance of psychological and information variables, suggesting that they can be included through a sequential initialization process or by engaging in hybrid modeling (e.g., by using machine learning to create adaptive agents). However, COVID-19 models may ultimately become too complex, given the pursuit to "covering the full behavioral and social complexity of societies under pandemic crisis" [292] through an ever-expanding set of rules and states. The design of COVID-19 models going forward may thus benefit from a shift from a monolithic piece onto a set of integrated sub-models. This shift would come with its own challenges, as risks for model integration have been discussed extensively elsewhere [293]. However, it may be simpler to develop and reuse dedicated modules, since many COVID-19 models have significant overlaps [294]. For example, this would facilitate the integration of a sub-model dedicated to capturing the perceived utility of certain actions (e.g., getting a vaccine) for an agent, such as modeling vaccination as a function of personal beliefs (e.g., via the Theory of Planned Behavior [295]) or through an emphasis on government accountability [296]. This paper focused on improving models of COVID-19. However, the actions taken to prevent COVID-19 will also impact other diseases. For instance, facemasks and social distancing can reduce other airborne diseases, while the prioritization of hospital resources for COVID-19 impacts other operations [297]. In addition, there is a growing interest in coinfection, particularly for coinfections of COVID-19 and bacteria [298], such as tuberculosis [299]. Consequently, COVID-19 cannot always be designed or expected to be utilized in isolation. Emerging models have started to include COVID-19 alongside other diseases [300]. Future COVID-19 models may thus have to be integrated alongside modules for other diseases. Given this requirement, there may be a tradeoff between the sophistication of a COVID-19 model and the ability to integrate it alongside other disease models.

Determinant	**Category**	**Get Vaccine**	**Effect Strength**	**References**
Age	18-29	No	Strong	[263, 264]
	30-49	Yes		[265]
	50-64	Yes		
	65+	Yes		
Sex	Male	No		[263]
Ethnicity	Non-Hispanic White	Yes		[265]
	Non-Hispanic Black	No		[263, 266, 267]
	Hispanic	No		
	Asian/Pacific Islander	Yes		[266]
	Other	No		[265, 266]
Employment	Unemployed	Yes	Weak	[263]
	Employed (full or part time)	No	Strong	
Education Level	Bachelor's degree or more	Yes		[265, 266, 268]
	No college degree	No		[266, 268]
Annual Income	<25,000	No		[267]
	>= 70,000	Yes		[266]
Comorbidities	Yes	Yes		
Political Party	Republican	No		[265]
	Democrat	Yes		
Prior COVID-19 Infection	Yes	Yes		[263]
Know someone who died	Yes	Yes		
Religion	Catholic	No	Weak	

Table 4.2: Propensity of U.S. individuals in specific socio-demographic categories to get vaccinated or not, and strength of the effect as reported in the references. We counted a reduction in refusal as being equivalent to an increase in acceptance.

1st Wave of Initialization of Four Categorial Features Jointly [266]						
2nd wave of initialization	**Ref**	**Factors**	**Age**	**Income**	**Race and Ethnicity**	**Sex**
	[274, 275]	Bachelor's Degree	✓		✓	✓
	[276, 277]	Political Party			✓	✓
	[278]	Diabetes	✓		✓	✓
	[279, 280]	Hypertension	✓			✓
	[281]	less than or equal to 1 dose of vaccine	✓		✓	

Table 4.3: Creation of a large pool of agents by first initializing four attributes together, then determining the remaining five by accounting for several interdependencies.

Chapter 5

On the necessity of human decision-making errors to explain vaccination rates for COVID-19: an agent-based modeling study

COVID-19 vaccines are important for individuals to avoid severe illness and collectively to prevent significant societal disruptions from uncontrolled disease spread. Vaccine adoption depends both on objective data about vaccine efficiency and on perceptions, which are shaped by individual characteristics and peer influences. Despite the abundance of Agent-Based Models (ABMs) models for COVID-19 and the long-term need for booster doses, ABMs have not yet accounted for the interplay of individual and collective drivers of vaccine adoption. In this explanatory study, we modify the validated COVASIM framework such that agents observe their peers' characteristics (derived from several datasets), use machine learning to reflect and then take decisions based on their own characteristics. We show that specific decision-making errors are necessary to replicate the real-world prevalence of COVID-19 vaccine coverage in the USA. Specifically, agents must only observe simple features of their peers (e.g., age, sex) rather than personal information (e.g., comorbidities).

A slightly shorter version of this chapter has been accepted as:

- Beerman, J. T., Beaumont, G. G., & Giabbanelli, P. J. (2023). On the necessity of human decision-making errors to explain vaccination rates for COVID-19: an agent-based modeling study. In *Proceedings of the 2023 Annual Modeling and Simulation Conference* (ANNSIM), IEEE/ACM.

5.1 Introduction

COVID-19 is an infection caused by the SARS-CoV-2 virus and responsible for almost 7M deaths worldwide by December 2022 [301]. COVID-19 is currently classified as a *pandemic*, which signifies that it is spread worldwide, as was the case for other viral respiratory diseases such as the H1N1 influenza pandemic or SARS [302]. The immunity (albeit temporary) acquired from natural infections or one of the 33 approved COVID-19 vaccines [303] is contributing to a transition from a pandemic into an *endemic* status, which means that overall infection rates will become static. Concretely, it signifies that the virus will become a constant presence and will make a resurgence in regions with low cases [304]. Several reminders, such as [305], have been issued to stress the implications of an endemic status. For example, "there can still be disruptive waves from endemic infections". In addition, an endemic state only means that the number of deaths will become more predictable, not necessarily lower: when authors forecast COVID-19 to turn into an influenza-like endemic disease, they note that there are 290,000 to 650,000 influenza-related deaths per year [303]. One of the most striking illustrations comes from China, where a sudden transition into the endemic phase from the 'Zero Covid' [306] has visible consequences for the healthcare system [307]. It is thus essential to prevent unconstrained spread and focus on a low-incidence strategy [308], in particular by using vaccines. For instance, the high vaccination rate of Singapore has resulted in an endemic state for COVID-19, with fewer disruptions on the economy or the social fabric of society [309].

Surveys offer widely different takes (e.g., from 41% to 93% in [310]) regarding the percentage of the US populations that would take additional vaccine doses (i.e., 'booster doses'). One of the largest cross-sectional survey studies concluded than half of US individuals would take boosters [311]. These numbers are potentially problematic, since a low-incidence strategy may require the yearly administration of an updated vaccine [312, 208]. Responses are also highly heterogeneous since they are shaped by geographical, occupational, and sociodemographical factors [313, 311]. The variety of factors involved demonstrate that a successful vaccination campaign is not merely a matter of vaccine efficacy or access: it also strongly depends on public compliance, where *perceptions* are important determinants of vaccine uptake [314, 315]. While perception has been almost exclusively investigated at the individual level, a study released in November 2022 on a representative sample of the US population also examined predictors at the *collective* level [316]. The study found that perceptions are driven both by individual characteristics *and social networks*, measured as the percentage of friends and family that were vaccinated or contracted the virus.

Agent-Based Models (ABMs) allow to represent heterogeneous individuals (thus capturing variations in individual-level predictors) and their interactions through social networks. While early COVID-19 research employed compartmental models, ABMs have become about as prevalent as the tool of choice in recent studies [317]. Examples of ABMs for COVID-19 simulations have appeared at ANNSIM [165] and numerous other venues [164, 318]. However, social networks have only served to model either the spread of the pathogen [226, 217, 317] and/or contact tracing [319]. The present study thus seeks to address an urgent research gap by using ABMs to examine vaccine choices as a result of both individual- and collective-level factors. Our aim is *explanatory*, as we seek to build a model of individual decision-making processes which reproduces the observed pattern of 81% vaccination among US adults as of January 29, 2023. In sum, the contributions of our study are twofold:

- We extend the validated `COVASIM` framework [226] by creating the first Agent-Based Model that combines individual demographic factors with social network influences to accurately reproduce the vaccination coverage observed in the USA.
- We demonstrate that specific individual decision-making *errors* are necessary to reproduce existing patterns, thus providing a model that can be reused for future COVID-19 ABMs that will need to account for yearly vaccine adoption.

The remainder of this paper is structured as follows. In Section 5.2, we briefly cover the use of ABMs for vaccine hesitancy and the inclusion of decision-making errors in COVID-19 ABMs. We introduce our methods and US-focused datasets in Section 5.3 and present our results in Section 5.4, with an emphasis on identifying combinations of parameters that reproduce the target vaccination rate of 81.0%. The implications of these results are discussed in Section 5.5 with respect to policy implications and future ABM developments.

5.2 Background

The percentage of individuals who have received at least one dose of any COVID-19 vaccine varies across nations (Table 5.1). In Western Europe, similarly to our setting of the USA, first dose coverage ranges from 70% to 80% [315]. Although numerous determinants are involved in shaping individual decisions regarding vaccination [313], the majority of simulation models for COVID-19 do not represent how individuals arrive at a decision. Many models were developed *prior* to the availability of vaccines, hence they focus on non-pharmaceutical interventions such as mask wearing and social distance. As vaccines became available, newer ABMs starting incorporating mechanisms to assign vaccines to specific agents, but assignments tended to be based on priority categories such as the elderly [169] or individuals in nursing homes [320], people at severe risk or healthcare workers [321]. These allocation mechanisms are perpetuated in more recent ABMs [240]. Such models have made it clear that vaccine hesitancy is harmful for public health, as it leads to slower vaccination rates and ultimately increases fatality [322].

In parallel, ABMs have been developed solely to study the spread of beliefs regarding vaccines. While ABMs of *disease spread* are often rooted in SEIR models from computational epidemiology, ABMs focused on individual beliefs resemble models of *rumor spread* [323]. For example, in [324], agents have an opinion (drawn from a normal distribution) and some agents whose opinions are constant will send up to five messages (or opinions) per step. The action of anti-vaccination messages may be countered as agents may be convinced to vaccinate if they visit a supportive doctor; otherwise they will be influenced by the circulating messages. A similar model was proposed in [325], where agents also had demographic attributes (age, sex, race, income, education). A more abstract approach was taken by [326], who used an ABM to simulate how a person's sentiment towards vaccines may change when reading Facebook pages. In all three cases, the model only accounted for the spread of rumors, although in reality there is a strong *interplay* between disease spread and information spread. For example, personally knowing someone who died of COVID-19 increases the odds of getting a vaccine [327], and getting a vaccine reduces the odds of dying from COVID-19. The need to *jointly* simulate disease spread and information spread is a core motivation for the present work.

Table 5.1: Sample of worldwide rates, sorted alphabetically by country [1]

Country	**Single-Vaccination**	**Full-Vaccination**
Argentina	92%	84%
Canada	92%	84%
China	94%	91%
Costa Rica	91%	85%
France	81%	79%
Mexico	78%	65%
Japan	83%	82%
Spain	88%	86%
United States	81%	68%

5.3 Methods

While early ABMs for COVID-19 were developed from scratch or built on prior efforts by the same team, several frameworks have made it possible to instantiate an ABM by leveraging a validated model and adding relevant aspects for a given research problem. In particular, `COVASIM` "has become one of the most widely adopted COVID models, and is used by researchers and policymakers in dozens of countries" [328]. In several cases [240, 169], two reasons explain the choice of `COVASIM` for a new study: the framework automatically embeds agents in multiple realistic synthetic social networks based on their age (home, community, work or school if age relevant) and handles the entire disease progression, including age-based disease severity. `COVASIM` also contains an immunity module, which handles vaccines and their efficacy against the different variants that may spread simultaneously. To use this framework in our study, the next two paragraphs detail how we (i) expand the attributes of the agents and initialize them for our target population of the USA; and (ii) redesign the agents' decision-making activities such that they can account for errors typical of human behavior and are shaped by both individual attributes and peers. For both (i) and (ii), we implement the recommendations recently formulated by [327]. The section concludes with the design of our experiments.

`COVASIM` creates agents with a distribution of age and sex. Given recent reviews on determinants of COVID-19 vaccination [313, 311], we *added six individual attributes*: race and ethnicity, income, educational attainment (whether a person has a bachelor degree), diabetes, hypertension, and political belief. These attributes are added through through consecutive steps. First, we use one data source to generate agents by jointly assigning age, sex, race and ethnicity, and income (Figure 5.1). This creates realistic demographics for the US instead of assigning each factor based on a single dependency (e.g., age given sex, income given age). Second, since no dataset contains all of our target attributes, we use recent datasets to initialize each of the remaining four constructs. In each case, the initialization depends on three existing attributes (e.g., diabetes given age, sex, race and ethnicity) to capture as much as possible the joint distributions in the population (Figure 5.1). Third, we import these features into `COVASIM` by matching agents created with the platform with a pool of synthetic agent created through our process. In addition to socio-demographic attributes, we initialize the simulation by ensuring that a small subset (5% at random) of agents are currently actively infectious and some are vaccinated. It is important to accurately assign vaccines to the right agents at baseline, since the spread of adoption will account for peer influences (as detailed in the next paragraph). We thus seed the simulation with 10% of individuals vaccinated, identified among those most likely to have received the first dose given their age, race and ethnicity.

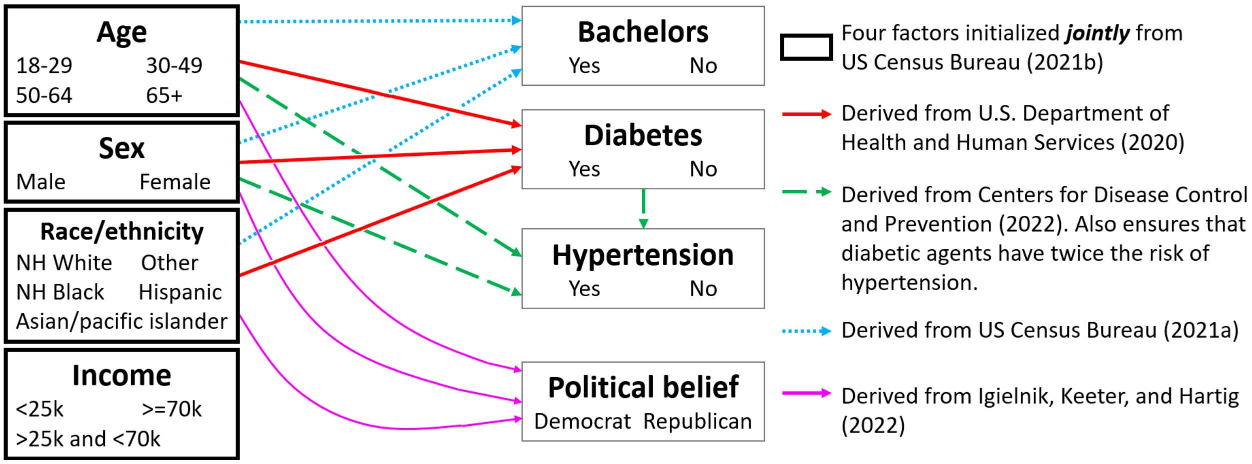

Figure 5.1: We first initialized four attributes jointly and then used a multitude of data sources to initialize additional (dependent) attributes. *Note: 'NH' means Non Hispanic.*

Every month each agent decides whether or not to vaccinate based on the knowledge accumulated about their peers (i.e., the cumulative observations up to the current month) and the decisions of their internal model. **First, agents observe** their peers. In reality, individuals may not know everything about others: for example, it is reasonable to know the age category of other agents, but we may not be aware of their political opinions or co-morbidities such as hypertension. We thus account for errors in decision-making by allowing agents to observe only a *percentage* of their peers and *a subset* of their attributes. The attributes are added gradually (Table 5.2) to test the resemble the more information an individual learns about another as their relationship strengthens. For example, the first few attributes would be commonly known about an acquaintance (e.g., age, sex, whether they died), while the next set of attributes adds personal information (e.g., political views and income bracket) and the last attributes disclose medical information (the two co-morbidities of diabetes and hypertension). **Second, agents reflect** on their observations by deriving a model, similarly to how humans form generalizations from experiences. Each agent was equipped with a decision tree classifier, with observations from peers as input and whether to vaccinate as output. We chose decision trees because they can conveniently be visualized (Figure 5.2) for debugging and constrained by a single parameter (the depth of the decision tree as in Figure 5.3) such that we can vary the sophistication of each agent's decision-making process. **Third, agents apply** the decision-tree classifier to themselves, given their own attributes. For example, they may have seen most of their older friends with co-morbidities taking the vaccine, but if they are young without co-morbidity then they do not feel concerned by their peers decisions. This mechanism replicates how individuals observe others' decisions and (partly) understand their motivations, but do not always feel personally concerned.

A simulation runs for a a full year starting at February 3, 2021 to October 3, 2022. This time period was selected to follow the timeline of the collected data for the United States vaccination total (Table 5.1). We initialize the `COVASIM` model, add agent attributes, seed the infection and vaccines, and run ML models on each agent as four variants of increasing strength emerge over a year. At initialization we seeded 10% of the population to be vaccinated by randomly selecting agents from the pool of agents who should have been vaccinated given the data. During the simulation, every agent (including those that were vaccinated at the start) records all attributes of the peers with whom they interact. Then, at each month, the agents train their own decision tree with their cumulative list of observations and finally predict whether or not they will vaccinate based on their own attributes. Note that the creation of the synthetic population (attributes and social ties) ensures that there is assortativity, hence an agent cannot decline the vaccine in perpetuity solely because it never finds its peers relatable.

In our experiments, we varied three model parameters as follows: decision tree depth from 1 to 4 (to examine the consequences of agents making simpler decisions); the amount of peers observed from 10, 25, 50, 75, or 100%; and the ten increasingly detailed subsets of peer information that were available to each agent (Table 5.2). We ran each combination of parameter values ten times to account for the stochastic behavior of the model. Our experiments used the following software ecosystem: `COVASIM` 3.1.2 and `Numpy` 1.20.3 for the simulation of disease spread, `scikit-learn` 1.1.1 for the machine learning activities of each agent, and `Pandas` 1.3.3 for data analysis.

Before interpreting the results from an ABM, we must ensure that (i) the model is sufficiently accurate for its purpose and (ii) the population size is sufficient to provide consistent results. We determine accuracy through a *confusion matrix* (Figure 5.4) by using our data to calculate which agents will vaccinate prior to simulation and then we compare those expectations with the simulation outcomes. Regarding the population size, it should not be too small as results may be incorrect and subject to significant variations, even as only a few hundred agents are added; this is exemplified in works such as [22]. The population

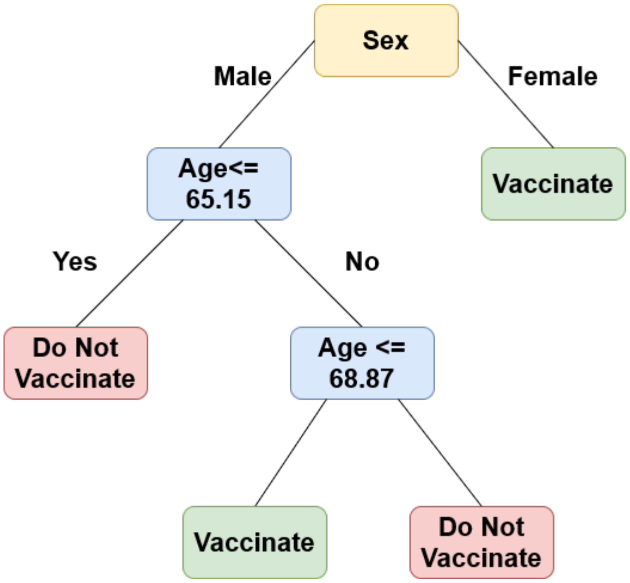

Figure 5.2: Agent's decision tree produced by our simulation (Parameters: Depth = 4, Attributes: {Sex, Age, Race}, Percentage of Observations: 100%).

should not be too large either, as computationals cost may become prohibitive and force us to compromise the number of combinations examined (i.e., reduction in search space) and/or the number of repeats [329]. Consequently, we perform simulations at increasingly large population sizes ($10,000$ agents, $25,000$ agents and $50,000$ agents) while looking for stability in the confusion matrix and the percentage of vaccinated agents.

5.4 Results

For full disclosure, our data is permanently hosted on a third-party repository at `https://doi.org/10.5281/zenodo.7582642`. The data consists of two files: supplementary online material S1 provides the percentage of vaccinated population for each simulation run (i.e., each combination and each repeat) while supplementary online material S2 provides the average vaccination percentage across repeats for analysis. Our analysis of the average vaccination percentage at different population sizes confirms that we have enough agents. Specifically, results across population sizes differ by 0.45 ± 0.84 *percentage points* on average, or a *relative* average difference of 1.55 ± 3.82. For example, for a decision tree depth of 2, the first combination of features (age only), and 75% of peers observed, we have the following vaccination rates: 81.45% for $10,000$ agents, 84.00% for $25,000$ agents, and 85.71% for $50,000$ agents. The widest difference is 4.25 percentage points (85.71 - 81.45) or a relative difference of 5.23%. The fact that most results are very close is further observed as 174 out of 200 combinations have a difference of less than 0.5 percentage points.

The heatmap in Figure 5.6 summarizes the impact of the percentage of available data (i.e., observations) for the agent's internal models and the combination of attributes (Table 5.2).

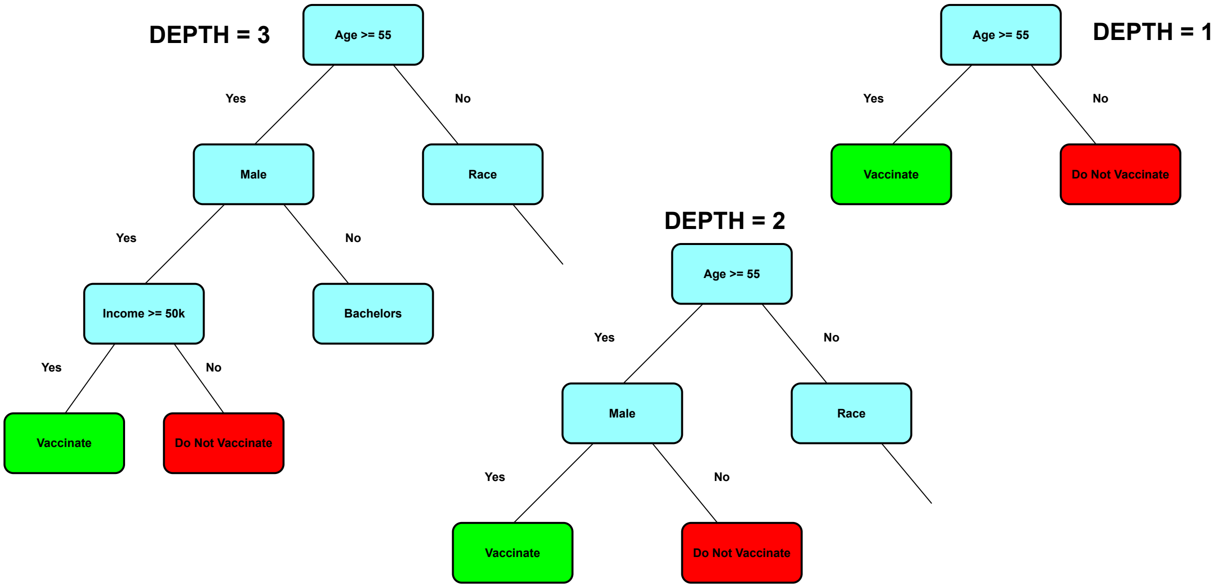

Figure 5.3: Each agent has a decision tree classifier, where the output is whether to vaccinate. The *depth* of the decision tree is a key parameter. As the depth of a decision tree increases, the vaccination decision of an individual may depend on a larger number of factors and/or revisit some factors to refine their choices.

This aggregate visualization of the parameter sweep shows that the real-world coverage of 81% in the U.S.A. can only be obtained if agents observe enough of their peers. That is, if agents ignored most of their peers and decisions were not subject to social influences, the simulations suggest that almost the entire population would have been vaccinated. We also analyzed the number of agents changing their mind regarding vaccination. Figure 5.5 shows that most agents change their belief after one year of simulation (i.e., between months 12 and 14). To further examine these results, we break down the output per depth of the decision tree in Figure 5.7. The best parameter combination to reproduce the target coverage of 81% consists of a decision tree depth of 4, 100% of observations, and three attributes (age, sex, race and ethnicity). Using this combination produced an accuracy over 70% when using a sufficient population size, per the confusion matrices in Figure 5.4. The second best combination is a decision tree depth of 2, 75% of observations, and only one attribute (age). If agents observe fewer peers, then they almost all get vaccinated. If agents have a very limited ability to reflect on the evidence (i.e., lower depths of the decision tree), then too few of them get vaccinated. The sensitivity of the model to the parameters is further visualized in Figure 5.8.

Table 5.2: Our 10 combinations (or simulation scenarios) add one factor at a time, from most to least potentially important based on prior reviews. For example, combination 3 has three factors: age, sex, race.

Combination	Attribute added
1	age
2	+sex
3	+race
4	+dead
5	+bachelors
6	+income
7	+political
8	+diagnosed
9	+diabetes
10	+hypertension

5.5 Discussion

A recent study showed that perceptions (and ultimately adoption) regarding the COVID-19 vaccine were driven by both individual characteristics and the social influences conveyed by peers [316]. Although many ABMs have been developed to study COVID-19, none of them has so far accounted for the interplay of individual and collective influences on vaccine decisions. Using machine learning to operationalize the decision-making module of agents, we found that few combinations of individual and collective features could accurately replicate the real-world coverage in the USA. Since a model is a *simplification* of reality, our results *should not be literally interpreted* to mean that only the two combinations found here explain the real-world vaccine coverage. Rather, the trends and high sensitivity of our model suggest that real-world patterns can be explained by the ability to observe most neighbors and derive sufficient rules from observations. These rules are based on commonly low-level observed features (e.g., age, sex) rather than very personal information (e.g., co-morbidities). In other words, individuals are not blind to their peers, unable to make judgments, or engaged in complex rules that take into account intimate details about their peers. Rather, they take into account simple features about most people around them.

The implications for the development of ABMs going forward is that accounting for individual and collective drivers of vaccine choices can be achieved by letting agents observe all peers at each round and run relatively light models (decision tree). The characteristics of peers that are needed for decision-making are already used in many ABMs (many of which use age in their disease severity module), hence minor to no modifications are needed in terms of agent features.

We focused on vaccine engagement as a product of a *local* social context, but it is also impacted by community- and societal-level factors (e.g., conceptions of health, encounters with the healthcare system) [330]. For instance, our study setting of the USA is different from

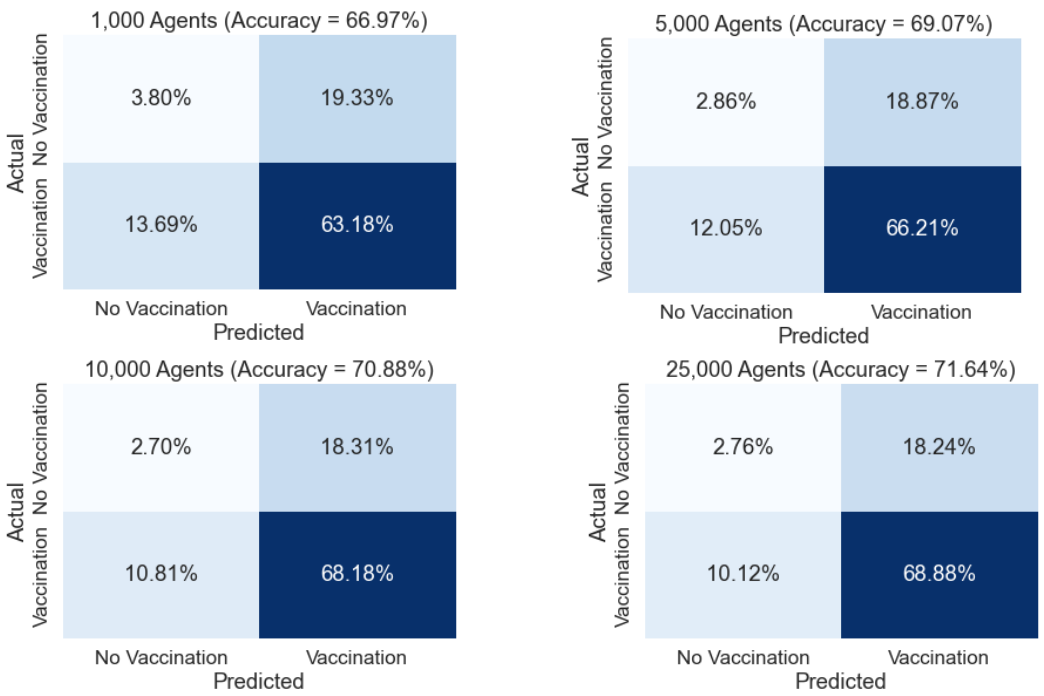

Figure 5.4: Confusion matrices for various populations where *Actual* represents the agents we determined would actually vaccinate and *Predicted* represents the agents that were predicted to vaccinate during the simulation. Parameters: Depth = 4, Attributes: {Sex, Age, Race}, Percentage of Observations: 100%.

western European countries in terms of legal system and policy choices. Although article 8 of the European Court of Human Rights considers that compulsory vaccination may interfere with private rights, vaccination can legally be mandatory if treatment is not dangerous and can help others [331]. Austria was the only nation to introduce a vaccination mandate and it abandoned it a few months later, but other countries use COVID-19 Vaccination Certificates (known in EU Regulation 2021/953 as 'Green Digital Certificate') as incentives [331]. As a result, societal-level drivers for vaccination may be higher in these countries than in the USA. In addition, the individual-level constructs most strongly associated with vaccine intention are different across places [332]. Consequently, if our model is re-calibrated to a different location, simulation results may show that a different combination of variables best explains the current rate in the location of interest.

Furthermore, future works could conduct these simulations at a smaller geographical scale to capture precise demographics which may produce more accurate results. For example, we may focus on a location such as New York City and only initialize attributes from data sets accordingly. These data sets could change our demographic variables. The New York City Community Health Survey [333] (CHS) depicts age groupings to be the following: 0-17 (21%) 18-24 (8%), 25-44 (30%), 45-64 (25%), 65+ (16%). The American Community Survey [334] would switch our race percentages to the following: Asian (15%), Black (22%),

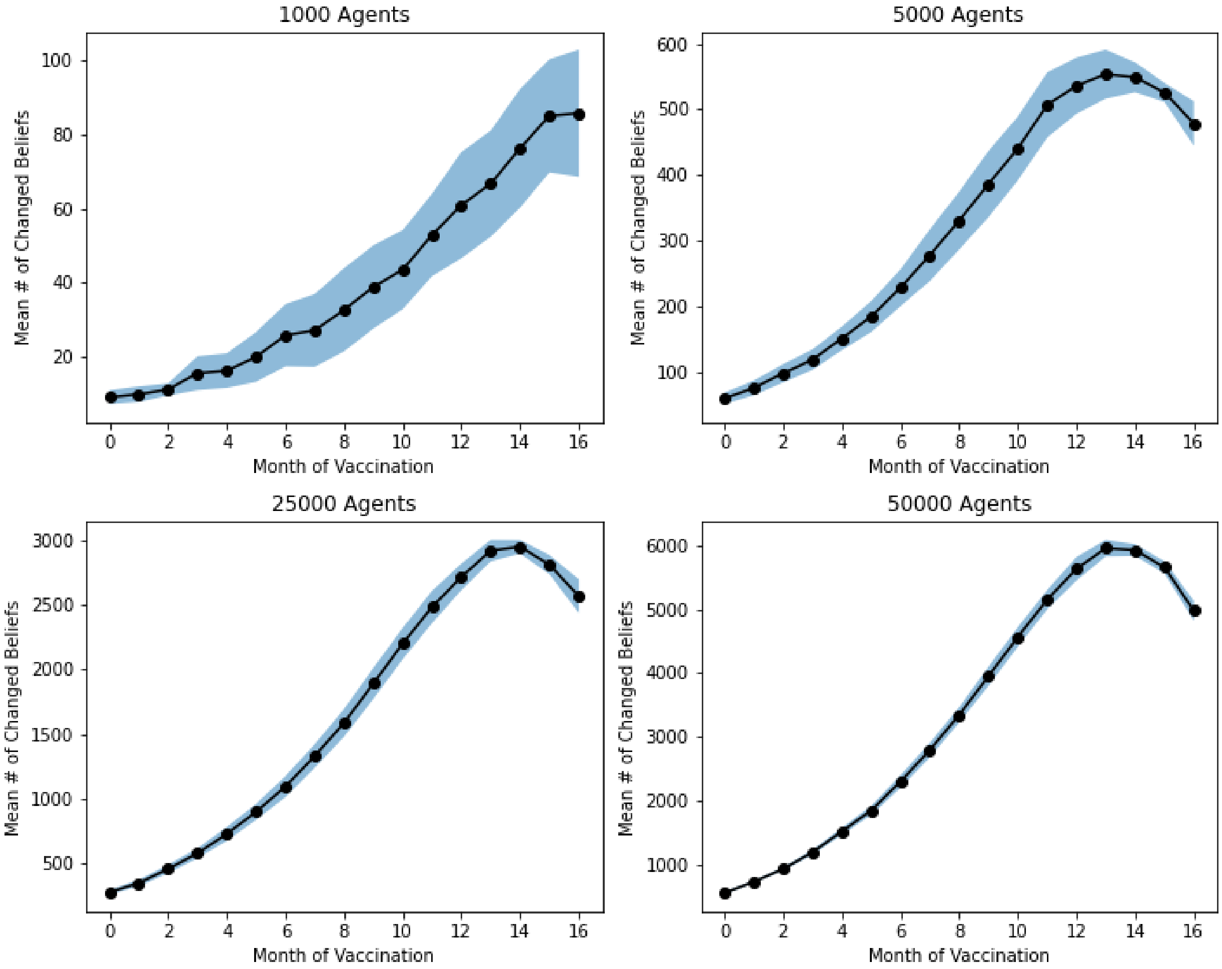

Figure 5.5: Agents changing their beliefs on vaccination over time.

Latino (29%), White (32%). Ultimately, a specific geographical location and its associated demographic data could change the vaccination rate.

Since it is a simplification, future works could extend our model in numerous ways. Our results suggest that extensions may not be as necessary when it comes to agent features, since accounting for a few of them suffices to replicate core results. However, extensions may be beneficial to examine how agents deal with their memories. Indeed, the observations of each agent are strictly cumulative, hence there is a perfect recollection of every that was observed previously. This may artificially reduce the possibility that agents make a different decision later in the simulation, since their new observations become diluted among their extensive records of the past. In practice, it is likely that people 'forget' some of these past observations. A simple approach adopted in other ABMs would be to express that the probability of forgetting a past observation increases as time advances [335]. Most interestingly, computational models of cognitive science offer different approaches to handle *reconsolida-*

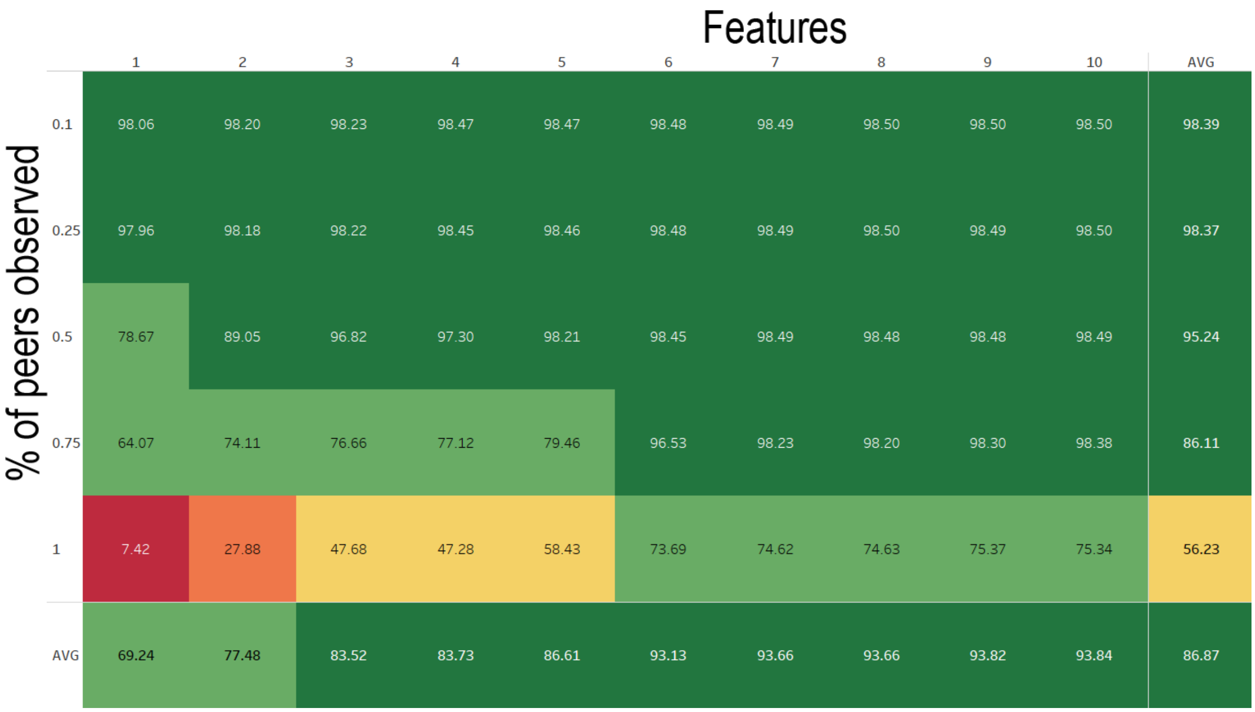

% of peers observed	Features 1	2	3	4	5	6	7	8	9	10	AVG
0.1	98.06	98.20	98.23	98.47	98.47	98.48	98.49	98.50	98.50	98.50	**98.39**
0.25	97.96	98.18	98.22	98.45	98.46	98.48	98.49	98.50	98.49	98.50	**98.37**
0.5	78.67	89.05	96.82	97.30	98.21	98.45	98.49	98.48	98.48	98.49	**95.24**
0.75	64.07	74.11	76.66	77.12	79.46	96.53	98.23	98.20	98.30	98.38	**86.11**
1	7.42	27.88	47.68	47.28	58.43	73.69	74.62	74.63	75.37	75.34	**56.23**
AVG	**69.24**	**77.48**	**83.52**	**83.73**	**86.61**	**93.13**	**93.66**	**93.66**	**93.82**	**93.84**	**86.87**

Figure 5.6: Average percentage of vaccinated agents as a function of the percentage of peers observed (y-axis) and the features examined in each peer.

tion, which deals with updating, distorting, or even erasing past observations [336]. As we shift our focus from a mechanical model of disease progression onto an investigation of human health behaviors, opportunities abound to incorporate cognitive models into ABMs for COVID-19.

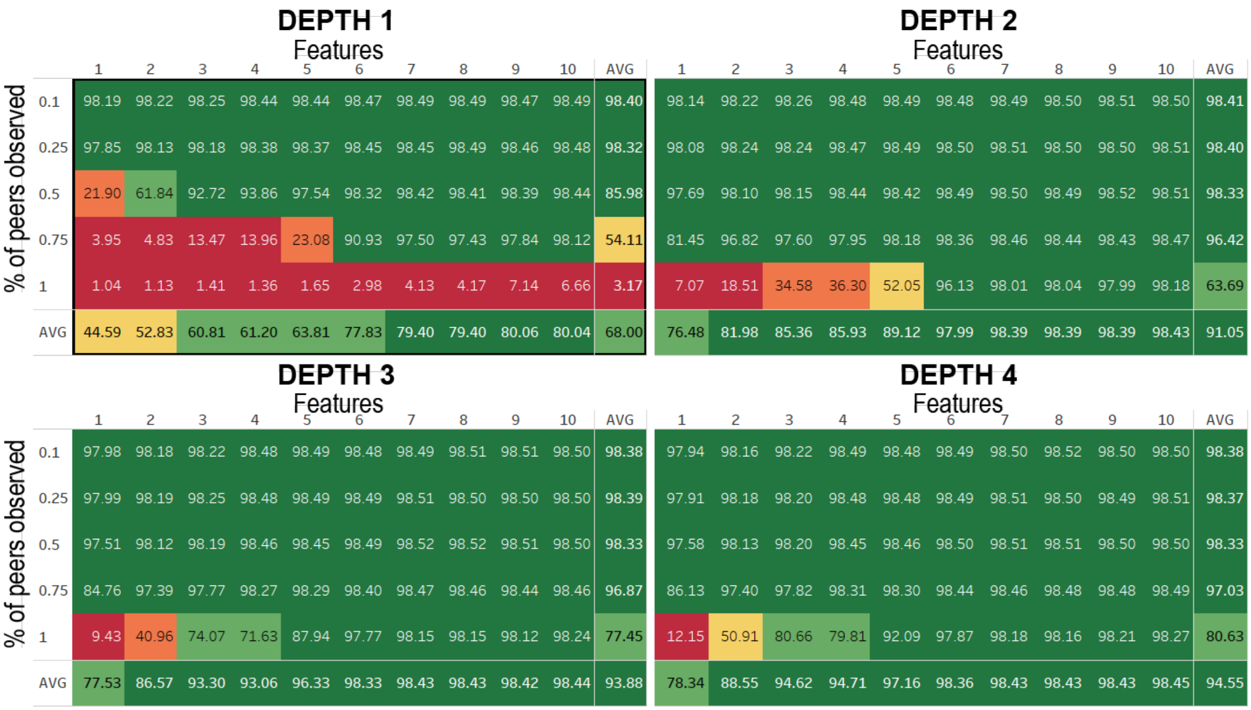

DEPTH 1

Features

% of peers observed	1	2	3	4	5	6	7	8	9	10	AVG
0.1	98.19	98.22	98.25	98.44	98.44	98.47	98.49	98.49	98.47	98.49	98.40
0.25	97.85	98.13	98.18	98.38	98.37	98.45	98.45	98.49	98.46	98.48	98.32
0.5	21.90	61.84	92.72	93.86	97.54	98.32	98.42	98.41	98.39	98.44	85.98
0.75	3.95	4.83	13.47	13.96	23.08	90.93	97.50	97.43	97.84	98.12	54.11
1	1.04	1.13	1.41	1.36	1.65	2.98	4.13	4.17	7.14	6.66	3.17
AVG	44.59	52.83	60.81	61.20	63.81	77.83	79.40	79.40	80.06	80.04	68.00

DEPTH 2

Features

% of peers observed	1	2	3	4	5	6	7	8	9	10	AVG
0.1	98.14	98.22	98.26	98.48	98.49	98.48	98.49	98.50	98.51	98.50	98.41
0.25	98.08	98.24	98.24	98.47	98.49	98.50	98.51	98.50	98.50	98.51	98.40
0.5	97.69	98.10	98.15	98.44	98.42	98.49	98.50	98.49	98.52	98.51	98.33
0.75	81.45	96.82	97.60	97.95	98.18	98.36	98.46	98.44	98.43	98.47	96.42
1	7.07	18.51	34.58	36.30	52.05	96.13	98.01	98.04	97.99	98.18	63.69
AVG	76.48	81.98	85.36	85.93	89.12	97.99	98.39	98.39	98.39	98.43	91.05

DEPTH 3

Features

% of peers observed	1	2	3	4	5	6	7	8	9	10	AVG
0.1	97.98	98.18	98.22	98.48	98.49	98.48	98.49	98.51	98.51	98.50	98.38
0.25	97.99	98.19	98.25	98.48	98.49	98.49	98.51	98.50	98.50	98.50	98.39
0.5	97.51	98.12	98.19	98.46	98.45	98.49	98.52	98.52	98.51	98.50	98.33
0.75	84.76	97.39	97.77	98.27	98.29	98.40	98.47	98.46	98.44	98.46	96.87
1	9.43	40.96	74.07	71.63	87.94	97.77	98.15	98.15	98.12	98.24	77.45
AVG	77.53	86.57	93.30	93.06	96.33	98.33	98.43	98.43	98.42	98.44	93.88

DEPTH 4

Features

% of peers observed	1	2	3	4	5	6	7	8	9	10	AVG
0.1	97.94	98.16	98.22	98.49	98.48	98.49	98.50	98.52	98.50	98.50	98.38
0.25	97.91	98.18	98.20	98.48	98.48	98.49	98.51	98.50	98.49	98.51	98.37
0.5	97.58	98.13	98.20	98.45	98.46	98.50	98.51	98.51	98.50	98.50	98.33
0.75	86.13	97.40	97.82	98.31	98.30	98.44	98.46	98.48	98.48	98.49	97.03
1	12.15	50.91	80.66	79.81	92.09	97.87	98.18	98.16	98.21	98.27	80.63
AVG	78.34	88.55	94.62	94.71	97.16	98.36	98.43	98.43	98.43	98.45	94.55

Figure 5.7: Vaccination rate as a function of the depth of the decision tree, simulation combination (x-axis), and percentage of peers observed (y-axis). Values close or above the observed vaccination rate are in green, while values below are in red.

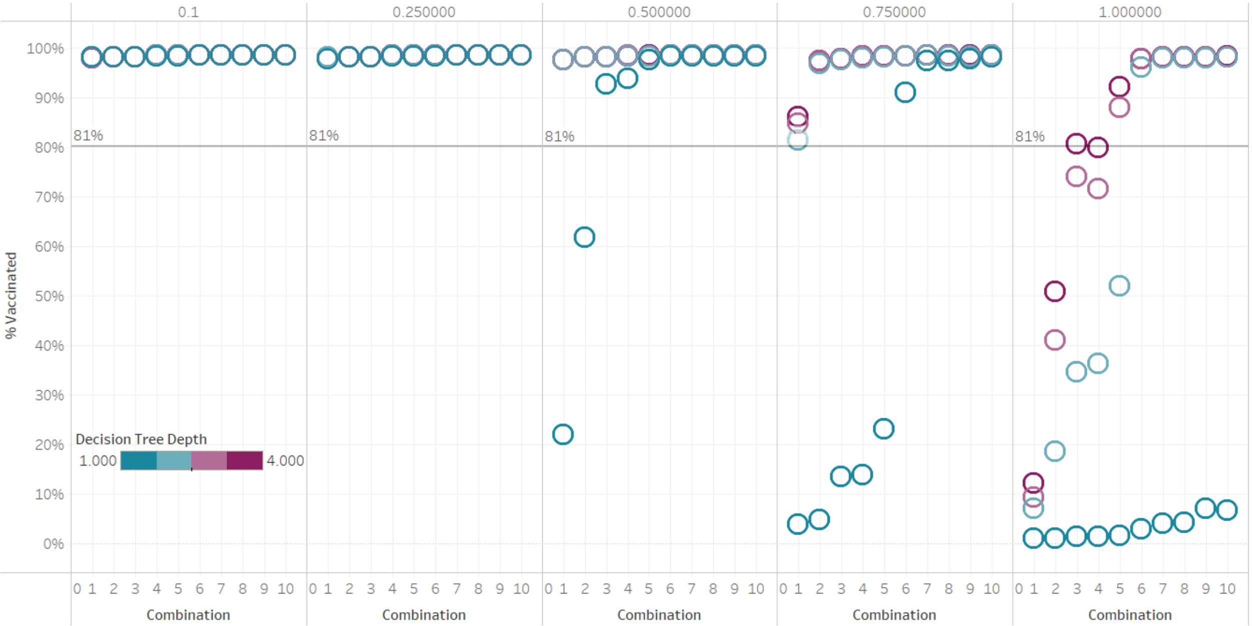

Figure 5.8: Effect of the percentage of observations, depth of the decision tree, and attribute combination onto the vaccination rate.

Chapter 6

Clustering Like-Minded Agents

A variety of models in Modeling & Simulation require a steep computational cost. Specifically, the combination of two separate models: Agent Based Models and Fuzzy Cognitive Maps, known as Hybrid Modeling requires an expensive computational cost for large agent populations. Researchers may attempt to offset these costs, by developing more efficient algorithms or utilizing faster processing units. In our work, we decide if we can reduce the cost of Hybrid Models by shrinking the agent population while maintaining accuracy of the initial simulation. We determine how to decrease our model's computational costs by implementing three innovative and a variety of existing metrics that assess whether agents within a population are similar (i.e, they think alike). Then, group agents based on their level of similarities, and construct super nodes (i.e., representative agents) from entire groups of agents. These super nodes are then reconnected and simulated from their initial values so we can measure how a reduction in the agent population impacts the accuracy of the overall model. The accuracy of these models are compared by recording each models: average output, standard deviation, quartile ranges, minimum values, and maximum values. At most, the simplified models average output deviate from the original model by 1.8%. Ultimately, we focus on determining the best metrics to utilize when comparing agents, and the impact super agents have on accuracy which in turn would help reduce computational costs.

6.1 Introduction

Agent-Based Modeling (ABM) serves to represent physical entities as virtual entities in a simulation for a plethora of real world scenarios [337]. These entities known as “agents” can imitate living organisms such as cells or physical objects such as cities. Furthermore, ABMs are constructed with specific rule sets and laws governing the actions of agents depending on the problem that modelers are attempting to analyze. For example, we may want to study the spread of HIV in the human body and incorporate biological concepts into the rule sets [90], or focus on the travel of humans in an urban society with traffic laws governing the system [338]. Regardless of the problem at hand, there is a balance to be struck between model size, which we use as a measure of accuracy, and the resources required for computation. For example, HIV can infect billions of cells in the human body [339], and cities may have tens of thousands of cars that are affected by traffic systems and pedestrians [340, 341]. While an accurate model would require accounting for every entity in these systems, doing so would likely exceed available computational resources. Therefore, it is necessary to find a compromise between model resolution (i.e., how many entities should be included) and available computational resources. Because lower resolution does not necessarily result in reduced accuracy. Simulating millions of cells instead of billions can still yield valuable insights, such as whether a particular treatment is effective. Due to this occurrence, we may want to utilize faster processing devices [342]; however, these items my not be accessible. Therefore we may aim to reduce the computational cost of agents by creating “super nodes“ [343, 344, 345].

Another type of informative model in Modeling & Simulation are known as Fuzzy Cognitive Maps (FCMs) [346]. FCMs are designed to depict the behavior of various concepts in relation to a scenario or select topic. These models are digraphs (i.e., directed graphs) constructed by a team of subject matter experts (SMEs) in their respective fields. This process incorporates surveying of subjects, defining causality, and implementing fuzzy logic to define edge and node weights of the FCM. Node weights vary from 0 to 1 where 0 is the absence of a concept and 1 is the full presence of a concept. Edge weights vary from -1 to 1 where a negative edge weight from a source node to a target node depicts that an increase in the source node causes a negative decrease in the concept of the target node. Once initialized, an FCM will iteratively update its node weights at each time step (Figure 6.1). The model finishes it simulations once a set amount of iterations have been reached or the focus concept has changed by a threshold amount.

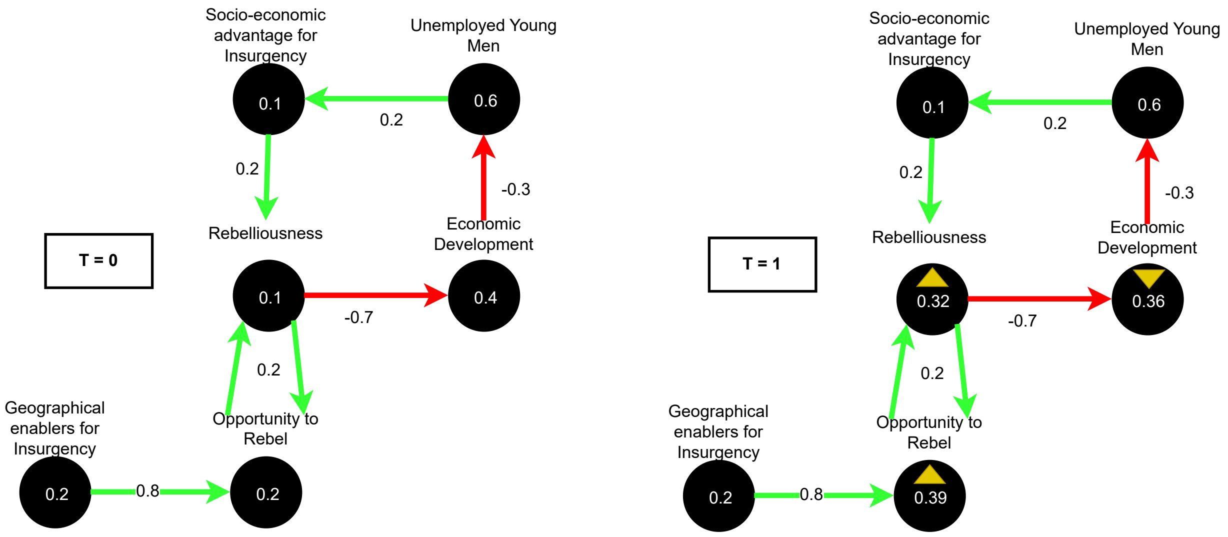

Figure 6.1: Simulating an FCM for one time step, using the example from [58, 347].

A methodology to incorporate both ABMs and FCMs in Modeling & Simulation is known as Hybrid Modelling (HM) [348]. Moreover, HMs are constructed by developing an ABM and FCM for a particular problem and attaching an FCM or various FCMs to agents in the ABM (i.e., we add the FCM as an attribute of the agent). This process allows us to understand how concepts depicted in the FCM may shift due to the interactions of agents in an ABM [342]. However the combination of two individual models for a population of agents creates concern for computational cost.

In our work, we address this concern by reducing the population sizes of HM by establishing representative communities of agents while maintaining accuracy. Furthermore, we implement new and existing techniques to compare FCMs for community detection and division. Ultimately our work contributes in two areas:

- Reduce computational costs of existing HMs
- Introduce new measures to compare weighted digraphs

We detail these new and existing metrics in Section 6.2 with a variety of equations, illustrations, and examples with FCMs. Once these metrics are established, in Section 6.3 we described how we compared FCMs in our simulations, assigned social ties between agents to represent the similarity/dissimilarity between their FCMs, and how we utilized community detection algorithms to cluster agents. Agents are selected from these clusters as representatives and reconnected to form smaller HMs that are simulated again with the initial values of the main HM. Finally, in Section 6.4 we present our results.

6.2 Background

Due to the heterogeneity and malleability of these models, ABMs have flourished in numerous disciplines and have been utilized specifically in Network Science [349]. Network scientists have designed these models to fit specific network topologies such as small-world, scale free, or random graphs [350, 351]. Small-world networks have agents with a high clustering coefficient and groups of communities with few links between the clusters [352]. Scale Free networks illustrate the rarity of humans having a disproportionally large distribution of social capital compared to the majority of humans in a social network [353]. Furthermore the topology is established with a power-law degree distribution [342]. Random graphs could resemble a variety of topologies but their construction must follow the probability that each node is equally likely to connect to any other node [354, 355].

6.2.1 Graph Metrics

Due to the prevalence of network models in Modeling & Simulation, we can implement a variety of metrics to characterize the cognitive map of an agent [356, 357] and hence compare maps [358, 359]. However, the purpose for comparison and properties of the graphs being compared dictate the types of measures that should be implemented. In our work, we focused on singular agents (i.e., nodes) representing a community of agents (i.e., group of related nodes) based on their FCM similarities and as a result, detail a number of graph metrics for this objective. We utilize both new and existing measures detailed in Table 6.1.

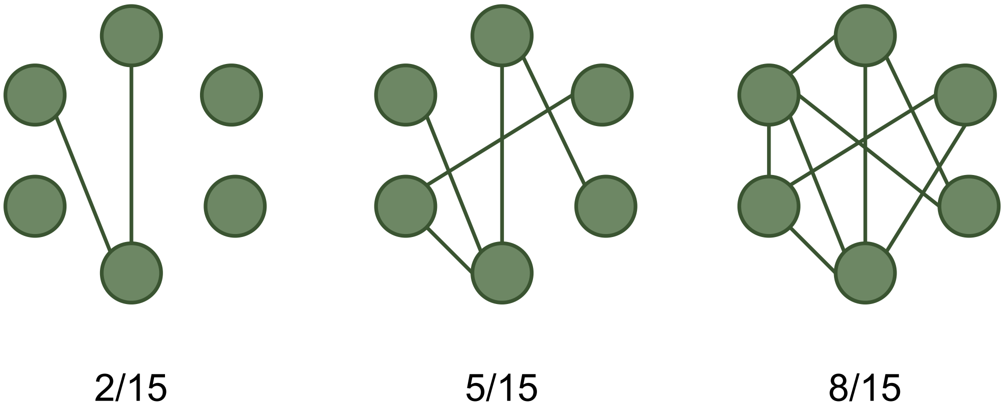

Figure 6.2: Graph Density Increasing from Left to Right

Graph Density is the number of connections in a map compared to the maximum number of connections possible for all concepts (**Figure** 6.2). Ultimately, the density of a graph depicts the interwovenness of concepts within an FCM [358]. The density of a graph is calculated in one of two ways which depends on whether the graph is directed (Equation 6.1) or not (Equation 6.2).

$$D = \frac{|E|}{2\binom{|V|}{2}} = \frac{|E|}{|V|(|V|-1)} \tag{6.1}$$

$$D = \frac{|E|}{\binom{|V|}{2}} = \frac{2|E|}{|V|(|V|-1)} \tag{6.2}$$

Graph kernels can be used to compare a variety of information attributed to a graph. Graph kernels provide a comprehensive measurement of diverse structural features or properties of a graph and return a single number [76]. Specifically, graph kernels focus on the patterns of graph structure during comparison [360]. Numerous methods have been implemented with graph kernels such as using graph kernels with loops or triads. A triad represents a subgraph of three nodes in a larger graph [361]. With this metric, we focus on the Triad Significance Profile (TSP). With 16 possible types of triads and we would calculate the total number of occurrences for each of these triads and then use that to calculate the percent difference between two FCMs. In order to extract a TSP from a given graph you would iteratively search for three nodes linked by 1 or more of the 16 possible types of triads. Once every profile is accounted for in two graphs, we would then compare the prevalence of each specific type of triad discovered in the network through frequency or distribution measures. This statistical significance can be quantified in Equation 6.3 using its Z-score, denoted Z_M, where n_M represents the frequency of motif M in the given network, and $\langle n_M^{\text{rand}} \rangle$ and σ_M^{rand} represent the mean and standard deviation of M's occurrences in a set of randomly generated networks, respectively [362, 363].

$$Z_M = \frac{N_M - \left\langle N_M^{\text{rand}} \right\rangle}{\sigma_M^{\text{rand}}} \tag{6.3}$$

Number of Concepts is similar to the aspect of comparing node properties. The number of concepts compares the total number of nodes in graph A to the total number of nodes in graph B [364]. This measure is known as *number of concepts*. When comparing FCMs, this metric can be implemented to compare the complexity of entire graphs and how comprehensive the data might be.

Clustering Coefficient of a node is how close a node and its neighbors are to being a complete graph. This is defined in Equation 6.7. The clustering coefficient of a graph is then found by averaging the clustering coefficient of all nodes. The clustering coefficient of a graph measures the relative frequency of triangles (level of connection) and is similar to the transitivity of a graph [365]. Let $G = (V, E)$ be a graph with a set of vertices V and edges E. Then, the neighborhood $N - i$ of $v_i \in V$ is given by Equation 6.4:

$$N_i = \{v_j | e_{ij} \in E \vee e_{ji} \in E\} \tag{6.4}$$

The clustering coefficient of a vertex $v_i \in V$ is given by Equation 6.5 for the directed case and Equation 6.6 for the undirected case.

$$C_i = \frac{|e_{jk}|}{|N_i| \cdot (|N_i| - 1)}, v_j, v_k \in N_i, e_{jk} \in E \text{ if } G \text{ is directed.} \tag{6.5}$$

$$C_i = \frac{2|e_{jk}|}{|N_i| \cdot (|N_i| - 1)}, v_j, v_k \in N_i, e_{jk} \in E \text{ if } G \text{ is un-directed.} \tag{6.6}$$

If $|N_i| = 0$ we set $C_i = 0$

Finally the clustering coefficient is defined per Equation 6.7:

$$C = \frac{1}{|V|} \cdot \sum_{i}^{n} C_i \tag{6.7}$$

Receiver-transmitter ratio may be employed when examining graph similarities due to the properties and focus of FCMs. Receiver transmitter ratio can be broken down into two parts: receiver nodes and transmitter nodes [366]. Receiver nodes are commonly denoted as R and do not influence any nodes in a graph which means R nodes have directed edges but serve as the target node (**Figure** 6.3) (i.e., they are never a source node) [358]. Transmitter nodes are the exact opposite. Denoted by T, transmitter nodes are always a source node and never serve as a target node (**Figure** 6.3). Once both transmitters and receivers are defined (Figure 6.4), the Receiver-transmitter ratio can be calculated via Equation 6.8.

$$\text{ratio} = \frac{R}{T} \tag{6.8}$$

Weighted Jaccard similarity measures the distance between two sets or vectors with

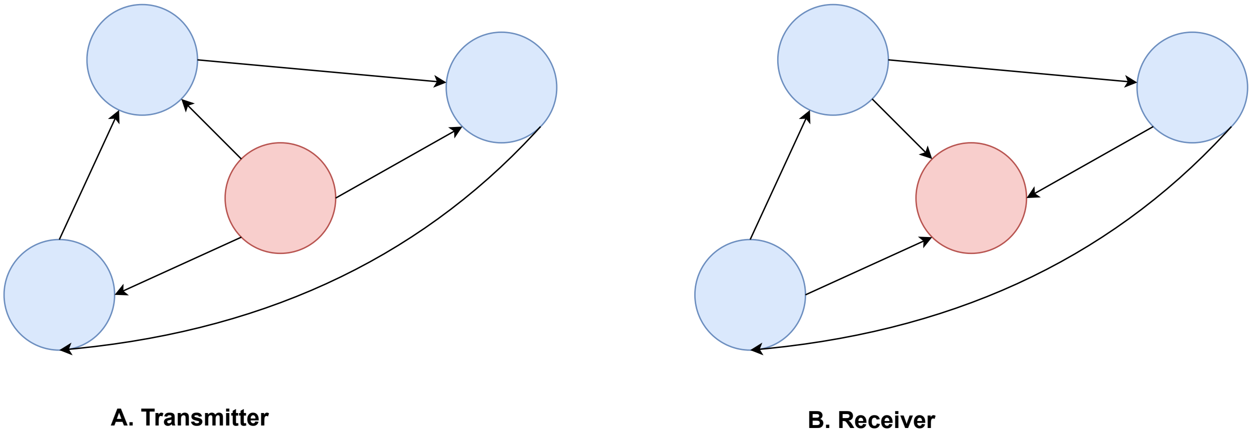

Figure 6.3: A transmitter is a source node (a) and a receiver is a target node (b).

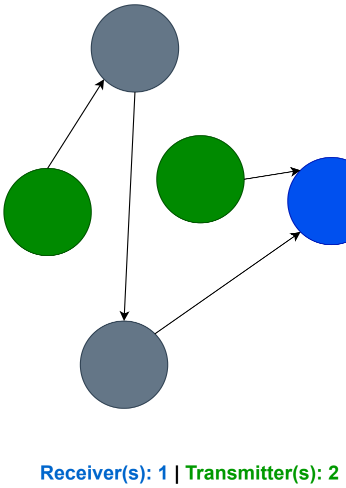

Figure 6.4: One receiver node (Blue) and two transmitter nodes (Green). The Receiver Transmitter Ratio is 0.5.

all positive real numbers for both x_i and y_i. First the similarity coefficient $J_W(x, y)$ must be determined through the summation of the minimum x_i and y_i values divided by the summation of the maximum x_i and y_i values (Equation 6.9). To calculate the distance the similarity coefficient is subtracted from the value of 1 (Equation 6.10). In network science, the Jaccard similarity is often defined between two nodes on the basis of the intersection and union of their neighborhood sets [367]. However, note that our work uses the Jaccard similarity between discrete distributions (e.g., the degree distribution) at the graph-level, rather than between sets of neighbors at the node-level. For example, our measure takes two FCMs' set of edges and their corresponding weights and computes the Jaccard similarity coefficient. This value is then utilized to calculate the distance between the two sets.

$$J_W(x,y) = \frac{\sum_i min(x_i, y_i)}{\sum_i max(x_i, y_i)} \tag{6.9}$$

$$d_{JW}(x,y) = 1 - J_W(x,y) \tag{6.10}$$

Measuring a node's importance to a graph can be determined by various **centrality** measures and then comparing the output of these measures via **cosine similarity**. Centrality calculates the rank or importance of nodes in a graph. Some of the most common centrality measures used are betweenness, closeness, and degree [368]. Betweenness centrality measures the importance of a node by determining the shortests paths that flow through that node and the rest of the network. Furthermore, this measure can incorporate edge weights into the ranking by accounting for the lowest total edge weight to traverse a network from a node.

Similar to betweenness centrality, closeness centrality places an importance on the distance of nodes; however, this measure is focused on the average distance instead of shortest distance. This is computed by taking the shortest distance from one node to each respective node in the graph. The average distance is then computed and the lower the average distance the higher ranking a node will have. A higher closeness centrality depicts that a node is more central or important to a network.

Degree centrality focuses on the direct contact or edges associated with each node. For an undirected graph, degree is simply calculated by the summation of the number of edges of a node. For directed graphs degree centrality can be divided into two categories : In-Degree and Out-Degree. In-degree calculates the number of edges directed to the selected node whereas Out-degree is the exact opposite and computes the number of edges the selected node directs to its neighbors.

In relation to the various centralities and their differing rankings, a common issue that arises is comparing the results of various centralities. Due to the discrepancies, cosine similarity may be used to compare the rank. Cosine similarity converts vectors into normal vectors and determine how they compare against one another by computing the dot product and scaling the dot product by the magnitude of the two vectors (Equation 6.11). This computation results in output between the values -1 and 1 where -1 depicts the least amount of similarity [369].

$$\frac{A \cdot B}{\|A\| \, \|B\|} \tag{6.11}$$

Kullback-Leibler Divergence (KL Divergence) can be used in a variety of applications for classification and comparison of distributions. This is defined in Equation 6.12 by two distributions P and Q which are independent of each other. We then take the summation over all possible values of the random variable, x, for $Q(x)$ and $P(x)$which are the probabilities assigned to each value x by the distributions Q and P. The output of this metric is always positive and will only equal to zero if the two distributions are identical. The greater the value of KL divergence between two distributions, the greater the difference between them.

$$D(P\|Q) = \sum_{i=1}^{k} P_i \log \frac{P_i}{Q_i} \tag{6.12}$$

Another statistical test to measure distributions is known as **Kolmogorov-Smirnov** (KS) statistic, defined in Equation 6.13. This test is designed to compute the maximum difference between the two distributions and determine whether the select distributions are from the same cumulative distribution [370].

$$D_n = \sup_{x\in\mathbb{R}} |F_n(x) - F(x)| \tag{6.13}$$

Table 6.1: Measures in previous work or implemented for FCM comparison for the first time.

Measure	**Implementation**
Graph Density	[358]
Graph Kernels (TSP)	[358]
Number of Concepts	[358]
Clustering Coefficient	[358]
Receiver-transmitter Ratio	[358]
Weighted Jaccard similarity	Not previously implemented
Centralities and Cosine Similarity	Not previously implemented
Kullback-Leibler Divergence	Not previously implemented
Kolmogorov-Smirnov	[358]

6.2.2 Community Detection Algorithm

Community detection algorithms are used to identify groups within a network. These algorithms attempt to identify the nodes in a network that are more closely related to each other than to the rest of the network. The goal of community detection is to identify these groups in a way that maximizes the number of connections within a group and minimizes the number of connections between groups. The resulting groups of nodes are known as communities. Having these communities can help reveal the underlying structure of a network and provide insight into the relationships between the nodes.

It is important to carefully evaluate the strengths and limitations of different community detection algorithms. Different algorithms are better suited for different types of networks. Some will perform better on networks with a high degree of connectivity, while others may

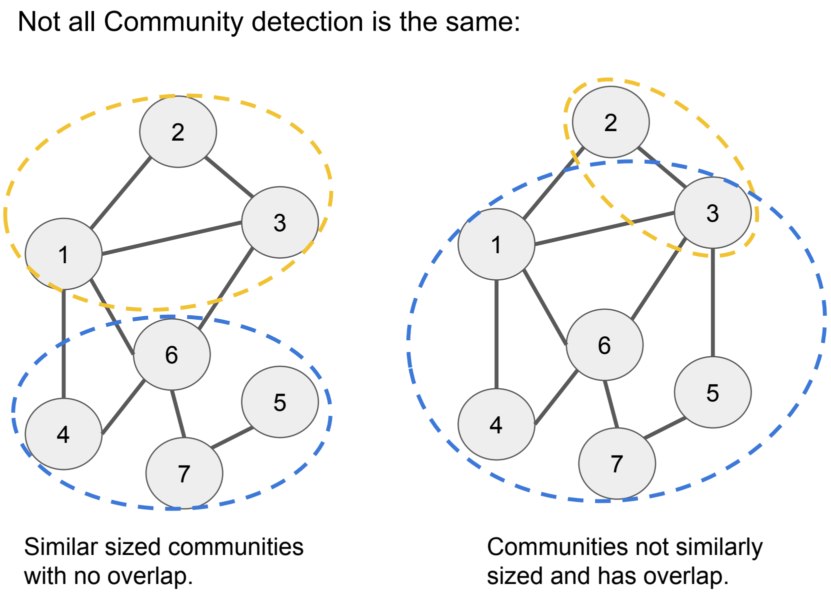

Figure 6.5: Variation of Quality from Community Detection

work better with more complex structures. Each algorithm will also have different quality communities. Some may produce high-quality communities that are well-defined, while others may produce communities that overlap as shown in figure 6.5. These communities may make possible the formation of suoer nodes. Community detection is complex and can be prone to bias and error, so iterating through different community detection algorithms and function parameters will allow you to find one that is the most balanced and best suited for the use case.

6.3 Methods

6.3.1 Case Studies

To analyze the effectiveness of utilizing various graph metrics to compare FCMs, we recreated two case studies: fast generation of heterogeneous mental models [371] and modeling joint effects on obesity [372]. Each case study was designed with three network topologies, small-world, scale free, and random. We randomly attached each agent in the ABM an attribute of an entire graph as their FCM. To simulate the population interacting with each other we first created a deep copy of the model to serve as a buffer. Once we copied the current state of the model we replicated interaction and influence of agents by looping through each agent and randomly and selecting one of their neighboring agents. Once a pair of agents was determined, we defined the influence that one agent had on another agent's FCM's concepts through a random probability. This random probability was designed so that each agent had an equal chance to influence a particular concept of the other agent. Then each agent's FCM was iterated through for each concept. At each concept, each agent was given a random probability between 0 and 1;whichever agent had the higher probability, that agent's concept value was going to influence the current concept of the neighbor with the lower probability. The influence was computed by taking the hyperbolic tangent of the two values and the buffer was updated with the result. Once every agent had been iterated through these new values were then loaded into the original model and the FCM was simulation.

For the FCM's simulation, a similar process was followed regarding the buffering of values. First, we defined our concept or focus node to be the Perceived Intake of agents and our max number of iterations to be 100 if the model did not stabilize on its own. In order to stabilize, we measured whether the Perceived Intake value had increased by 0.05. If it had not, we updated the values of the concepts nodes in its buffer by also taking the hyperbolic tangent of the concept nodes and overall summation of the weights.

6.3.2 Assigning Social Ties

After each case study was constructed, we simulated the original model. After the model was simulated we compared every pair of neighbors' FCMs in the HM. This was completed by looping through the edges of the HM. Then, both the selected agent and its neighbor's FCM were analyzed for 11 various measures that utilized the computations discussed in Section 6.2.1:

- KS for edge weight distributions
- Jaccard for edge weight distributions
- Centrality: Betweenness, Degree, Closeness Averaged and compared w Cosine Similarity
- Graph Density
- KL for edge weight distributions
- Graph TSP
- KL for node weight distributions
- KL for node, KS for edge
- Receiver-transmitter ratio
- Clustering coefficient
- Number of concepts

The computed value was assigned as the value of the edge weight between the selected agent and its neighbor (Figure 6.6). Assigning social ties was the process of assigning weighted social ties in an ABM. Each agent's FCM in the model is compared to every other connected agent (Figure 6.6). In this example, the total number of graph concepts is being used to calculate similarities between the FCMs. Agents one and two have the same number of concepts so the resulting weight between them will be 1. Agents one and three have a different number of concepts, so when calculating the weight it won't be 1 as they are not as structurally similar. To find the weight between these agents we used Equation 6.14. In this equation, we have variables n_1 and n_2 which represent the number of concepts of two different agents FCMs. So, solving for agent one and agent two, we arrive at our answer of $\frac{6}{7}$ as shown in the graph.

Measure	**Metric**	**Network Topology**							
		Scale Free				**small-world**			
		Algorithm							
		chinese-whispers	**der**	**paris**	**pycombo**	**chinese-whispers**	**der**	**paris**	**pycombo**
Average # of Agents	**Clustering Coefficient**	15.1	361.0	128.7	50.7	5.8	361.0	193.1	38.5
	# of Concepts	102.2	361.0	135.6	48.9	12.1	361.0	240.7	45.1
	Graph Density	16.4	361.0	83.5	48.2	5.9	361.0	185.3	36.3
	R/T Ratio	104.7	361.0	135.6	48.9	12.1	361.0	240.7	45.1
	TSP	15.7	361.0	123.2	48.1	5.9	361.0	187.7	32.0
Max # of Agents	**Clustering Coefficient**	306.0	414.3	268.6	123.5	13.0	375.4	235.4	44.0
	# of Concepts	532.7	448.9	276.1	123.3	27.7	374.1	256.0	46.0
	Graph Density	331.6	411.9	194.1	125.8	13.7	371.0	223.8	43.3
	R/T Ratio	530.0	422.8	276.1	123.3	27.3	373.0	256.0	46.0
	TSP	305.8	403.3	249.4	126.3	13.1	370.0	223.6	41.6
Min # of Agents	**Clustering Coefficient**	1.9	307.7	22.4	11.2	3.0	346.6	150.6	33.3
	# of Concepts	2.9	273.1	30.9	6.7	2.6	347.9	210.0	45.0
	Graph Density	1.9	310.1	11.6	11.9	3.0	351.0	153.8	29.6
	R/T Ratio	2.8	299.2	30.9	6.7	2.5	349.0	210.0	45.0
	TSP	1.9	318.7	17.9	7.9	3.0	352.0	147.5	21.6
# of Communities	**Clustering Coefficient**	55.2	2.0	15.7	14.6	123.8	2.0	4.3	18.8
	# of Concepts	10.6	2.0	13.1	15.1	59.8	2.0	3.0	16.0
	Graph Density	51.4	2.0	19.9	15.3	122.9	2.0	4.2	19.9
	R/T Ratio	10.8	2.0	13.1	15.1	59.9	2.0	3.0	16.0
	TSP	54.3	2.0	10.0	15.3	123.1	2.0	4.0	22.6

Table 6.2: Exploration of community detection algorithms.

$$1 - abs\frac{(n_1 - n_2)}{(n_1 + n_2)} \tag{6.14}$$

6.3.3 Clustering with a Community Detection Algorithm

Once every pair of agents were assigned a social tie, we transitioned to utilizing a community detection algorithm on the ABM to cluster agents. When determining how to cluster our agents with community detection algorithms, we were focused on avoiding super clusters (i.e., large grouping of agents), overlapping clusters (i.e., agents were a part of multiple communities), and a large amount of small communities. To find the most effective community

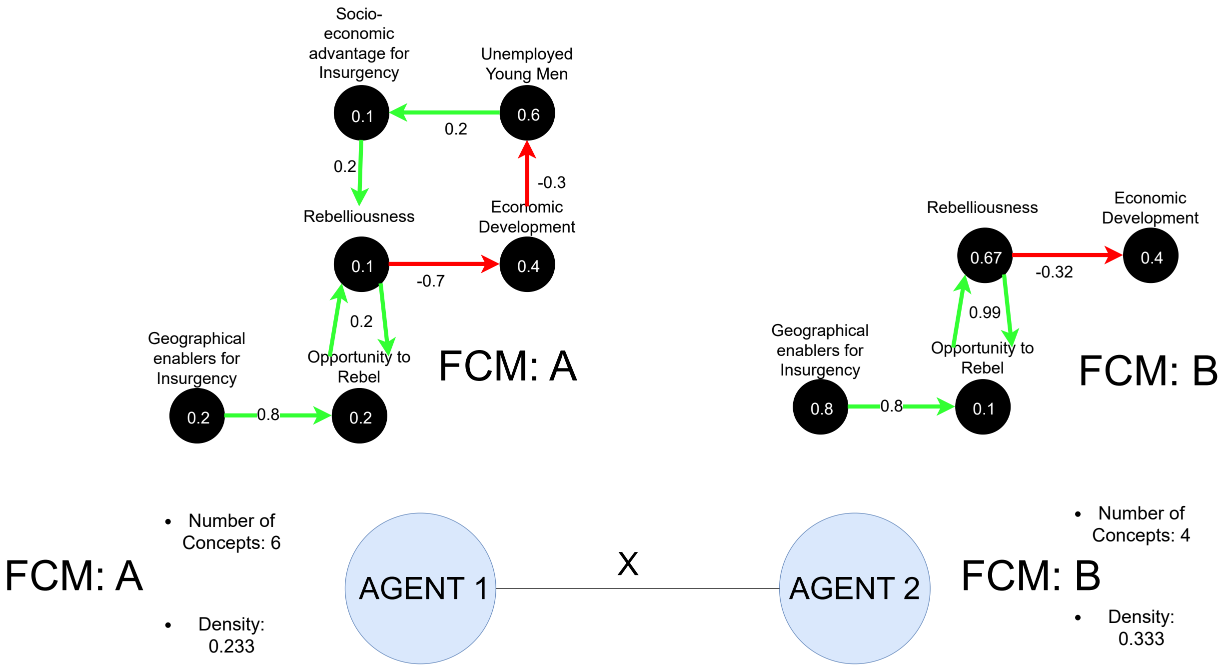

Figure 6.6: Assigning social ties, where X can be various metrics.

detection algorithm we examined a variety of detection algorithms from NetworkX that included the weight of edges during community detection. From our initial search, we narrowed down four algorithms: chinesewhispers [373], DER [374], paris [375], and pycombo [376]. We then selected one algorithm for our work by comparing the four algorithms performance on the CMAES case study for both the small-world and scale free network topology. To meet our criteria above we recorded four values: (i) the number of communities, (ii) the average number of agents in a community, (iii) the number of agents in the largest community, (iiii) the number of agents in the smallest community (Table 6.2). Our analysis determined that chinesewhispers was the best algorithm to use due it having the most variable distributions depending on the measure and network topology. For example, the average number of communities for chinesewhispers for a scale free network and the metric clustering coefficient was 55.2 where as the same network topology, but different metric such as Receiver Transmitter ratio was 10.8. These results illustrated that chinesewhispers was able to balance the variety of metrics and not analyze metrics as the exact same (e.g., DER results in 2 communities every time and pycombo results in approximately 15 communities every time).

After determining chinesewhispers as our detection algorithm, we clustered the HM by focusing on the social ties computed for every pair of agents. Once these communities were established, we iterated through each cluster, calculated the sum of each agent's FCM's concept values, and then selected an agent that represented a median of these values. This agent was selected to be representative of the communities aggregate concept values. Once an agent was selected as a representative of each community, we rebuilt the HM with the representative of each community, and connected the representative agents by verifying two communities had a edge(s) to each other from the previous model. Once these reduced HM were constructed, we restored the initial values of each agent before the original model was simulated. Finally, we simulated the reduced HM with the same ruleset as before and collected the output for each run. To analyze the impact of reducing HMs by creating super nodes, we calculated the KL Divergence between each distribution, recorded the number of reduced nodes, measured common statistics such as mean, quartile ranges, and standard deviation, and plotted the most similar distributions to the original model as violin plots.

Algorithm 1 Algorithm to Reduce HMs

```
create communities;
for each cluster in communities
    calculate sum of each agent's FCM concept values;
    select an agent as median of these values to represent the community;
//Build Reduced HM
for each representative agent
    connect to representatives of other communities with edge(s) from previous HM;
    rebuild HM with representative agents;
//Restore Initial Values of Agents:
for each agent
    restore initial values;
//Simulate Reduced HM:
run simulation with same ruleset as before;
collect output for each run;
//Analyze Impact of Reducing HMs:
calculate KL divergence between each distribution;
record number of reduced nodes;
measure common statistics (mean, quartile ranges, standard deviation);
plot most similar distributions to original model as violin plots;
```

6.4 Results

6.4.1 CMAES

To capture diversity in individual thought and behavior we utilized a variety of heterogeneous FCMs. This was accomplished by applying our previous work that created 722 unique FCMs from longitudinal data [371]. CMA-ES was integrated in our work to establish a FCM for our population of 722 agents in each of the three graph topologies for specific concepts regarding nutrition intake (Table 6.3).

6.4.2 Obesity

Due to obesity being shaped by a variety of interacting psycho-social factors in an environment, HMs may be deployed to understand the complexity surrounding the concept [377]. In previous work, we analyzed experts' knowledge pertaining to obesity among Canadian adults and the social factors that attributed to the prevalence of obesity. First, the FCM was created from an original system dynamics model [377] by aggregating experts' knowledge on obesity and then simplified due to the availability of operationalizing current data. More importantly, we introduced the concept of *knowledge* which impacted physical exercise and food intake in the FCM. We wanted to increase the heterogeneity of the FCM to resemble that of CMAES so we created the FCM and varied the edge weights for 722 FCMs. These were initialized by a random uniform distribution between -1.0 and 1.0 for each edge between the defined concepts in the original FCM. Once created, the FCMs were randomly assigned to the population of 722 agents for the three topologies where every agent in the same topology had a unique FCM. The simulation then followed the same rules as CMAES except the focus node was "Obesity".

For both case studies, we analyzed the output of the new hybrid models to their original model in three ways: (i) KL divergence between the distributions of output values, (ii) violin plots of the distributions, and (iii) statistical measures such as mean, median, and quartile ranges. We reported the KL divergence between the two distributions of each metric's HM and the original model (Table 6.5) and found that most distributions were similar with the majority of values being less than. We further analyzed these results by plotting the most similar distributions for each case study in Figure 6.7 and Figure 6.8. Finally we created a Table 6.6 that depicts the mean, standard deviation, minimum value, maximum value, and quartile ranges for each case study, every topology, and all measures.

6.5 Conclusion

In our work, we provided a comprehensive analysis of the impact of reducing the number of nodes in an HM based on the comparison of FCMs. We incorporated three new metrics along with existing metrics to measure the similarities of FCMs of various agents and studied the impact of clustering agents into representative super agents. These simplified models were compared to the original results of the initial model to emphasize an important balance between model accuracy and computational costs. In future work, we hope to examine how various population sizes of ABMs may impact the accuracy of the model as reduction takes place. Furthermore, analyzing the exact differences in run time would allow us to better determine how valuable simplifications may be to an overall model.

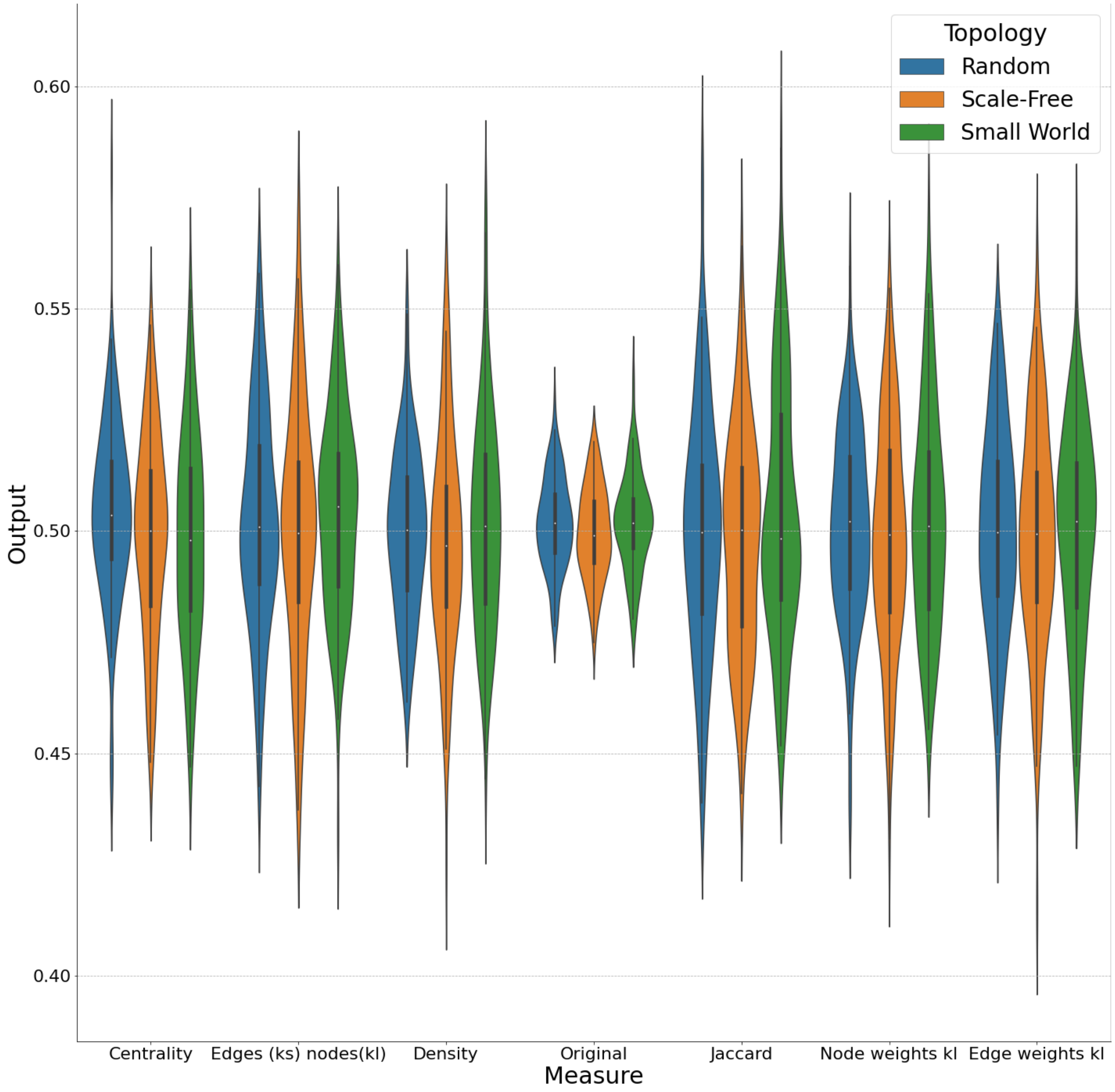

Figure 6.7: Violin Plot of Super Node Simulations CMAES

Table 6.3: CMAE's Concepts

Concept #	**Construct**	**Operationalization**
1.	Awareness	One's awareness of the number of fruits s/he thinks s/he eats?
2.	Attitude	One's belief that eating 2 servings of fruits daily is healthy.
3.	Attitude Price	One's belief that eating 2 servings of fruits daily is expensive.
4.	Self-efficacy	One's belief that s/he can eat more fruit per day in the next six months if s/he really wants to?
5.		One's belief about the extent to which it is difficult to eat more fruit in the next six months?
6.	Social-influence	One's belief that most people who are important to her/him think s/he should eat two pieces of fruit per day.
7.		One's belief that most people who are important to him/her consume two pieces of fruit per day.
8.	Intention	One's intention to eat two pieces of fruit per day?
9.	Action-planning	One has a clear plan for when s/he is going to eat more fruit.
10.		One has a clear plan for which fruit s/he is going to eat more/less.
11.		One has a clear plan for how many fruits s/he is going to eat more/less.
12.	Coping planning	One has a clear plan for what s/he is going to do when something interferes with his/her plans to eat more fruit.
13.		One has a clear plan for what s/he is going to do in situations in which it is difficult to eat more fruit.
14.	Perception of availability at home	How often does one have fruit products available at home?
15.	Visibility at home	Visibility of fruits at home

Source Node	**Target Node**	**Edge Weight**
Age	Exercise	-0.44
Income	Exercise	0.548
Income	Fatness Perceived as Negative	0.478
Fatness Perceived as Negative	Weight Discrimination	0.739
Belief in Personal Responsibility	Weight Discrimination	0.578
Obesity	Weight Discrimination	0.840
Weight Discrimination	Depression	0.732
Exercise	Depression	-0.649
Exercise	Obesity	-0.638
Depression	Anti-Depressants	0.592
Anti-Depressants	Obesity	0.528
Anti-Depressants	Food Intake	0.526
Food Intake	Obesity	0.637
Knowledge	Food Intake	-0.500
Knowledge	Exercise	0.500
Obesity	Physical Health	-0.795
Exercise	Physical Health	0.860
Stress	Depression	0.540
Stress	Food Intake	0.607
Stress	Physical Health	-0.694

Table 6.4: Nutrition FCM's Edge Value

Topology	**Measure**	**Case Study**	
		CMAES	**NUTR**
		Entropy	**Entropy**
Scale Free	**KS Edges**	0.000870775	0.008200573
	Jaccard	0.001041824	0.000768558
	Centrality	0.000805587	0.015100711
	Density	0.000915756	0.010683189
	Edge KL	0.001147539	0.00879268
	TSP	0.000712275	0.008513862
	Node KL	0.000981851	0.000910494
	Graphs	0.001265705	0.000966754
	RT	0.015818707	0.01707571
	Clustering	0.000957229	0.012937348
	Concepts	0.009017314	0.012548926
small-world	**KS Edges**	0.000887428	0.0028738
	Jaccard	0.00114878	0.000944116
	Centrality	0.000921387	0.002506133
	Density	0.001132987	0.002756311
	Edge KL	0.000898797	0.001757961
	TSP	0.000976396	0.002445733
	NodeWeights	0.00102551	0.001044938
	Graphs	0.000711031	0.001006291
	RT	0.002344465	0.002411796
	Clustering	0.001190033	0.002115926
	Concepts	0.002385118	0.002533634
Random	**KS Edges**	0.000858849	0.004756609
	Jaccard	0.001229995	0.000699844
	Centrality	0.000587468	0.004140896
	Density	0.000635022	0.005002704
	Edge KL	0.000803183	0.004376142
	TSP	0.00057372	0.00363466
	Node KL	0.000644129	0.000897676
	Graphs	0.000922512	0.000898402
	RT	0.004680375	0.004151029
	Clustering	0.000528615	0.00463623
	Concepts	0.003638542	0.003159536

Table 6.5: Comparison of Case Studies' Distributions of Output via KL Divergence

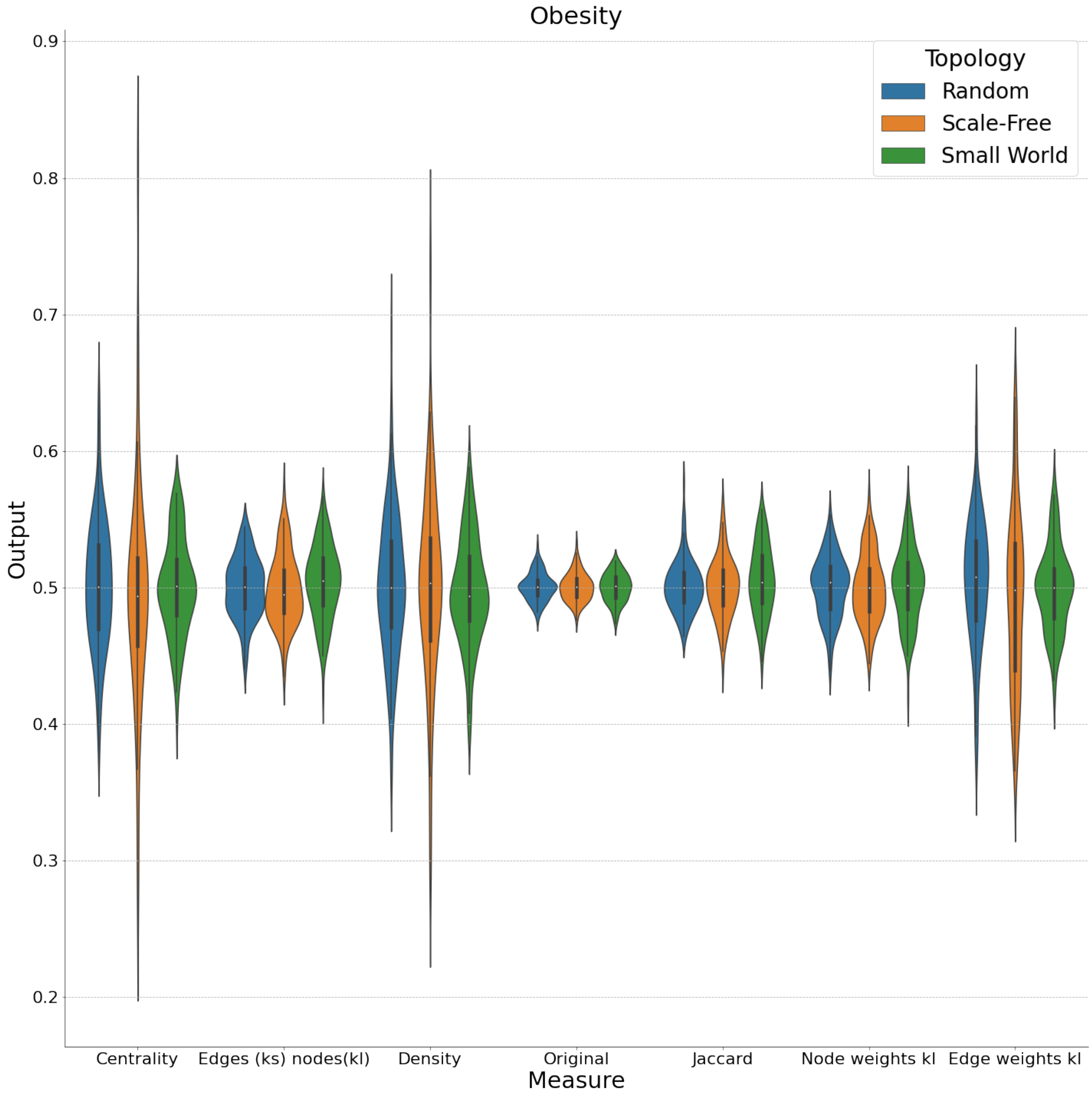

Figure 6.8: Violin Plot of Super Node Simulations Obesity

Table 6.6: The output is computed at the end of each simulation by taking the concept node value and average it across 100 runs.

		Nutrition								**CMAES**						
		Output								**Output**						
Topology	**Measure**	**mean**	**std**	**min**	**25%**	**50%**	**75%**	**max**		**mean**	**std**	**min**	**25%**	**50%**	**75%**	**max**
Random	**Original**	0.501	0.010	0.476	0.494	0.501	0.506	0.531		0.502	0.010	0.479	0.495	0.502	0.508	0.529
	centrality	0.502	0.047	0.385	0.470	0.501	0.531	0.643		0.504	0.020	0.444	0.494	0.504	0.516	0.581
	clustering	0.503	0.048	0.382	0.474	0.505	0.529	0.623		0.502	0.019	0.450	0.490	0.498	0.514	0.556
	compare graphs	0.500	0.022	0.440	0.485	0.500	0.515	0.544		0.502	0.024	0.442	0.488	0.501	0.519	0.558
	concepts	0.502	0.041	0.420	0.473	0.507	0.530	0.588		0.499	0.044	0.389	0.465	0.496	0.530	0.604
	density	0.501	0.052	0.363	0.471	0.500	0.534	0.688		0.500	0.018	0.462	0.487	0.500	0.512	0.549
	edge weight kl	0.504	0.047	0.371	0.476	0.508	0.534	0.626		0.500	0.023	0.439	0.485	0.500	0.516	0.547
	Jaccard	0.501	0.019	0.464	0.489	0.500	0.511	0.577		0.500	0.027	0.439	0.481	0.500	0.515	0.581
	KS edges	0.504	0.051	0.373	0.472	0.500	0.537	0.624		0.504	0.023	0.445	0.488	0.502	0.519	0.578
	node weights kl	0.501	0.022	0.439	0.484	0.504	0.515	0.553		0.501	0.021	0.439	0.487	0.502	0.517	0.559
	rt ratio	0.504	0.046	0.387	0.476	0.505	0.529	0.598		0.505	0.051	0.379	0.473	0.506	0.537	0.643
	tsp	0.501	0.044	0.408	0.466	0.497	0.527	0.634		0.499	0.019	0.456	0.486	0.496	0.513	0.551
Scale-Free	**Original**	0.500	0.010	0.476	0.493	0.500	0.507	0.533		0.500	0.010	0.475	0.493	0.499	0.507	0.520
	centrality	0.493	0.085	0.265	0.457	0.494	0.522	0.807		0.499	0.022	0.448	0.483	0.500	0.514	0.546
	clustering	0.494	0.076	0.200	0.461	0.498	0.528	0.736		0.499	0.024	0.443	0.484	0.499	0.518	0.546
	compare graphs	0.499	0.026	0.435	0.481	0.495	0.513	0.571		0.500	0.028	0.437	0.484	0.500	0.516	0.568
	concepts	0.504	0.079	0.266	0.475	0.505	0.541	0.712		0.504	0.070	0.267	0.482	0.500	0.522	0.832
	density	0.500	0.073	0.280	0.461	0.503	0.537	0.748		0.498	0.024	0.425	0.483	0.497	0.510	0.559
	edge weight kl	0.492	0.065	0.365	0.440	0.498	0.532	0.639		0.499	0.025	0.416	0.484	0.499	0.513	0.561
	Jaccard	0.500	0.022	0.441	0.487	0.501	0.513	0.562		0.498	0.025	0.441	0.479	0.500	0.514	0.564
	KS edges	0.500	0.064	0.350	0.454	0.493	0.548	0.652		0.497	0.022	0.448	0.485	0.496	0.509	0.592
	node weights kl	0.500	0.025	0.444	0.483	0.500	0.514	0.567		0.499	0.025	0.431	0.482	0.499	0.518	0.555
	rt ratio	0.496	0.098	0.251	0.442	0.493	0.519	0.895		0.504	0.089	0.201	0.461	0.494	0.535	0.903
	tsp	0.504	0.068	0.316	0.472	0.502	0.532	0.768		0.499	0.022	0.438	0.486	0.501	0.514	0.550
small-world	**Original**	0.500	0.010	0.473	0.492	0.501	0.508	0.520		0.502	0.011	0.478	0.496	0.502	0.507	0.535
	centrality	0.500	0.035	0.403	0.480	0.501	0.521	0.569		0.498	0.023	0.447	0.482	0.498	0.514	0.554
	clustering	0.499	0.035	0.426	0.472	0.496	0.522	0.597		0.501	0.025	0.445	0.483	0.503	0.520	0.555
	compare graphs	0.504	0.027	0.422	0.487	0.505	0.522	0.566		0.504	0.022	0.433	0.488	0.506	0.518	0.560
	concepts	0.502	0.039	0.416	0.479	0.498	0.530	0.592		0.497	0.036	0.430	0.471	0.497	0.516	0.635
	density	0.497	0.039	0.394	0.476	0.494	0.523	0.588		0.501	0.024	0.444	0.484	0.501	0.517	0.573
	edge weight kl	0.499	0.031	0.421	0.478	0.500	0.514	0.577		0.500	0.023	0.447	0.483	0.502	0.515	0.564
	Jaccard	0.505	0.025	0.446	0.488	0.504	0.523	0.557		0.504	0.028	0.452	0.485	0.498	0.526	0.586
	KS edges	0.501	0.039	0.421	0.473	0.502	0.525	0.612		0.501	0.023	0.444	0.486	0.502	0.514	0.554
	node weights kl	0.501	0.027	0.420	0.484	0.502	0.518	0.568		0.502	0.025	0.455	0.483	0.501	0.518	0.572
	rt ratio	0.501	0.037	0.389	0.477	0.500	0.528	0.593		0.503	0.037	0.383	0.479	0.504	0.532	0.575
	tsp	0.499	0.036	0.418	0.476	0.495	0.527	0.583		0.502	0.023	0.450	0.484	0.503	0.517	0.561

Chapter 7

Conclusion

7.0.1 Contribution

Our work demonstrates the importance of incorporating heterogeneity of human behavior to increase the realism of computational models and additionally aims to offset this incorporation of various data by lowering computational costs.

We developed an open source framework that can inject human errors (insufficient observations, superficial observations, biases, and limited abilities) into pre-existing and future Agent Based Models. Furthermore, this framework allows us to incorporate various Machine Learning models such as Decision Tree Classifiers or Logistic Regressor to aid in realistically replicating human errors.

Once we were able to replicate these errors, we shifted to demonstrating that these decision-making errors are critical to constructing accurate models. This was accomplished through a comprehensive review of improving COVID-19 vaccination models and implementation of our recommendations on our fork of a popular model known as COVASIM. These modifications to the existing COVASIM model confirm that both heterogeneous data and human error are essential to achieving expected results.

Finally, we introduced innovative measures to compare the similarities of agents' decision-making processes. These similarities are incorporated when creating super nodes to reduce the size of various case studies' agent populations. After establishing these reduced populations, we compare the simplified hybrid models to the original model's results. These processes are developed to stress the importance of maintaining accuracy while balancing the overall computational cost.

7.0.2 Future Work

Improving our Framework to Incorporate Cognitive Theories

Because there are boundless errors that humans may make, our framework for the comparison of errors is not all-encompassing. In the future, we can expand our model to account for other facets of human behavior and cognitive theories such as cognitive biases and status asymmetries [188]. This can be explored by replicating how humans may be selective in social learning through the balance theory which details how individuals assimilate new knowledge with existing knowledge [189]. Furthermore, status asymmetries would depict how particular social contacts have more social influence over one individual than other contacts. This unbalanced influence could sway the dissemination of information across particular models [190]. Ultimately, we can continue to build upon this framework and incorporate countless errors to increase the realism of our models.

Smaller Geographical Scales and Human Memory

Socio-demographics fluctuate from one geographical region to the next [333]. To account for these heterogeneous regions, we can explore loading relevant data for small-scale regions based on user specifications. For example, the race/ethnicity demographics for Memphis Tennessee are broken-down as the following: White 27.1%, African American 64.6% Asian 1.7%, and Hispanic 7.7%. In contrast, Boise Idaho follows different proportions: White 86.4%, Black 1.7%, Asian 3.4% and Hispanic 8.8% [378, 379]. These varying distributions of demographics may result in entirely different populations vaccinating over time.

It is also important to explore the longevity of human memory over time. Although humans may have experienced a situation in the past or learned previous material, some of this information may be lost over an extended duration. Our improvements in COVASIM could account for this loss of information from past observations by introducing functions from previous works [335] that reduce retained information over an extended period.

Account for Changing Beliefs Over Time

The notion of 'green computing' is all about saving energy. In a simulation, it often leads us to avoid any redundancy, thus computing only what is strictly necessary and reusing results whenever possible [380]. In a social simulation, it means that modelers can aggregate agents as a group if they are similar, compute what happens for one 'sample' agent from the group, and use that sample as the result for each individual of the group. While this practice of 'grouping agents' and reusing results does save on computations, it faces one challenge: people change over time [381]. New beliefs form, others are modified, and some are forgotten. In a simulation, it means that agents that may have shared similar beliefs at a specific moment can later differentiate. As a result, some agents may be assigned to a group for several steps, but group composition may later have to be re-done. The notion of dynamically grouping agents during a simulation has been well-researched from the perspective of dynamic or 'adaptive' workload balancing, which seeks to group agents onto compute cores for distributed simulations by creating an equal distribution of workloads while minimizing communication between cores [382, 383, 384]. In contrast to a focus on workloads, there has been a paucity of research devoted to dynamically managing groups based on the cognitive similarities of their constituting members. It would be possible to utilize graph distance metrics to analyze (i) how to assign individuals to groups based on a balance between similar beliefs and their interactions in a social network and (ii) under which conditions the composition of a group should be revised (**Figure 7.1**).

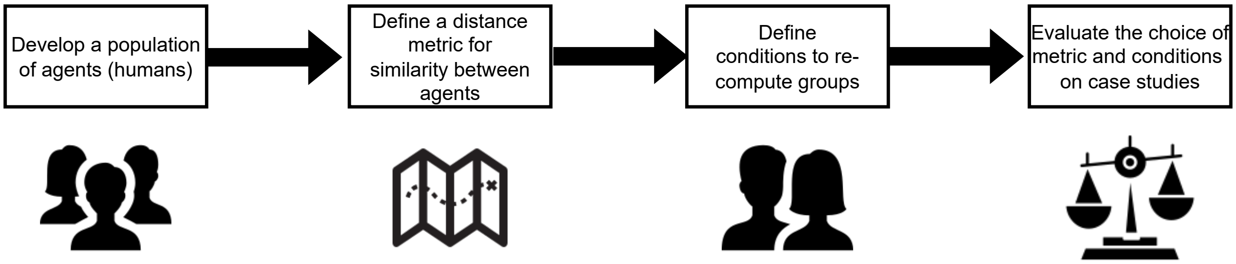

Figure 7.1: Potential future research

Bibliography

[1] Edouard Mathieu, Hannah Ritchie, Lucas Rodés-Guirao, Cameron Appel, Charlie Giattino, Joe Hasell, Bobbie Macdonald, Saloni Dattani, Diana Beltekian, Esteban Ortiz-Ospina, and et al. Coronavirus (covid-19) vaccinations. *Our World in Data*, Mar 2020. Available via `https://ourworldindata.org/covid-vaccinations`. Accessed Dec. 31, 2022.

[2] Tina Balke and Nigel Gilbert. How do agents make decisions? a survey. *Journal of Artificial Societies and Social Simulation*, 17(4):13, 2014.

[3] Dali Wang, Michael W Berry, Eric A Carr, and Louis J Gross. A parallel fish landscape model for ecosystem modeling. *Simulation*, 82(7):451–465, 2006.

[4] Charles M Macal. Everything you need to know about agent-based modelling and simulation. *Journal of Simulation*, 10(2):144–156, 2016.

[5] Nina Holden and Scott Sheffield. Scaling limits of the schelling model. *Probability Theory and Related Fields*, 176(1):219–292, 2020.

[6] Juana Castro, Stefan Drews, Filippos Exadaktylos, Joël Foramitti, Franziska Klein, Théo Konc, Ivan Savin, and Jeroen van den Bergh. A review of agent-based modeling of climate-energy policy. *Wiley Interdisciplinary Reviews: Climate Change*, 11(4):e647, 2020.

[7] Patricia L Mabry, Stephen E Marcus, Pamela I Clark, Scott J Leischow, and David Méndez. Systems science: a revolution in public health policy research, 2010.

[8] Patricia L Mabry and Robert M Kaplan. Systems science: a good investment for the public's health. *Health Education & Behavior*, 40(1_suppl):9S–12S, 2013.

[9] Herbert A Simon. Bounded rationality. In *Utility and probability*, pages 15–18. Springer, 1990.

[10] David O'Sullivan, James Millington, George Perry, and John Wainwright. Agent-based models–because they're worth it? In *Agent-based models of geographical systems*, pages 109–123. Springer, 2012.

[11] Miadreza Shafie-khah and João P. S. Catalão. A stochastic multi-layer agent-based model to study electricity market participants behavior. *IEEE Transactions on Power Systems*, 30(2):867–881, 2015.

[12] Florian Klapproth. Time and decision making in humans. *Cognitive, Affective, & Behavioral Neuroscience*, 8(4):509–524, 2008.

[13] John C Turner and Katherine J Reynolds. Self-categorization theory. *Handbook of theories in social psychology*, 2(1):399–417, 2011.

[14] Paul K Davis and Angela O'Mahony. Improving social-behavioral modeling. *Social-Behavioral Modeling for Complex Systems*, pages 15–48, 2019.

[15] Philippe J. Giabbanelli. Solving challenges at the interface of simulation and big data using machine learning. In *2019 Winter Simulation Conference (WSC)*, pages 572–583, 2019.

[16] Ashkan Negahban and Philippe J Giabbanelli. Hybrid agent-based simulation of adoption behavior and social interactions: Alternatives, opportunities, and pitfalls. *IEEE Transactions on Computational Social Systems*, 9(3):770–780, 2021.

[17] Andrew Evans. Uncertainty and error. In Alison J. Heppenstall, Andrew T. Crooks, Linda M. See, and Michael Batty, editors, *Agent-Based Models of Geographical Systems*, pages 309–346. Springer Netherlands, Dordrecht, 2012.

[18] Ethan O. Grantham and Philippe J. Giabbanelli. Creating perceptual uncertainty in agent-based models with social interactions. In *2020 Spring Simulation Conference (SpringSim)*, pages 1–12, May 2020.

[19] Sander van der Hoog. Surrogate modelling in (and of) agent-based models: A prospectus. *Computational Economics*, 53(3):1245–1263, 2019.

[20] Srikanth B. Yoginath, Maksudul Alam, and Kalyan S. Perumalla. Energy conservation through cloned execution of simulations. In *2019 Winter Simulation Conference (WSC)*, pages 2572–2582, 2019.

[21] Soufiane Bouarfa, Henk AP Blom, Richard Curran, and Mariken HC Everdij. Agent-based modeling and simulation of emergent behavior in air transportation. *Complex Adaptive Systems Modeling*, 1(1):1–26, 2013.

[22] Matthew Gibson, Joana Portugal Pereira, Raphael Slade, and Joeri Rogelj. Agent-based modelling of future dairy and plant-based milk consumption for uk climate targets. *Journal of Artificial Societies and Social Simulation*, 25(2), 2022.

[23] Miroslaw Malek. The art of creating models and models integration. In *International Workshop on Model-Based Software and Data Integration*, pages 1–7. Springer, 2008.

[24] Jay W Forrester. Urban dynamics. *IMR; Industrial Management Review (pre-1986)*, 11(3):67, 1970.

[25] Jay W Forrester. *World dynamics*. Wright-Allen Press, 1971.

[26] Jay Wright Forrester. Industrial dynamics. *Journal of the Operational Research Society*, 48(10):1037–1041, 1997.

[27] Bruce Edmonds and Ruth Meyer. *Simulating social complexity*. Springer, 2015.

[28] Robert P Abelson and Alex Bernstein. A computer simulation model of community referendum controversies. *Public Opinion Quarterly*, 27(1):93–122, 1963.

[29] Thomas C Schelling. Dynamic models of segregation. *Journal of mathematical sociology*, 1(2):143–186, 1971.

[30] Andreas Tolk and Christopher G Glazner. Representing socio-behavioral understanding with models. *Social-Behavioral Modeling for Complex Systems*, pages 545–567, 2019.

[31] Joshua M. Epstein. Why model? *Journal of Artificial Societies and Social Simulation*, 11(4):12, 2008.

[32] Andreas Tolk. Learning something right from models that are wrong: Epistemology of simulation. In *Concepts and methodologies for modeling and simulation*, pages 87–106. Springer, 2015.

[33] Emma Norling, Bruce Edmonds, and Ruth Meyer. Informal approaches to developing simulation models. In *Simulating Social Complexity*, pages 61–79. Springer, 2017.

[34] Paul Davidsson and Harko Verhagen. Types of simulation. In *Simulating Social Complexity*, pages 23–36. Springer, 2013.

[35] Christophe Le Page, Didier Bazile, Nicolas Becu, Pierre Bommel, François Bousquet, Michel Etienne, Raphael Mathevet, Véronique Souchere, Guy Trébuil, and Jacques Weber. Agent-based modelling and simulation applied to environmental management. In *Simulating social complexity*, pages 499–540. Springer, 2013.

[36] Charlotte Hemelrijk. Simulating complexity of animal social behaviour. In *Simulating Social Complexity*, pages 633–670. Springer, 2017.

[37] Saurabh Mittal, Umut Durak, and Tuncer Ören. *Guide to simulation-based disciplines: Advancing our computational future*. Springer, 2017.

[38] Rosaria Conte, Nigel Gilbert, Giulia Bonelli, Claudio Cioffi-Revilla, Guillaume Deffuant, Janos Kertesz, Vittorio Loreto, Suzy Moat, J-P Nadal, Anxo Sanchez, et al. Manifesto of computational social science. *The European Physical Journal Special Topics*, 214(1):325–346, 2012.

[39] Gert Jan Hofstede, Christopher Frantz, Jesse Hoey, Geeske Scholz, and Tobias Schröder. Artificial sociality manifesto. *Review of Artificial Societies and Social Simulation, 8th April*, 2021.

[40] Jonathan Pfautz, Paul K Davis, and Angela O'Mahony. Understanding and improving the human condition: A vision of the future for social-behavioral modeling. *Social-Behavioral Modeling for Complex Systems*, pages 1–xliii, 2019.

[41] Andrew Schotter et al. The economic theory of social institutions. *Cambridge Books*, 2008.

[42] Robert Luce, Robert R Bush, and Eugene Ed Galanter. *Handbook of mathematical psychology: I.* John Wiley, 1963.

[43] Samvel Mkhitaryan and Philippe J. Giabbanelli. How modeling methods for fuzzy cognitive mapping can benefit from psychology research. In *2021 Winter Simulation Conference (WSC)*, pages 1–12, 2021.

[44] Jennifer Badham. *A compendium of modelling techniques.* Number 12 in Integration Insights. ANU College of Medicine, Biology & Environment, May 2010.

[45] Philippe J Giabbanelli and Rik Crutzen. Using agent-based models to develop public policy about food behaviours: future directions and recommendations. *Computational and mathematical methods in medicine*, 2017, 2017.

[46] Charles M. Macal. Tutorial on agent-based modeling and simulation: Abm design for the zombie apocalypse. In *2018 Winter Simulation Conference (WSC)*, pages 207–221, 2018.

[47] Ivan Garibay, Chathika Gunaratne, Niloofar Yousefi, and Steve Scheinert. The agent-based model canvas: A modeling lingua franca for computational social science. *Social-Behavioral Modeling for Complex Systems*, pages 521–544, 2019.

[48] José Manuel Galán, Luis R. Izquierdo, Segismundo S. Izquierdo, José Ignacio Santos, Ricardo del Olmo, Adolfo López-Paredes, and Bruce Edmonds. Errors and artefacts in agent-based modelling. *Journal of Artificial Societies and Social Simulation*, 12(1):1, 2009.

[49] Frederick William Lanchester. Mathematics in warfare. *The world of mathematics*, 4(Part XX):2138–2157, 1956.

[50] Alexey Voinov, Karen Jenni, Steven Gray, Nagesh Kolagani, Pierre D Glynn, Pierre Bommel, Christina Prell, Moira Zellner, Michael Paolisso, Rebecca Jordan, et al. Tools and methods in participatory modeling: Selecting the right tool for the job. *Environmental Modelling & Software*, 109:232–255, 2018.

[51] Philippe Giabbanelli, Michele Fattoruso, and Max L Norman. Cofluences: simulating the spread of social influences via a hybrid agent-based/fuzzy cognitive maps architecture. In *Proceedings of the 2019 ACM SIGSIM conference on principles of advanced discrete simulation*, pages 71–82, 2019.

[52] Antonie J. Jetter and Kasper Kok. Fuzzy cognitive maps for futures studies—a methodological assessment of concepts and methods. *Futures*, 61:45–57, 2014.

[53] Osonde Osoba and Bart Kosko. Causal modeling with feedback fuzzy cognitive maps. *Social-Behavioral Modeling for Complex Systems*, pages 587–615, 2019.

[54] Brian Moon, Robert R Hoffman, Joseph Novak, and Alberto Canas. *Applied concept mapping: Capturing, analyzing, and organizing knowledge*. CRC Press, 2011.

[55] Samvel Mkhitaryan, Philippe Giabbanelli, Maciej K Wozniak, Gonzalo Nápoles, Nanne De Vries, and Rik Crutzen. Fcmpy: a python module for constructing and analyzing fuzzy cognitive maps. *PeerJ Computer Science*, 8:e1078, 2022.

[56] Samvel Mkhitaryan, Philippe J Giabbanelli, Nanne K de Vries, and Rik Crutzen. Dealing with complexity: How to use a hybrid approach to incorporate complexity in health behavior interventions. *Intelligence-Based Medicine*, 3:100008, 2020.

[57] Zhong Li. *Fuzzy chaotic systems*. Springer, 2006.

[58] Philippe J Giabbanelli. Modelling the spatial and social dynamics of insurgency. *Security Informatics*, 3(1):1–15, 2014.

[59] Eric A. Lavin and Philippe J. Giabbanelli. Analyzing and simplifying model uncertainty in fuzzy cognitive maps. In *2017 Winter Simulation Conference (WSC)*, pages 1868–1879, 2017.

[60] Eric A Lavin, Philippe J Giabbanelli, Andrew T Stefanik, Steven A Gray, and Robert Arlinghaus. Should we simulate mental models to assess whether they agree? In *Proceedings of the Annual Simulation Symposium*, pages 1–12, 2018.

[61] Payam Aminpour, Heike Schwermer, and Steven Gray. Do social identity and cognitive diversity correlate in environmental stakeholders? a novel approach to measuring cognitive distance within and between groups. *Plos one*, 16(11):e0244907, 2021.

[62] Francisco Aparecido Rodrigues. Network centrality: an introduction. In *A mathematical modeling approach from nonlinear dynamics to complex systems*, pages 177–196. Springer, 2019.

[63] Jennifer Golbeck. Chapter 3 - network structure and measures. In Jennifer Golbeck, editor, *Analyzing the Social Web*, pages 25–44. Morgan Kaufmann, Boston, 2013.

[64] Jennifer Golbeck. Chapter 21 - analyzing networks. In Jennifer Golbeck, editor, *Introduction to Social Media Investigation*, pages 221–235. Syngress, Boston, 2015.

[65] Thomas W Valente, Kathryn Coronges, Cynthia Lakon, and Elizabeth Costenbader. How correlated are network centrality measures? *Connections (Toronto, Ont.)*, 28(1):16, 2008.

[66] Andreas Christoforou and Andreas S. Andreou. A framework for static and dynamic analysis of multi-layer fuzzy cognitive maps. *Neurocomputing*, 232:133–145, 2017. Advances in Fuzzy Cognitive Maps Theory.

[67] Marta Olazabal and Unai Pascual. Use of fuzzy cognitive maps to study urban resilience and transformation. *Environmental Innovation and Societal Transitions*, 18:18–40, 2016.

[68] Veysel Çoban and Sezi Çevik Onar. Modelling solar energy usage with fuzzy cognitive maps. *Intelligence systems in environmental management: theory and applications*, pages 159–187, 2017.

[69] Derek L Hansen, Ben Shneiderman, Marc A Smith, and Itai Himelboim. Social network analysis: measuring, mapping, and modeling collections of connections. *Analyzing social media networks with NodeXL*, pages 31–51, 2020.

[70] Mamoon Obiedat and Sandhya Samarasinghe. A new method for identifying the central nodes in fuzzy cognitive maps using consensus centrality measure. In *Proceedings of 19th International Congress on Modelling and Simulation*, pages 1084–1091. Modelling and Simulation Society of Australia and New Zealand, 2011.

[71] Byung Sung Yoon and Antonie J. Jetter. Comparative analysis for fuzzy cognitive mapping. In *2016 Portland International Conference on Management of Engineering and Technology (PICMET)*, pages 1897–1908, 2016.

[72] Pasquale Marcello Falcone and Salvatore Paolo De Rosa. Use of fuzzy cognitive maps to develop policy strategies for the optimization of municipal waste management: A case study of the land of fires (italy). *Land Use Policy*, 96:104680, 2020.

[73] Konstantinos Papageorgiou, Gustavo Carvalho, Elpiniki I. Papageorgiou, Dionysis Bochtis, and George Stamoulis. Decision-making process for photovoltaic solar energy sector development using fuzzy cognitive map technique. *Energies*, 13(6), 2020.

[74] Marc Barthelemy. Betweenness centrality in large complex networks. *The European physical journal B*, 38(2):163–168, 2004.

[75] Xinbo Gao, Bing Xiao, Dacheng Tao, and Xuelong Li. A survey of graph edit distance. *Pattern Analysis and applications*, 13(1):113–129, 2010.

[76] Philippe J Giabbanelli, Andrew A Tawfik, and Vishrant K Gupta. Learning analytics to support teachers' assessment of problem solving: A novel application for machine learning and graph algorithms. *Utilizing learning analytics to support study success*, pages 175–199, 2019.

[77] Christopher WH Davis, Philippe J Giabbanelli, and Antonie J Jetter. The intersection of agent based models and fuzzy cognitive maps: a review of an emerging hybrid modeling practice. In *2019 Winter Simulation Conference (WSC)*, pages 1292–1303. IEEE, 2019.

[78] Philippe J Giabbanelli, Steven A Gray, and Payam Aminpour. Combining fuzzy cognitive maps with agent-based modeling: Frameworks and pitfalls of a powerful hybrid modeling approach to understand human-environment interactions. *Environmental modelling & software*, 95:320–325, 2017.

[79] Thomas M Mitchell et al. *Machine learning*. McGraw-Hill, Inc., New York, NY, USA, 1997.

[80] Iqbal H Sarker. Machine learning: Algorithms, real-world applications and research directions. *SN Computer Science*, 2(3):1–21, 2021.

[81] Ravinder Ahuja, Aakarsha Chug, Shaurya Gupta, Pratyush Ahuja, and Shruti Kohli. Classification and clustering algorithms of machine learning with their applications. In *Nature-inspired computation in data mining and machine learning*, pages 225–248. Springer, 2020.

[82] Michael W Berry, Azlinah Mohamed, and Bee Wah Yap. *Supervised and unsupervised learning for data science*. Springer, 2019.

[83] Mohammed J Zaki and Wagner Meira Jr. *Data Mining and Machine Learning: Fundamental Concepts and Algorithms*. Cambridge University Press, 2020.

[84] Tammy Jiang, Jaimie L Gradus, and Anthony J Rosellini. Supervised machine learning: a brief primer. *Behavior Therapy*, 51(5):675–687, 2020.

[85] In Lee and Yong Jae Shin. Machine learning for enterprises: Applications, algorithm selection, and challenges. *Business Horizons*, 63(2):157–170, 2020.

[86] Elpiniki I Papageorgiou. Learning algorithms for fuzzy cognitive maps—a review study. *IEEE Transactions on Systems, Man, and Cybernetics, Part C (Applications and Reviews)*, 42(2):150–163, 2011.

[87] Dale K Brearcliffe and Andrew Crooks. Creating intelligent agents: Combining agent-based modeling with machine learning. In *Proceedings of the 2020 Conference of The Computational Social Science Society of the Americas*, pages 31–58. Springer, 2021.

[88] William Rand. Machine learning meets agent-based modeling: When not to go to a bar. In *Conference on Social Agents: Results and Prospects*, 2006.

[89] Ellen-Wien Augustijn, Shaheen A. Abdulkareem, Mohammed Hikmat Sadiq, and Ali A. Albabawat. Machine learning to derive complex behaviour in agent-based modellzing. In *2020 International Conference on Computer Science and Software Engineering (CSASE)*, pages 284–289, 2020.

[90] Christopher B. Lutz, Philippe J. Giabbanelli, Andrew Fisher, and Vijay K. Mago. How many costly simulations do we need to create accurate metamodels? a case study on predicting hiv viral load in response to clinically relevant intervention scenarios. In *2021 Annual Modeling and Simulation Conference (ANNSIM)*, pages 1–12, 2021.

[91] Christopher B Lutz and Philippe J Giabbanelli. When do we need massive computations to perform detailed covid-19 simulations? *Advanced Theory and Simulations*, 5(2):2100343, 2022.

[92] Hamdi Kavak, Jose J Padilla, Christopher J Lynch, and Saikou Y Diallo. Big data, agents, and machine learning: towards a data-driven agent-based modeling approach. In *Proceedings of the Annual Simulation Symposium*, ANSS '18, pages 1–12, San Diego, CA, USA, 2018. Society for Computer Simulation International.

[93] Maria Isabel Aldinhas Ferreira. Cognitive architectures: The dialectics of agent/environment. In *Cognitive Architectures*, pages 1–12. Springer, 2019.

[94] Samarth Swarup. Adequacy: what makes a simulation good enough? In *2019 Spring Simulation Conference (SpringSim)*, pages 1–12. IEEE, 2019.

[95] Paul M Torrens and Atsushi Nara. Modeling gentrification dynamics: A hybrid approach. *Computers, environment and urban systems*, 31(3):337–361, 2007.

[96] Virginia Dignum and Frank Dignum. Agents are dead. long live agents! In *Proceedings of the 19th International Conference on Autonomous Agents and MultiAgent Systems*, pages 1701–1705, 2020.

[97] William G. Kennedy. Modelling human behaviour in agent-based models. In Alison J. Heppenstall, Andrew T. Crooks, Linda M. See, and Michael Batty, editors, *Agent-Based Models of Geographical Systems*, pages 167–179. Springer Netherlands, Dordrecht, 2012.

[98] Dimitris Kremmydas, Ioannis N. Athanasiadis, and Stelios Rozakis. A review of agent based modeling for agricultural policy evaluation. *Agricultural Systems*, 164:95–106, 2018.

[99] Amin Khademi, Donglan Zhang, Philippe J Giabbanelli, Shirley Timmons, Chengqian Luo, and Lu Shi. An agent-based model of healthy eating with applications to hypertension. In *Advanced Data Analytics in Health*, pages 43–58. Springer, 2018.

[100] Ida NS Djenontin, Arika Ligmann-Zielinska, and Leo C Zulu. Landscape-scale effects of farmers' restoration decision making and investments in central malawi: an agent-based modeling approach. *Journal of Land Use Science*, 17(1):281–306, 2022.

[101] David Burden and Maggi Savin-Baden. *Virtual humans: Today and tomorrow*. Chapman and Hall/CRC, 2019.

[102] Benjamin Nyblade, Angela O'Mahony, and Katharine Sieck. Building on social science: Theoretic foundations for modelers. *Social-Behavioral Modeling for Complex Systems*, pages 63–99, 2019.

[103] Jieting Luo and Mehdi Dastani. Modeling affective reaction in multi-agent systems. In *Proceedings of the 21st International Conference on Autonomous Agents and Multiagent Systems*, pages 1681–1683, 2022.

[104] Herbert Simon. A behavioral model of rational choice. *Models of man, social and rational: Mathematical essays on rational human behavior in a social setting*, pages 241–260, 1957.

[105] Ron Sun. Cognitive social simulation for policy making. *Policy Insights from the Behavioral and Brain Sciences*, 5(2):240–246, 2018.

[106] Swapna Thorve, Zhihao Hu, Kiran Lakkaraju, Joshua Letchford, Anil Vullikanti, Achla Marathe, and Samarth Swarup. A framework for the comparison of agent-based models. *Autonomous Agents and Multi-Agent Systems*, 36(2):1–24, 2022.

[107] Christopher Vendome, Dhananjai M Rao, and Philippe J Giabbanelli. How do modelers code artificial societies? investigating practices and quality of netlogo codes from large repositories. In *2020 Spring Simulation Conference (SpringSim)*, pages 1–12. IEEE, 2020.

[108] Philippe J Giabbanelli. Solving challenges at the interface of simulation and big data using machine learning. In *2019 Winter Simulation Conference (WSC)*, pages 572–583. IEEE, 2019.

[109] Marco Hauff and Annika Lurz. Agent-based models using artificial intelligence: A literature review. In *Proceedings of the 2022 Pacific Asia Conference on Information Systems*, volume 106, page 1265, 2022.

[110] Ashkan Negahban. Neural networks and agent-based diffusion models. In *2017 Winter Simulation Conference (WSC)*, pages 1407–1418. IEEE, 2017.

[111] Rachel L Kendal, Neeltje J Boogert, Luke Rendell, Kevin N Laland, Mike Webster, and Patricia L Jones. Social learning strategies: Bridge-building between fields. *Trends in cognitive sciences*, 22(7):651–665, 2018.

[112] Olivier Morin, Pierre Olivier Jacquet, Krist Vaesen, and Alberto Acerbi. Social information use and social information waste. *Philosophical Transactions of the Royal Society B*, 376(1828):20200052, 2021.

[113] Mehdi Dastani and Leendert Van Der Torre. A classification of cognitive agents. In *Proceedings of the Twenty-Fourth Annual Conference of the Cognitive Science Society*, pages 256–261. Routledge, 2002.

[114] Iuliia Kotseruba and John K Tsotsos. 40 years of cognitive architectures: core cognitive abilities and practical applications. *Artificial Intelligence Review*, 53(1):17–94, 2020.

[115] R Sun. Cognitive modeling. In P. Atkinson, S. Delamont, A. Cernat, J.W. Sakshaug, and R.A. Williams, editors, *SAGE Research Methods Foundations*. SAGE, 2020.

[116] Mohammad Ramshani, Xueping Li, Anahita Khojandi, and Lorna Treffert. An optimization via agent-based simulation framework to integrate stochastic programming with human introduced uncertainty. In *2019 Winter Simulation Conference (WSC)*, pages 809–818, 2019.

[117] Julia Schindler. On emergent errors in agent-based models-the need for fundamental research, 2011.

[118] Wander Jager. Enhancing the realism of simulation (eros): On implementing and developing psychological theory in social simulation. *Journal of Artificial Societies and Social Simulation*, 20(3):14, 2017.

[119] Mathieu Bourgais, Patrick Taillandier, and Laurent Vercouter. Ben: An agent architecture for explainable and expressive behavior in social simulation. In Davide Calvaresi, Amro Najjar, Michael Schumacher, and Kary Främling, editors, *Explainable, Transparent Autonomous Agents and Multi-Agent Systems*, pages 147–163, Cham, 2019. Springer International Publishing.

[120] John E Laird, Allen Newell, and Paul S Rosenbloom. Soar: An architecture for general intelligence. *Artificial intelligence*, 33(1):1–64, 1987.

[121] John R. Anderson and Christian J. Lebiere. *The Atomic Components of Thought*. Psychology Press, 1 2014.

[122] Mathieu Bourgais, Patrick Taillandier, and Laurent Vercouter. Enhancing the behavior of agents in social simulations with emotions and social relations. In Graçaliz Pereira Dimuro and Luis Antunes, editors, *Multi-Agent Based Simulation XVIII*, pages 89–104, Cham, 2018. Springer International Publishing.

[123] Seunghan Lee, Saurabh Jain, Keeli Ginsbach, and Young-Jun Son. Dynamic-data-driven agent-based modeling for the prediction of evacuation behavior during hurricanes. *Simulation Modelling Practice and Theory*, 106:102193, 2021.

[124] Peijun Ye, Shuai Wang, and Fei-Yue Wang. A general cognitive architecture for agent-based modeling in artificial societies. *IEEE Transactions on Computational Social Systems*, 5(1):176–185, March 2018.

[125] Alexander Pokahr, Lars Braubach, Christopher Haubeck, and Jan Ladiges. Programming bdi agents with pure java. In *German Conference on Multiagent System Technologies*, pages 216–233. Springer, 2014.

[126] Parantapa Bhattacharya, A Mooij, Davide Dell'Anna, Mehdi Dastani, Brian Logan, and Samarth Swarup. Pansim+ sim-2apl: a framework for large-scale distributed simulation with complex agents. In *International Workshop on Engineering Multi-Agent Systems*, pages 1–21. Springer, 2021.

[127] Mathieu Bourgais, Patrick Taillandier, and Laurent Vercouter. Ben: An architecture for the behavior of social agents. *Journal of Artificial Societies & Social Simulation*, 23(4):1–26, 2020.

[128] Rijk Mercuur, Virginia Dignum, and Catholijn M. Jonker. Integrating social practice theory in agent-based models: A review of theories and agents. *IEEE Transactions on Computational Social Systems*, 7:1131–1145, 10 2020.

[129] F. Dignum, D. Morley, E.A. Sonenberg, and L. Cavedon. Towards socially sophisticated bdi agents. In *Proceedings Fourth International Conference on MultiAgent Systems*, pages 111–118, 2000.

[130] R Sun. The clarion cognitive architecture: Extending cognitive modeling to social simulation. In R Sun, editor, *Cognition and multi-agent interaction: From cognitive modeling to social simulation*, pages 79–99. Cambridge University Press, New York, NY, USA, 2006.

[131] Shelley D Dionne, Janaki Gooty, Francis J Yammarino, and Hiroki Sayama. Decision making in crisis: A multilevel model of the interplay between cognitions and emotions. *Organizational Psychology Review*, 8(2-3):95–124, 2018.

[132] Gian Paolo Cimellaro, Stephen Mahin, and Marco Domaneschi. Integrating a human behavior model within an agent-based approach for blasting evacuation. *Computer-Aided Civil and Infrastructure Engineering*, 34(1):3–20, 2019.

[133] Alexei V Samsonovich. Intellectual agents based on a cognitive architecture supporting humanlike social emotionality and creativity. In *International Conference on Neuroinformatics*, pages 39–50. Springer, 2018.

[134] Alexei V Samsonovich. Socially emotional brain-inspired cognitive architecture framework for artificial intelligence. *Cognitive Systems Research*, 60:57–76, 2020.

[135] Vladimir S Tsarkov, Vladislav A Enikeev, and Alexei V Samsonovich. Toward a socially acceptable model of emotional artificial intelligence. *Procedia Computer Science*, 190:771–788, 2021.

[136] Andrew Crooks, Alison Heppenstall, Nick Malleson, and Ed Manley. Agent-based modeling and the city: A gallery of applications. In Wenzhong Shi, Michael F. Goodchild, Michael Batty, Mei-Po Kwan, and Anshu Zhang, editors, *Urban Informatics*, pages 885–910. Springer Singapore, Singapore, 2021.

[137] Catriona Kennedy, Georgios Theodoropoulos, Volker Sorge, Edward Ferrari, Peter Lee, and Chris Skelcher. Aimss: An architecture for data driven simulations in the social sciences. In *International Conference on Computational Science*, pages 1098–1105. Springer, 2007.

[138] Mazhar Sajjad, Karandeep Singh, Euihyun Paik, and Chang-Won Ahn. A data-driven approach for agent-based modeling: Simulating the dynamics of family formation. *Journal of Artificial Societies and Social Simulation*, 19(1):9, 2016.

[139] Guoyin Jiang, Xiaodong Feng, Wenping Liu, and Xingjun Liu. Clicking position and user posting behavior in online review systems: A data-driven agent-based modeling approach. *Information Sciences*, 512:161–174, 2020.

[140] Alexander Amini, Igor Gilitschenski, Jacob Phillips, Julia Moseyko, Rohan Banerjee, Sertac Karaman, and Daniela Rus. Learning robust control policies for end-to-end autonomous driving from data-driven simulation. *IEEE Robotics and Automation Letters*, 5(2):1143–1150, 2020.

[141] Yinghui Pan, Jing Tang, Biyang Ma, Yifeng Zeng, and Zhong Ming. Toward data-driven solutions to interactive dynamic influence diagrams. *Knowledge and Information Systems*, 63(9):2431–2453, 2021.

[142] Shaheen A Abdulkareem, Yaseen T Mustafa, Ellen-Wien Augustijn, and Tatiana Filatova. Bayesian networks for spatial learning: a workflow on using limited survey data for intelligent learning in spatial agent-based models. *Geoinformatica*, 23(2):243–268, 2019.

[143] Haifeng Zhang, Yevgeniy Vorobeychik, Joshua Letchford, and Kiran Lakkaraju. Data-driven agent-based modeling, with application to rooftop solar adoption. *Autonomous Agents and Multi-Agent Systems*, 30(6):1023–1049, 2016.

[144] Fatema T Johora, Hao Cheng, Jörg P Müller, and Monika Sester. An agent-based model for trajectory modelling in shared spaces: a combination of expert-based and deep learning approaches. In *Proceedings of the 19th International Conference on Autonomous Agents and MultiAgent Systems*, pages 1878–1880, 2020.

[145] Koen de Koning, Tatiana Filatova, and Okmyung Bin. Capitalization of flood insurance and risk perceptions in housing prices: an empirical agent-based model approach. *Southern Economic Journal*, 85(4):1159–1179, 2019.

[146] Peggy J Liu, Jessica Wisdom, Christina A Roberto, Linda J Liu, and Peter A Ubel. Using behavioral economics to design more effective food policies to address obesity. *Applied Economic Perspectives and Policy*, 36(1):6–24, 2014.

[147] Y Tony Yang and Sara E Benjamin-Neelon. Recent progress in children's meals law in restaurants in baltimore city and california state: Making a healthy beverage option the default choice. *Preventive medicine*, 123:160–162, 2019.

[148] Gerd Gigerenzer and Wolfgang Gaissmaier. Decision making: Nonrational theories. In *International encyclopedia of the social & behavioral sciences*, pages 911–916. Elsevier, 2015.

[149] N Sánchez-Maroño, A Alonso-Betanzos, O Fontenla-Romero, J Gary Polhill, and T Craig. Empirically-derived behavioral rules in agent-based models using decision trees learned from questionnaire data. In *Agent-Based Modeling of Sustainable Behaviors*, pages 53–76. Springer, 2017.

[150] Navreet Kaur, Manuel Gonzales, Cristian Garcia Alcaraz, Laura E. Barnes, Kristen J. Wells, and Jiaqi Gong. Theory-guided randomized neural networks for decoding medication-taking behavior. In *2021 IEEE EMBS International Conference on Biomedical and Health Informatics (BHI)*, pages 1–4, 2021.

[151] Yanchang Liang, Chunlin Guo, Zhaohao Ding, and Huichun Hua. Agent-based modeling in electricity market using deep deterministic policy gradient algorithm. *IEEE Transactions on Power Systems*, 35(6):4180–4192, 2020.

[152] Dielle Horne, Romina Palermo, Markus F Neumann, Regan Housley, and Jason Bell. Can people accurately estimate the calories in food images? an optimised set of low- and high-calorie images from the food-pics database. *Appetite*, 139:189–196, 2019.

[153] Melissa Oldham and Eric Robinson. Visual weight status misperceptions of men: Why overweight can look like a healthy weight. *Journal of health psychology*, 21(8):1768–1777, 2016.

[154] Jackie Kazil, David Masad, and Andrew Crooks. Utilizing python for agent-based modeling: The mesa framework. In *International Conference on Social Computing, Behavioral-Cultural Modeling and Prediction and Behavior Representation in Modeling and Simulation*, pages 308–317. Springer, 2020.

[155] Joël Foramitti. Agentpy: A package for agent-based modeling in python. *Journal of Open Source Software*, 6(62):3065, 2021.

[156] Nicholson T Collier, Jonathan Ozik, and Eric R Tatara. Experiences in developing a distributed agent-based modeling toolkit with python. In *2020 IEEE/ACM 9th Workshop on Python for High-Performance and Scientific Computing (PyHPC)*, pages 1–12. IEEE, 2020.

[157] Kendra E Kaiser, AN Flores, and Christopher R Vernon. Janus: a python package for agent-based modeling of land use and land cover change. *Journal of Open Research Software*, 8(PNNL-SA-148545), 2020.

[158] Erez Hatna and Itzhak Benenson. The schelling model of ethnic residential dynamics: Beyond the integrated - segregated dichotomy of patterns. *Journal of Artificial Societies and Social Simulation*, 15(1):6, 2012.

[159] Robert Axelrod. The dissemination of culture: A model with local convergence and global polarization. *Journal of conflict resolution*, 41(2):203–226, 1997.

[160] Edmund Chattoe-Brown. Un drôle de type: The schelling model, calibration, specification, validation and using relevant data. In *Conference of the European Social Simulation Association*, pages 243–255. Springer, 2019.

[161] Thomas C Schelling. Models of segregation. *The American economic review*, 59(2):488–493, 1969.

[162] Marcos E Gaudiano and Jorge A Revelli. On the role of structured initial conditions in the schelling model. *Physica A: Statistical Mechanics and its Applications*, 587:126476, 2022.

[163] Janyce Eunice Gnanvi, Kolawolé Valère Salako, Gaëtan Brezesky Kotanmi, and Romain Glèlè Kakaï. On the reliability of predictions on covid-19 dynamics: A systematic and critical review of modelling techniques. *Infectious Disease Modelling*, 6:258–272, 2021.

[164] Fabian Lorig, Emil Johansson, and Paul Davidsson. Agent-based social simulation of the covid-19 pandemic: A systematic review. *JASSS: Journal of Artificial Societies and Social Simulation*, 24(3), 2021.

[165] Philippe J Giabbanelli, Jennifer Badham, Brian Castellani, Hamdi Kavak, Vijay Mago, Ashkan Negahban, and Samarth Swarup. Opportunities and challenges in developing covid-19 simulation models: Lessons from six funded projects. In *2021 Annual Modeling and Simulation Conference (ANNSIM)*, pages 1–12. IEEE, 2021.

[166] Erik Cuevas. An agent-based model to evaluate the covid-19 transmission risks in facilities. *Computers in biology and medicine*, 121:103827, 2020.

[167] Trevor S Farthing and Cristina Lanzas. Assessing the efficacy of interventions to control indoor sars-cov-2 transmission: an agent-based modeling approach. *Epidemics*, 37:100524, 2021.

[168] Christopher R Williams and Armin R Mikler. Incorporating disgust as disease-avoidant behavior in an agent-based epidemic model. In *International Conference on Social Computing, Behavioral-Cultural Modeling and Prediction and Behavior Representation in Modeling and Simulation*, pages 107–116. Springer, 2016.

[169] Junjiang Li and Philippe Giabbanelli. Returning to a normal life via covid-19 vaccines in the united states: a large-scale agent-based simulation study. *JMIR medical informatics*, 9(4):e27419, 2021.

[170] Seyed M Moghadas, Pratha Sah, Affan Shoukat, Lauren Ancel Meyers, and Alison P Galvani. Population immunity against covid-19 in the united states. *Annals of Internal Medicine*, 174(11):1586–1591, 2021.

[171] C.D.C. Cdc covid data tracker: Vaccinations in the us. https://covid.cdc.gov/covid-data-tracker/#vaccinations_vacc-total-admin-rate-total, 2022. Accessed: 2022-08-07.

[172] Refrigerating and American National Standards Institute. *Thermal environmental conditions for human occupancy*, volume 55. American Society of Heating, Refrigerating and Air-Conditioning Engineers, 2004.

[173] Covid-19 risk calculator - covid-19. https://covid-19.forhealth.org/covid-19-transmission-calculator/, 2022. Accessed: 2022-08-07.

[174] Shirley Collie, Jared Champion, Harry Moultrie, Linda-Gail Bekker, and Glenda Gray. Effectiveness of bnt162b2 vaccine against omicron variant in south africa. *New England Journal of Medicine*, 386(5):494–496, 2022.

[175] IHME. Ihme covid-19 insights blog — institute for health metrics and evaluation. https://www.healthdata.org/news-events/blogs/covid-19-insights-blog, 2022. Accessed: 2022-08-07.

[176] Abhiteja Konda, Abhinav Prakash, Gregory A Moss, Michael Schmoldt, Gregory D Grant, and Supratik Guha. Aerosol filtration efficiency of common fabrics used in respiratory cloth masks. *ACS nano*, 14(5):6339–6347, 2020.

[177] Sima Asadi, Christopher D Cappa, Santiago Barreda, Anthony S Wexler, Nicole M Bouvier, and William D Ristenpart. Efficacy of masks and face coverings in controlling outward aerosol particle emission from expiratory activities. *Scientific reports*, 10(1):1–13, 2020.

[178] Anand Sahasranaman and Henrik Jeldtoft Jensen. Dynamics of transformation from segregation to mixed wealth cities. *PloS one*, 11(11):e0166960, 2016.

[179] Luca De Sanctis and Tobias Galla. Effects of noise and confidence thresholds in nominal and metric axelrod dynamics of social influence. *Physical Review E*, 79(4):046108, 2009.

[180] Konstantin Klemm, Víctor M Eguíluz, Raúl Toral, and Maxi San Miguel. Global culture: A noise-induced transition in finite systems. *Physical Review E*, 67(4):045101, 2003.

[181] Nuno Crokidakis. Role of noise and agents' convictions on opinion spreading in a three-state voter-like model. *Journal of Statistical Mechanics: Theory and Experiment*, 2013(07):P07008, 2013.

[182] Federico Vazquez, Juan Carlos Gonzalez-Avella, Victor M Eguiluz, and Maxi San Miguel. Time-scale competition leading to fragmentation and recombination transitions in the coevolution of network and states. *Physical Review E*, 76(4):046120, 2007.

[183] Carlos Gracia-Lázaro, Fernando Quijandría, Laura Hernández, Luis Mario Floría, and Yamir Moreno. Coevolutionary network approach to cultural dynamics controlled by intolerance. *Physical Review E*, 84(6):067101, 2011.

[184] Rémi Perrier, Yérali Gandica, and Laura Hernández. The consequences of hesitation: Axelrod model with intrinsic noise. *Plos one*, 16(11):e0259295, 2021.

[185] Akond Rahman and Effat Farhana. An exploratory characterization of bugs in covid-19 software projects. *arXiv preprint arXiv:2006.00586*, 2020.

[186] John Pesavento, Andy Chen, Rayan Yu, Joon-Seok Kim, Hamdi Kavak, Taylor Anderson, and Andreas Züfle. Data-driven mobility models for covid-19 simulation. In *Proceedings of the 3rd ACM SIGSPATIAL International Workshop on Advances in Resilient and Intelligent Cities*, pages 29–38, 2020.

[187] Adrienne Grêt-Regamey, Sibyl H Huber, and Robert Huber. Actors' diversity and the resilience of social-ecological systems to global change. *Nature Sustainability*, 2(4):290–297, 2019.

[188] Manvir Singh, Alberto Acerbi, Christine A Caldwell, Étienne Danchin, Guillaume Isabel, Lucas Molleman, Thom Scott-Phillips, Monica Tamariz, Pieter Van Den Berg, Edwin JC Van Leeuwen, et al. Beyond social learning. *Philosophical Transactions of the Royal Society B*, 376(1828):20200050, 2021.

[189] Fredrik Jansson, Elliot Aguilar, Alberto Acerbi, and Magnus Enquist. Modelling cultural systems and selective filters. *Philosophical Transactions of the Royal Society B*, 376(1828):20200045, 2021.

[190] Marcela Moraes, John Gountas, Sandra Gountas, and Piyush Sharma. Celebrity influences on consumer decision making: New insights and research directions. *Journal of marketing management*, 35(13-14):1159–1192, 2019.

[191] Chris Jackson, Mallory Newall, Jocelyn Duran, and Jeremy Golden. Most americans not worrying about covid going into 2022 holidays. https://www.ipsos.com/en-us/news-polls/axios-ipsos-coronavirus-index, 2022. Accessed: 2022-08-02.

[192] Wen Wen, Chen Chen, Jiake Tang, Chunyi Wang, Mengyun Zhou, Yongran Cheng, Xiang Zhou, Qi Wu, Xingwei Zhang, Zhanhui Feng, et al. Efficacy and safety of three new oral antiviral treatment (molnupiravir, fluvoxamine and paxlovid) for covid-19: a meta-analysis. *Annals of medicine*, 54(1):516–523, 2022.

[193] Ying Liu and Qing Ye. Safety and efficacy of the common vaccines against covid-19. *Vaccines*, 10(4):513, 2022.

[194] National Center for Health Statistics. Provisional death counts for coronavirus disease 2019 (covid-19. https://www.cdc.gov/nchs/nvss/vsrr/covid19/index.htm, 2022. Accessed: 2022-08-02.

[195] Thomas Lyttelton and Emma Zang. Occupations and sickness-related absences during the covid-19 pandemic. *Journal of health and social behavior*, 63(1):19–36, 2022.

[196] Whitney Thurman, Elizabeth Heitkemper, and Karen E Johnson. Challenges facing public health nursing faculty in the united states: Covid-19 as a catalyst for change. *American Journal of Public Health*, 112(S3):S314–S320, 2022.

[197] Desiree Carver-Thomas, Dion Burns, Melanie Leung, and Naomi Ondrasek. Teacher shortages during the pandemic: How california districts are responding. *Learning Policy Institute*, 2022.

[198] Gabriela Ksinan Jiskrova. Impact of covid-19 pandemic on the workforce: from psychological distress to the great resignation. *J Epidemiol Community Health*, 76(6):525–526, 2022.

[199] Steven R Schmid and Shreyes N Melkote. Manufacturing and the great resignation. *Mechanical Engineering*, 144(3):38–43, 2022.

[200] Mihajla Gavin, Mahan Poorhosseinzadeh, and Jim Arrowsmith. The transformation of work and employment relations: Covid-19 and beyond, 2022.

[201] Nico P Pronk. Addressing covid-19 disruptions at the workplace while preparing for a postpandemic future. *ACSM's Health & Fitness Journal*, 26(3):52–55, 2022.

[202] Beamish Rita Aidan Vaziri. Covid in california: Reinfections account for 1 in 7 coronavirus cases in state. https://www.sfchronicle.com/bayarea/article/COVID-in-California-Latest-updates-about-the-17342154.php, 2022. Accessed: 2022-08-02.

[203] Tapan Behl, Ishnoor Kaur, Aayush Sehgal, Sukhbir Singh, Neelam Sharma, Md Khalid Anwer, Hafiz A Makeen, Mohammed Albratty, Hassan A Alhazmi, Saurabh Bhatia, et al. There is nothing exempt from the peril of mutation–the omicron spike. *Biomedicine & Pharmacotherapy*, 148:112756, 2022.

[204] Peter Marks. Fall 2022 covid-19 vaccine strain composition selection recommendation. https://www.fda.gov/media/159597/download, 2022. Accessed: 2022-08-03.

[205] Justin Mccarthy. Roundup of gallup covid-19 coverage. https://news.gallup.com/opinion/gallup/308126/roundup-gallup-covid-coverage.aspx, 2022. Accessed: 2022-08-03.

[206] Alec Tyson. 57% of americans say masks should be required on airplanes and public transportation. https://www.pewresearch.org/fact-tank/2022/05/11/57-of-americans-say-masks-should-be-required-on-airplanes-and-public-transportation/, 2022. Accessed: 2022-08-03.

[207] Robert P Lennon, Ray Block Jr, Eric C Schneider, Laurie Zephrin, Arnav Shah, The African American Research Collaborative, 2021 COVID Group, et al. Underserved population acceptance of combination influenza-covid-19 booster vaccines. *Vaccine*, 40(4):562–567, 2022.

[208] Peter Marks, Janet Woodcock, and Robert Califf. Covid-19 vaccination—becoming part of the new normal. *JAMA*, 327(19):1863–1864, 2022.

[209] Sawsan Abuhammad, Omar F Khabour, Karem H Alzoubi, Shaher Hamaideh, Baker A Alzoubi, Waed S Telfah, and Farah K El-Zubi. The public's attitude to and acceptance of periodic doses of the covid-19 vaccine: A survey from jordan. *PLoS One*, 17(7):e0271625, 2022.

[210] Laura Reifferscheid, Janet Sau Wun Lee, Noni E MacDonald, Manish Sadarangani, Ali Assi, Samuel Lemaire-Paquette, and Shannon E MacDonald. Transition to endemic: acceptance of additional covid-19 vaccine doses among canadian adults in a national cross-sectional survey. *BMC Public Health*, 22(1):1745, 2022.

[211] Jakob Weitzer, Brenda M Birmann, Ilja Steffelbauer, Martin Bertau, Lukas Zenk, Guido Caniglia, Manfred D Laubichler, Gerald Steiner, and Eva S Schernhammer. Willingness to receive an annual covid-19 booster vaccine in the german-speaking dach region in europe: A cross-sectional study. *The Lancet Regional Health-Europe*, 18:100414, 2022.

[212] Ryan C Lee, Howard Hu, Eric S Kawaguchi, Andre E Kim, Daniel W Soto, Kush Shanker, Jeffrey D Klausner, Sarah Van Orman, and Jennifer B Unger. Covid-19 booster vaccine attitudes and behaviors among university students and staff in the united states: The usc trojan pandemic research initiative. *Preventive Medicine Reports*, 28:101866, 2022.

[213] Yudong Tao, Chuang Yang, Tianyi Wang, Erik Coltey, Yanxiu Jin, Yinghao Liu, Renhe Jiang, Zipei Fan, Xuan Song, Ryosuke Shibasaki, et al. A survey on data-driven covid-19 and future pandemic management. *ACM computing surveys*, 55(7):1–36, 2022.

[214] Usama Bilal, Pricila H Mullachery, Alina Schnake-Mahl, Heather Rollins, Edwin McCulley, Jennifer Kolker, Sharrelle Barber, and Ana V Diez Roux. Heterogeneity in spatial inequities in covid-19 vaccination across 16 large us cities. *American journal of epidemiology*, 191(9):1546–1556, 2022.

[215] Nina B Masters, Tianyi Zhou, Lu Meng, Peng-Jun Lu, Jennifer L Kriss, Carla Black, Amel Omari, Kwanza Boone, Debora Weiss, Rosalind J Carter, et al. Geographic heterogeneity in behavioral and social drivers of covid-19 vaccination. *American Journal of Preventive Medicine*, 63(6):883–893, 2022.

[216] Joan Saldaña and Caterina Scoglio. Influence of heterogeneous age-group contact patterns on critical vaccination rates for herd immunity to sars-cov-2. *Scientific Reports*, 12(1):2640, 2022.

[217] Junjiang Li and Philippe J Giabbanelli. Identifying synergistic interventions to address covid-19 using a large scale agent-based model. In *Computational Science–ICCS 2021: 21st International Conference, Krakow, Poland, June 16–18, 2021, Proceedings, Part III*, pages 655–662. Springer, 2021.

[218] Mª Àngels Colomer, Antoni Margalida, Francesc Alos, Pilar Oliva-Vidal, Anna Vilella, and Lorenzo Fraile. Modelling the sars-cov-2 outbreak: Assessing the usefulness of protective measures to reduce the pandemic at population level. *Science of the Total Environment*, 789:147816, 2021.

[219] Navid Ghaffarzadegan, Lauren M Childs, and Uwe C TÄuber. Diverse computer simulation models provide unified lessons on university operation during a pandemic. *BioScience*, 71(2):113–114, 2021.

[220] Shuli Zhou, Suhong Zhou, Zhong Zheng, and Junwen Lu. Optimizing spatial allocation of covid-19 vaccine by agent-based spatiotemporal simulations. *GeoHealth*, 5(6):e2021GH000427, 2021.

[221] Santiago Romero-Brufau, Ayush Chopra, Alex J Ryu, Esma Gel, Ramesh Raskar, Walter Kremers, Karen S Anderson, Jayakumar Subramanian, Balaji Krishnamurthy, Abhishek Singh, et al. Public health impact of delaying second dose of bnt162b2 or mrna-1273 covid-19 vaccine: simulation agent based modeling study. *bmj*, 373, 2021.

[222] Agnieszka Truszkowska, Lorenzo Zino, Sachit Butail, Emanuele Caroppo, Zhong-Ping Jiang, Alessandro Rizzo, and Maurizio Porfiri. Predicting the effects of waning vaccine immunity against covid-19 through high-resolution agent-based modeling. *Advanced theory and simulations*, 5(6):2100521, 2022.

[223] Sherrie L Kelly, Epke A Le Rutte, Maximilian Richter, Melissa A Penny, and Andrew J Shattock. Covid-19 vaccine booster strategies in light of emerging viral variants: Frequency, timing, and target groups. *Infectious Diseases and Therapy*, 11(5):2045–2061, 2022.

[224] Matthew D Johnston, Bruce Pell, and Patrick Nelson. A mathematical study of covid-19 spread by vaccination status in virginia. *Applied Sciences*, 12(3):1723, 2022.

[225] Constantino Caetano, Maria Luísa Morgado, Paula Patrício, Andreia Leite, Ausenda Machado, André Torres, João Freitas Pereira, Sónia Namorado, Ana Sottomayor, André Peralta-Santos, et al. Measuring the impact of covid-19 vaccination and immunity waning: A modelling study for portugal. *Vaccine*, 40(49):7115–7121, 2022.

[226] Cliff C Kerr, Robyn M Stuart, Dina Mistry, Romesh G Abeysuriya, Katherine Rosenfeld, Gregory R Hart, et al. Covasim: an agent-based model of covid-19 dynamics and interventions. *PLOS Computational Biology*, 17(7):e1009149, 2021.

[227] Robert Hinch, William JM Probert, Anel Nurtay, Michelle Kendall, Chris Wymant, Matthew Hall, Katrina Lythgoe, Ana Bulas Cruz, Lele Zhao, Andrea Stewart, et al. Openabm-covid19—an agent-based model for non-pharmaceutical interventions against covid-19 including contact tracing. *PLoS computational biology*, 17(7):e1009146, 2021.

[228] Benoit Gaudou, Nghi Quang Huynh, Damien Philippon, Arthur Brugière, Kevin Chapuis, Patrick Taillandier, Pierre Larmande, and Alexis Drogoul. Comokit: A modeling kit to understand, analyze, and compare the impacts of mitigation policies against the covid-19 epidemic at the scale of a city. *Frontiers in public health*, 8:563247, 2020.

[229] Joseph Aylett-Bullock, Carolina Cuesta-Lazaro, Arnau Quera-Bofarull, Miguel Icaza-Lizaola, Aidan Sedgewick, Henry Truong, Aoife Curran, Edward Elliott, Tristan Caulfield, Kevin Fong, et al. June: open-source individual-based epidemiology simulation. *Royal Society open science*, 8(7):210506, 2021.

[230] István Z Reguly, Dávid Csercsik, János Juhász, Kálmán Tornai, Zsófia Bujtár, Gergely Horváth, Bence Keömley-Horváth, Tamás Kós, György Cserey, Kristóf Iván, et al. Microsimulation based quantitative analysis of covid-19 management strategies. *PLoS computational biology*, 18(1):e1009693, 2022.

[231] Cliff C Kerr, Dina Mistry, Robyn M Stuart, Katherine Rosenfeld, Gregory R Hart, Rafael C Núñez, Jamie A Cohen, Prashanth Selvaraj, Romesh G Abeysuriya, et al. Controlling covid-19 via test-trace-quarantine. *Nature communications*, 12(1):2993, 2021.

[232] Jamie A Cohen, Robyn M Stuart, Rafael C Núñez, Bradley Wagner, Stewart Chang, Katherine Rosenfeld, Cliff C Kerr, Michael Famulare, and Daniel J Klein. Mechanistic modeling of sars-cov-2 immune memory, variants, and vaccines. *medRxiv*, pages 2021–05, 2021.

[233] Nick Scott, Anna Palmer, Dominic Delport, Romesh Abeysuriya, Robyn M Stuart, Cliff C Kerr, Dina Mistry, Daniel J Klein, Rachel Sacks-Davis, Katie Heath, et al.

Modelling the impact of relaxing covid-19 control measures during a period of low viral transmission. *Medical Journal of Australia*, 214(2):79–83, 2021.

[234] Romesh G Abeysuriya, Dominic Delport, Robyn M Stuart, Rachel Sacks-Davis, Cliff C Kerr, Dina Mistry, Daniel J Klein, Margaret Hellard, and Nick Scott. Preventing a cluster from becoming a new wave in settings with zero community covid-19 cases. *BMC Infectious Diseases*, 22(1):1–15, 2022.

[235] Paula Sanz-Leon, Nathan J Stevenson, Robyn M Stuart, Romesh G Abeysuriya, James C Pang, Stephen B Lambert, Cliff C Kerr, and James A Roberts. Risk of sustained sars-cov-2 transmission in queensland, australia. *Scientific Reports*, 12(1):6309, 2022.

[236] Davidson H Hamer, Laura F White, Helen E Jenkins, Christopher J Gill, Hannah E Landsberg, Catherine Klapperich, Katia Bulekova, Judy Platt, Linette Decarie, Wayne Gilmore, et al. Assessment of a covid-19 control plan on an urban university campus during a second wave of the pandemic. *JAMA network open*, 4(6):e2116425–e2116425, 2021.

[237] J Panovska-Griffiths, CC Kerr, W Waites, RM Stuart, D Mistry, D Foster, DJ Klein, RM Viner, and C Bonell. Modelling the potential impact of mask use in schools and society on covid-19 control in the uk. *Scientific reports*, 11(1):8747, 2021.

[238] Olga Krivorotko, Mariia Sosnovskaia, Ivan Vashchenko, Cliff Kerr, and Daniel Lesnic. Agent-based modeling of covid-19 outbreaks for new york state and uk: Parameter identification algorithm. *Infectious Disease Modelling*, 7(1):30–44, 2022.

[239] Quang D Pham, Robyn M Stuart, Thuong V Nguyen, Quang C Luong, Quang D Tran, Thai Q Pham, Lan T Phan, Tan Q Dang, Duong N Tran, Hung T Do, et al. Estimating and mitigating the risk of covid-19 epidemic rebound associated with reopening of international borders in vietnam: a modelling study. *The Lancet Global Health*, 9(7):e916–e924, 2021.

[240] Andrea Cattaneo, Andrea Vitali, Mirko Mazzoleni, and Fabio Previdi. An agent-based model to assess large-scale covid-19 vaccination campaigns for the italian territory: The case study of lombardy region. *Computer Methods and Programs in Biomedicine*, 224:107029, 2022.

[241] Kristie EN Clarke, Jefferson M Jones, Yangyang Deng, Elise Nycz, Adam Lee, Ronaldo Iachan, Adi V Gundlapalli, Aron J Hall, and Adam MacNeil. Seroprevalence of infection-induced sars-cov-2 antibodies—united states, september 2021–february 2022. *Morbidity and Mortality Weekly Report*, 71(17):606, 2022.

[242] Jamie A Cohen, Robyn M Stuart, Jasmina Panovska-Griffiths, Edinah Mudimu, Romesh G Abeysuriya, Cliff C Kerr, Michael Famulare, and Daniel J Klein. The changing impact of vaccines in the covid-19 pandemic. *medRxiv*, pages 2022–03, 2022.

[243] Serin Lee, Zelda B Zabinsky, Judith N Wasserheit, Jennifer M Ross, Shi Chen, and Shan Liu. Covid-19 endemic plan: Impact of vaccination and non-pharmaceutical interventions with viral variants and waning immunity using an agent-based simulation. *medRxiv*, pages 2022–06, 2022.

[244] Jun Cai, Xiaowei Deng, Juan Yang, Kaiyuan Sun, Hengcong Liu, Zhiyuan Chen, Cheng Peng, Xinhua Chen, Qianhui Wu, Junyi Zou, et al. Modeling transmission of sars-cov-2 omicron in china. *Nature medicine*, 28(7):1468–1475, 2022.

[245] Bruce Pell, Matthew D Johnston, and Patrick Nelson. A data-validated temporary immunity model of covid-19 spread in michigan. *Mathematical Biosciences and Engineering*, 19(10):10122–10142, 2022.

[246] Anyin Feng, Uri Obolski, Lewi Stone, and Daihai He. Modelling covid-19 vaccine breakthrough infections in highly vaccinated israel—the effects of waning immunity and third vaccination dose. *PLOS Global Public Health*, 2(11):e0001211, 2022.

[247] Marion Pepper. Immunity to sars-cov-2 infection. *Immunological Reviews*, 309(1):5, 2022.

[248] Nusrat J Epsi, Stephanie A Richard, David A Lindholm, Katrin Mende, Anuradha Ganesan, Nikhil Huprikar, Tahaniyat Lalani, Anthony C Fries, Ryan C Maves, Rhonda E Colombo, et al. Understanding'hybrid immunity': comparison and predictors of humoral immune responses to sars-cov-2 infection and covid-19 vaccines. *Clin. infect. dis*, 2022.

[249] Heba N Altarawneh, Hiam Chemaitelly, Houssein H Ayoub, Patrick Tang, Mohammad R Hasan, Hadi M Yassine, Hebah A Al-Khatib, Maria K Smatti, Peter Coyle, Zaina Al-Kanaani, et al. Effects of previous infection and vaccination on symptomatic omicron infections. *New England Journal of Medicine*, 387(1):21–34, 2022.

[250] Doan C Nguyen, Pedro A Lamothe, Matthew C Woodruff, Ankur S Saini, Caterina E Faliti, Ignacio Sanz, and Frances Eun-Hyung Lee. Covid-19 and plasma cells: Is there long-lived protection? *Immunological Reviews*, 309(1):40–63, 2022.

[251] Manojit Bhattacharya, Ashish Ranjan Sharma, Kuldeep Dhama, Govindasamy Agoramoorthy, and Chiranjib Chakraborty. Hybrid immunity against covid-19 in different countries with a special emphasis on the indian scenario during the omicron period. *International Immunopharmacology*, 108:108766, 2022.

[252] Alessandro Sette and Shane Crotty. Immunological memory to sars-cov-2 infection and covid-19 vaccines. *Immunological reviews*, 310(1):27–46, 2022.

[253] Timothy A Bates, Savannah K McBride, Hans C Leier, Gaelen Guzman, Zoe L Lyski, Devin Schoen, Bradie Winders, Joon-Yong Lee, David Xthona Lee, William B

Messer, et al. Vaccination before or after sars-cov-2 infection leads to robust humoral response and antibodies that effectively neutralize variants. *Science immunology*, 7(68):eabn8014, 2022.

[254] Farhina Mozaffer, Philip Cherian, Sandeep Krishna, Brian Wahl, and Gautam I Menon. Effect of hybrid immunity, school reopening, and the omicron variant on the trajectory of the covid-19 epidemic in india: a modelling study. *The Lancet Regional Health-Southeast Asia*, 8:100095, 2023.

[255] Peter Nordström, Marcel Ballin, and Anna Nordström. Risk of sars-cov-2 reinfection and covid-19 hospitalisation in individuals with natural and hybrid immunity: a retrospective, total population cohort study in sweden. *The Lancet Infectious Diseases*, 22(6):781–790, 2022.

[256] Stefan Pilz, Verena Theiler-Schwetz, Christian Trummer, Robert Krause, and John PA Ioannidis. Sars-cov-2 reinfections: Overview of efficacy and duration of natural and hybrid immunity. *Environmental research*, 209:112911, 2022.

[257] Michael P Busch, Susan L Stramer, Mars Stone, Elaine A Yu, Eduard Grebe, Edward Notari, Paula Saa, Robyn Ferg, Irene Molina Manrique, Natalia Weil, et al. Population-weighted seroprevalence from severe acute respiratory syndrome coronavirus 2 (sars-cov-2) infection, vaccination, and hybrid immunity among us blood donations from january to december 2021. *Clinical Infectious Diseases*, 75(Supplement_2):S254–S263, 2022.

[258] Jinal N Bhiman and Penny L Moore. Leveraging south african hiv research to define sars-cov-2 immunity triggered by sequential variants of concern. *Immunological Reviews*, 310(1):61–75, 2022.

[259] Sarah P Otto, Troy Day, Julien Arino, Caroline Colijn, Jonathan Dushoff, Michael Li, Samir Mechai, Gary Van Domselaar, Jianhong Wu, David JD Earn, et al. The origins and potential future of sars-cov-2 variants of concern in the evolving covid-19 pandemic. *Current Biology*, 31(14):R918–R929, 2021.

[260] P Ciunkiewicz, W Brooke, M Rogers, and S Yanushkevich. Agent-based epidemiological modeling of covid-19 in localized environments. *Computers in Biology and Medicine*, 144:105396, 2022.

[261] Thomas Usherwood, Zachary LaJoie, and Vikas Srivastava. A model and predictions for covid-19 considering population behavior and vaccination. *Scientific reports*, 11(1):1–11, 2021.

[262] Yuan Liu and Bin Wu. Coevolution of vaccination behavior and perceived vaccination risk can lead to a stag-hunt-like game. *Physical Review E*, 106(3):034308, 2022.

[263] Rachael Piltch-Loeb, Diana R Silver, Yeerae Kim, Hope Norris, Elizabeth McNeill, and David M Abramson. Determinants of the covid-19 vaccine hesitancy spectrum. *PLoS One*, 17(6):e0267734, 2022.

[264] Justin Xavier Moore, Keon L Gilbert, Katie L Lively, Christian Laurent, Rishab Chawla, Cynthia Li, Ryan Johnson, Robert Petcu, Mehul Mehra, Antron Spooner, et al. Correlates of covid-19 vaccine hesitancy among a community sample of african americans living in the southern united states. *Vaccines*, 9(8):879, 2021.

[265] Ying Wang and Yu Liu. Multilevel determinants of covid-19 vaccination hesitancy in the united states: A rapid systematic review. *Preventive medicine reports*, 25:101673, 2022.

[266] Madhura S Rane, Shivani Kochhar, Emily Poehlein, William You, McKaylee M Robertson, Rebecca Zimba, Drew A Westmoreland, Matthew L Romo, Sarah G Kulkarni, Mindy Chang, et al. Determinants and trends of covid-19 vaccine hesitancy and vaccine uptake in a national cohort of us adults: A longitudinal study. *American journal of epidemiology*, 191(4):570–583, 2022.

[267] Sonali Saluja, Chun Nok Lam, Danielle Wishart, Alec McMorris, Michael R Cousineau, and Cameron M Kaplan. Disparities in covid-19 vaccine hesitancy among los angeles county adults after vaccine authorization. *Preventive Medicine Reports*, 24:101544, 2021.

[268] Megan Halbrook, Adva Gadoth, Rachel Martin-Blais, Ashley N Gray, Saman Kashani, Clayton Kazan, Brian Kane, Nicole H Tobin, Kathie G Ferbas, Grace M Aldrovandi, et al. Longitudinal assessment of coronavirus disease 2019 vaccine acceptance and uptake among frontline medical workers in los angeles, california. *Clinical Infectious Diseases*, 74(7):1166–1173, 2022.

[269] Alexander J Freund and Philippe J Giabbanelli. The necessity and difficulty of navigating uncertainty to develop an individual-level computational model. In *Computational Science–ICCS 2021: 21st International Conference, Krakow, Poland, June 16–18, 2021, Proceedings, Part VI*, pages 407–421. Springer, 2021.

[270] United States Census Bureau. Pinc-01. selected characteristics of people 15 years and over, by total money income, work experience, race, hispanic origin, and sex. https://www.census.gov/data/tables/time-series/demo/income-poverty/cps-pinc/pinc-01.2019.html, 2022. Accessed: 2022-08-12.

[271] Vasileios Petrakis, Periklis Panagopoulos, Dimitrios Papazoglou, and Nikolaos Papanas. Diabetes mellitus and hypertension as major risk factors of mortality from covid-19 pneumonia. *Experimental and Clinical Endocrinology & Diabetes*, 130(03):205–206, 2022.

[272] Bedasa Taye Merga, Galana Mamo Ayana, Temam Beshir Raru, Addisu Alemu, Belay Negash, Miressa Bekana, Abdi Birhanu, and Yadeta Dessie. Association of pre-existing comorbidities with disease severity among covid-19 patients in eastern ethiopia. *Infection and Drug Resistance*, pages 2825–2834, 2022.

[273] Ewan McFarlane, Marijke Linschoten, Folkert W Asselbergs, Peter S Lacy, Dawid Jedrzejewski, Bryan Williams, and CAPACITY-COVID Consortium. The impact of pre-existing hypertension and its treatment on outcomes in patients admitted to hospital with covid-19. *Hypertension Research*, 45(5):834–845, 2022.

[274] United States Census Bureau. Educational attainment in the united states: 2019. https://www.census.gov/data/tables/2019/demo/educational-attainment/cps-detailed-tables.html, 2022. Accessed: 2022-08-12.

[275] United States Census Bureau. Annual estimates of the resident population by sex, age, race alone or in combination,1 and hispanic origin for the united states: April 1, 2010 to july 1, 2019. https://www2.census.gov/programs-surveys/popest/tables/2010-2019/national/asrh/nc-est2019-asr5h.xlsx, 2022. Accessed: 2022-08-12.

[276] Hannah Hartig Ruth Igielnik, Scott Keeter. Behind biden's 2020 victory. https://www.pewresearch.org/politics/2021/06/30/behind-bidens-2020-victory/, Nov 2022. Accessed: 2022-08-12.

[277] United States Census Bureau. Voting and registration in the election of november 2020. https://www.census.gov/data/tables/time-series/demo/voting-and-registration/p20-585.html, 2022. Accessed: 2022-08-16.

[278] Centers for Disease Prevention and Control. National diabetes statistics report 2020: Estimates of diabetes and its burden in the united states. https://www.census.gov/data/tables/2019/demo/educational-attainment/cps-detailed-tables.html, 2022. Accessed: 2022-08-12.

[279] National Center for Health Statistics. Hypertension among adults aged 20 and over, by selected characteristics: United states, selected years 1988–1994 through 2015–2018. https://ftp.cdc.gov/pub/Health_Statistics/NCHS/Publications/Health_US/hus19tables/table022.xlsx, 2022. Accessed: 2022-08-12.

[280] B Stierman, J Afful, MD Carroll, TC Chen, O Davy, S Fink, CD Fryar, Q Gu, CM Hales, JP Hughes, et al. National health and nutrition examination survey 2017–march 2020 prepandemic data. https://www.cdc.gov/nchs/data/nhsr/nhsr158-508.pdf, 2022. Accessed: 2022-08-16.

[281] Jennifer L Kriss, Mei-Chuan Hung, Anup Srivastav, Carla L Black, Megan C Lindley, James T Lee, Ram Koppaka, Yuping Tsai, Peng-Jun Lu, David Yankey, et al. Covid-19 vaccination coverage, by race and ethnicity—national immunization survey adult

covid module, united states, december 2020–november 2021. *Morbidity and Mortality Weekly Report*, 71(23):757, 2022.

[282] Dhananjai M Rao and Julius D Higiro. Managing pending events in sequential and parallel simulations using three-tier heap and two-tier ladder queue. *ACM Transactions on Modeling and Computer Simulation (TOMACS)*, 29(2):1–28, 2019.

[283] Alberto Giubilini and Julian Savulescu. Vaccination, risks, and freedom: the seat belt analogy. *Public Health Ethics*, 12(3):237, 2019.

[284] David Shaw. The side effects of not being vaccinated: Individual risk and vaccine hesitancy nationalism. *Journal of Bioethical Inquiry*, 19(1):7–10, 2022.

[285] Baltazar Espinoza, Samarth Swarup, Christopher L Barrett, and Madhav Marathe. Heterogeneous adaptive behavioral responses may increase epidemic burden. *Scientific Reports*, 12(1):11276, 2022.

[286] Alcides Castro e Silva, Américo Tristão Bernardes, Eduardo Augusto Gonçalves Barbosa, Igor Aparecido Santana das Chagas, Wesley Dáttilo, Alexandre Barbosa Reis, and Sérvio Pontes Ribeiro. Successive pandemic waves with different virulent strains and the effects of vaccination for sars-cov-2. *Vaccines*, 10(3):343, 2022.

[287] U.S. Department of Health & Human Services. Biden-harris administration secures 66 million doses of moderna's variant-specific covid-19 vaccine booster for potential use in fall and winter 2022. https://www.hhs.gov/about/news/2022/07/29/biden-harris-administration-secures-66-million-doses-modernas-variant-specific-covid-19-vaccine-booster-for-potential-use-in-fall-winter-2022.html, 2022. Accessed: 2022-08-08.

[288] Bruce Y. Lee. Is omicron ba.5 'worst version' of covid-19 coronavirus seen? https://www.forbes.com/sites/brucelee/2022/07/03/is-omicron-ba5-worst-version-of-covid-19-coronavirus-seen/?sh=7c83b4eb7918, 2022. Accessed: 2022-08-09.

[289] Weiwei Zhang, Shiyong Liu, Nathaniel Osgood, Hongli Zhu, Ying Qian, and Peng Jia. Using simulation modelling and systems science to help contain covid-19: A systematic review. *Systems research and behavioral science*, 40(1):207–234, 2023.

[290] Jeffrey D Sachs, Salim S Abdool Karim, Lara Aknin, Joseph Allen, Kirsten Brosbøl, Francesca Colombo, Gabriela Cuevas Barron, María Fernanda Espinosa, Vitor Gaspar, Alejandro Gaviria, et al. The lancet commission on lessons for the future from the covid-19 pandemic. *The Lancet*, 400(10359):1224–1280, 2022.

[291] Mariam Abdulmonem Mansouri, Leandro Garcia, Frank Kee, and Declan Terence Bradley. Systems-oriented modelling methods in preventing and controlling emerging infectious diseases in the context of healthcare policy: A scoping review. *Systems*, 10(5):182, 2022.

[292] Flaminio Squazzoni, J Gareth Polhill, Bruce Edmonds, Petra Ahrweiler, Patrycja Antosz, Geeske Scholz, Emile Chappin, Melania Borit, Harko Verhagen, Francesca Giardini, et al. Computational models that matter during a global pandemic outbreak: A call to action. *Journal of Artificial Societies and Social Simulation*, 23(2), 2020.

[293] Alexey Voinov and Herman H Shugart. 'integronsters', integral and integrated modeling. *Environmental Modelling & Software*, 39:149–158, 2013.

[294] Shane A Schroeder, Christopher Vendome, Philippe J Giabbanelli, and Alan M Montfort. Towards reusable building blocks to develop covid-19 simulation models. In *2022 Winter Simulation Conference (WSC)*, pages 569–580. IEEE, 2022.

[295] Kai Dou, Jin Yang, Lin-Xin Wang, and Jian-Bin Li. Theory of planned behavior explains males' and females' intention to receive covid-19 vaccines differently. *Human Vaccines & Immunotherapeutics*, 18(5):2086393, 2022.

[296] Artyom Jelnov and Pavel Jelnov. Vaccination policy and trust. *Economic Modelling*, 108:105773, 2022.

[297] Vieri Lastrucci, Francesca Collini, Silvia Forni, Sara D'Arienzo, Valeria Di Fabrizio, Primo Buscemi, Chiara Lorini, Fabrizio Gemmi, and Guglielmo Bonaccorsi. The indirect impact of covid-19 pandemic on the utilization of the emergency medical services during the first pandemic wave: A system-wide study of tuscany region, italy. *PLoS One*, 17(7):e0264806, 2022.

[298] Abdulrahman S Bazaid, Heba Barnawi, Husam Qanash, Ghaida Alsaif, Abdu Aldarhami, Hattan Gattan, Bandar Alharbi, Abdulaziz Alrashidi, Waleed Abu Al-Soud, Safia Moussa, et al. Bacterial coinfection and antibiotic resistance profiles among hospitalised covid-19 patients. *Microorganisms*, 10(3):495, 2022.

[299] Quan Wang, Shasha Guo, Xiaolin Wei, Quanfang Dong, Ning Xu, Hui Li, Jie Zhao, and Qiang Sun. Global prevalence, treatment and outcome of tuberculosis and covid-19 coinfection: a systematic review and meta-analysis (from november 2019 to march 2021). *BMJ open*, 12(6):e059396, 2022.

[300] Mayowa M Ojo, Temitope O Benson, Olumuyiwa James Peter, and Emile Franc Doungmo Goufo. Nonlinear optimal control strategies for a mathematical model of covid-19 and influenza co-infection. *Physica A: Statistical Mechanics and its Applications*, 607:128173, 2022.

[301] Google News. Coronavirus (covid-19), 2022. Available via `https://news.google.com/covid19/map`. Accessed Dec. 28, 2022.

[302] Rashed Noor and Syeda Muntaka Maniha. A brief outline of respiratory viral disease outbreaks: 1889–till date on the public health perspectives. *Virusdisease*, 31(4):441–449, 2020.

[303] Bruna Aparecida Souza Machado, Katharine Valéria Saraiva Hodel, Larissa Moraes dos Santos Fonseca, Vinícius Couto Pires, Luis Alberto Brêda Mascarenhas, Leone Peter Correia da Silva Andrade, Marcelo Albano Moret, and Roberto Badaró. The importance of vaccination in the context of the covid-19 pandemic: A brief update regarding the use of vaccines. *Vaccines*, 10(4):591, 2022.

[304] Nicky Phillips et al. The coronavirus is here to stay-here's what that means. *Nature*, 590(7846):382–384, 2021.

[305] Aris Katzourakis. Covid-19: endemic doesn't mean harmless. *Nature*, pages 485–485, 2022.

[306] Qianer Liu, Cheng Leng, Sun Yu, and Ryan McMorrow. China estimates 250mn people have caught covid in 20 days, 2022. Available via `https://www.ft.com/content/1fb6044a-3050-44d8-b715-80c18ca5c9ab`. Accessed Dec. 28, 2022.

[307] Farah Master and David Stanway. China lacked a 'zero covid' exit plan. its people are paying the price, 2022. Available via `https://www.reuters.com/world/china/china-lacked-zero-covid-exit-plan-its-people-are-paying-price-2022-12-23/`. Accessed Dec. 28, 2022.

[308] Thomas Czypionka, Emil N Iftekhar, Barbara Prainsack, Viola Priesemann, Simon Bauer, Andre Calero Valdez, Sarah Cuschieri, Enrico Glaab, Eva Grill, Jenny Krutzinna, et al. The benefits, costs and feasibility of a low incidence covid-19 strategy. *The Lancet Regional Health-Europe*, 13:100294, 2022.

[309] Jaffar A Al-Tawfiq, Dinh-Toi Chu, Van-Thuan Hoang, and Ziad A Memish. From pandemicity to endemicity: The journey of sars-cov-2. *Journal of Epidemiology and Global Health*, pages 1–3, 2022.

[310] Shaimaa Abdelaziz Abdelmoneim, Malik Sallam, Dina Mohamed Hafez, Ehab Elrewany, Hesham Metwalli Mousli, Elsayed Mohamed Hammad, Sally Waheed Elkhadry, Mohammed Fathelrahman Adam, Amr Abdelraouf Ghobashy, Manal Naguib, et al. Covid-19 vaccine booster dose acceptance: Systematic review and meta-analysis. *Tropical Medicine and Infectious Disease*, 7(10):298, 2022.

[311] Israel T Agaku, Caleb Adeoye, and Theodore G Long. Geographic, occupational, and sociodemographic variations in uptake of covid-19 booster doses among fully vaccinated us adults, december 1, 2021, to january 10, 2022. *JAMA Network Open*, 5(8):e2227680–e2227680, 2022.

[312] Ingrid Torjesen. Covid-19 will become endemic but with decreased potency over time, scientists believe. *BMJ: British Medical Journal (Online)*, 372, 2021.

[313] Emily Terry, Sapphire Cartledge, Sarah Damery, and Sheila Greenfield. Factors associated with covid-19 vaccine intentions during the covid-19 pandemic; a systematic

review and meta-analysis of cross-sectional studies. *BMC Public Health*, 22(1):1–16, 2022.

[314] Emil Nafis Iftekhar, Viola Priesemann, Rudi Balling, Simon Bauer, Philippe Beutels, André Calero Valdez, Sarah Cuschieri, Thomas Czypionka, Uga Dumpis, Enrico Glaab, et al. A look into the future of the covid-19 pandemic in europe: an expert consultation. *The Lancet Regional Health-Europe*, 8:100185, 2021.

[315] Guihong Fan, Haitao Song, Stan Yip, Tonghua Zhang, and Daihai He. Impact of low vaccine coverage on the resurgence of covid-19 in central and eastern europe. *One Health*, page 100402, 2022.

[316] Feng Hao. Multilevel determinants on covid-19 booster intention among americans. *Preventive Medicine*, 164:107269, 2022.

[317] Weiwei Zhang, Shiyong Liu, Nathaniel Osgood, Hongli Zhu, Ying Qian, and Peng Jia. Using simulation modelling and systems science to help contain covid-19: A systematic review. *Systems research and behavioral science*, 2022.

[318] Samar Ibrahim. A review of agent-based model simulation for covid 19 spread. In *International Conference on Emerging Technologies and Intelligent Systems*, pages 585–602. Springer, 2023.

[319] Jonatan Almagor and Stefano Picascia. Exploring the effectiveness of a covid-19 contact tracing app using an agent-based model. *Scientific reports*, 10(1):1–11, 2020.

[320] Emilio Sulis and Pietro Terna. An agent-based decision support for a vaccination campaign. *Journal of Medical Systems*, 45(11):1–7, 2021.

[321] Beate Jahn, Gaby Sroczynski, Martin Bicher, Claire Rippinger, Nikolai Mühlberger, Júlia Santamaria, Christoph Urach, Michael Schomaker, Igor Stojkov, Daniela Schmid, et al. Targeted covid-19 vaccination (tav-covid) considering limited vaccination capacities—an agent-based modeling evaluation. *Vaccines*, 9(5):434, 2021.

[322] Parantapa Bhattacharya, Dustin Machi, Jiangzhuo Chen, Stefan Hoops, Bryan Lewis, Henning Mortveit, Srinivasan Venkatramanan, Mandy L Wilson, Achla Marathe, Przemyslaw Porebski, et al. Ai-driven agent-based models to study the role of vaccine acceptance in controlling covid-19 spread in the us. In *2021 IEEE International Conference on Big Data (Big Data)*, pages 1566–1574. IEEE, 2021.

[323] Meksianis Z Ndii, Ema Carnia, and Asep K Supriatna. Mathematical models for the spread of rumors: a review. *Issues and trends in interdisciplinary behavior and social science*, pages 65–73, 2018.

[324] Pawel Sobkowicz and Antoni Sobkowicz. Agent based model of anti-vaccination movements: Simulations and comparison with empirical data. *Vaccines*, 9(8):809, 2021.

[325] Pooria Taghizadeh Naderi, Ali Asgary, Jude Kong, Jianhong Wu, and Fattaneh Taghiyareh. Covid-19 vaccine hesitancy and information diffusion: An agent-based modeling approach. *arXiv preprint arXiv:2109.01182*, 2021.

[326] Muhammad Al Atiqi, Shuang Chang, and Hiroshi Deguchi. Simulating the influence of facebook fan pages on individual attitudes toward vaccination using agent-based modelling. *Systems Research and Behavioral Science*, 2022.

[327] Jack T. Beerman, Gwendal G. Beaumont, and Philippe J. Giabbanelli. A scoping review of three dimensions for long-term covid-19 vaccination models: Hybrid immunity, individual drivers of vaccinal choice, and human errors. *Vaccines*, 10(10), 2022.

[328] Cliff C Kerr, Robyn M Stuart, Dina Mistry, Romesh G Abeysuriya, Jamie A Cohen, Lauren George, Michał Jastrzebski, Michael Famulare, Edward Wenger, and Daniel J Klein. Python vs. the pandemic: a case study in high-stakes software development. In *Proc. of the 21st Python in Science Conf. (SCIPY)*, 2022.

[329] Stewart Robinson. *Experimentation: Obtaining Accurate Results*, pages 166–199. Bloomsbury Publishing, second edition, 2014.

[330] Martyn Pickersgill, Lucinda Manda-Taylor, and Natalia Niño-Machado. Pandemic preparedness means policy makers need to work with social scientists. *The Lancet*, 2022.

[331] G Montanari Vergallo, A Del Rio, F Negro, and S Zaami. Covid-19 vaccine mandates: What are the current european public perspectives. *Eur. Rev. Med. Pharmacol. Sci*, 26:643–652, 2022.

[332] Yam B Limbu, Rajesh K Gautam, and Wencang Zhou. Predicting vaccination intention against covid-19 using theory of planned behavior: A systematic review and meta-analysis. *Vaccines*, 10(12):2026, 2022.

[333] NYC Health. Community health survey public use data. Available via `https://www.nyc.gov/site/doh/data/data-sets/community-health-survey-public-use-data.page`. Accessed March 26, 2023.

[334] US Census Bureau. American community survey data, Sep 2022. Available via `https://www.census.gov/programs-surveys/acs/data.html`. Accessed March 26, 2023.

[335] Haixin Ding and Li Xie. Simulating rumor spreading and rebuttal strategy with rebuttal forgetting: An agent-based modeling approach. *Physica A: Statistical Mechanics and its Applications*, page 128488, 2023.

[336] Ullrich KH Ecker and Stephan Lewandowsky. Computational constraints in cognitive theories of forgetting. *Frontiers in Psychology*, 3:400, 2012.

[337] Ali Khodabandelu and JeeWoong Park. Agent-based modeling and simulation in construction. *Automation in Construction*, 131:103882, 2021.

[338] Lei Zhang and David Levinson. Agent-based approach to travel demand modeling: Exploratory analysis. *Transportation Research Record*, 1898(1):28–36, 2004.

[339] Till Köster, Philippe J Giabbanelli, and Adelinde Uhrmacher. Performance and soundness of simulation: a case study based on a cellular automaton for in-body spread of hiv. In *2020 Winter Simulation Conference (WSC)*, pages 2281–2292. IEEE, 2020.

[340] Jinghui Zhong, Wentong Cai, Linbo Luo, and Haiyan Yin. Learning behavior patterns from video: A data-driven framework for agent-based crowd modeling. In *Proceedings of the 2015 international conference on autonomous agents and multiagent systems*, pages 801–809, 2015.

[341] Suiping Zhou, Dan Chen, Wentong Cai, Linbo Luo, Malcolm Yoke Hean Low, Feng Tian, Victor Su-Han Tay, Darren Wee Sze Ong, and Benjamin D Hamilton. Crowd modeling and simulation technologies. *ACM Transactions on Modeling and Computer Simulation (TOMACS)*, 20(4):1–35, 2010.

[342] Kareem A. Ghumrawi, Kim Ha, Jack T. Beerman, John-David Rudie, and Philippe J. Giabbanelli. Software technology to develop large-scale self-adaptive systems:accelerating agent-based models and fuzzy cognitive maps via cuda. In *Hawaii International Conference on System Sciences*, 2022.

[343] Melvin Lippe, Mike Bithell, Nick Gotts, Davide Natalini, Peter Barbrook-Johnson, Carlo Giupponi, Mareen Hallier, Gert Jan Hofstede, Christophe Le Page, Robin B Matthews, et al. Using agent-based modelling to simulate social-ecological systems across scales. *GeoInformatica*, 23:269–298, 2019.

[344] Hazel R Parry and Andrew J Evans. A comparative analysis of parallel processing and super-individual methods for improving the computational performance of a large individual-based model. *Ecological Modelling*, 214(2-4):141–152, 2008.

[345] Hazel R Parry and Mike Bithell. Large scale agent-based modelling: A review and guidelines for model scaling. *Agent-based models of geographical systems*, pages 271–308, 2012.

[346] Dimitris E Koulouriotis, Ioannis E Diakoulakis, and Dimitris M Emiris. Learning fuzzy cognitive maps using evolution strategies: a novel schema for modeling and simulating high-level behavior. In *Proceedings of the 2001 congress on evolutionary computation (IEEE Cat. No. 01TH8546)*, volume 1, pages 364–371. IEEE, 2001.

[347] Simon F Pratt, Philippe J Giabbanelli, Piper Jackson, and Vijay K Mago. Rebel with many causes: A computational model of insurgency. In *2012 IEEE International Conference on Intelligence and Security Informatics*, pages 90–95. IEEE, 2012.

[348] Christopher WH Davis, Antonie J Jetter, and Philippe J Giabbanelli. Fuzzy cognitive maps in agent based models: a practicial implementation example. In *2020 Spring Simulation Conference (SpringSim)*, pages 1–11. IEEE, 2020.

[349] Mark Newman. *Networks: An Introduction.* Oxford University Press, Inc., USA, 2010.

[350] Philippe J Giabbanelli. The small-world property in networks growing by active edges. *Advances in Complex Systems*, 14(06):853–869, 2011.

[351] Philippe J Giabbanelli, Dorian Mazauric, and Jean-Claude Bermond. On the average path length of deterministic and stochastics recursive networks. In *Complex Networks: Second International Workshop, CompleNet 2010, Rio de Janeiro, Brazil, October 13-15, 2010, Revised Selected Papers*, pages 1–12. Springer, 2011.

[352] Duncan J Watts and Steven H Strogatz. Collective dynamics of 'small-world'networks. *nature*, 393(6684):440–442, 1998.

[353] Albert-László Barabási and Eric Bonabeau. Scale-free networks. *Scientific american*, 288(5):60–69, 2003.

[354] Albert-László Barabási and Réka Albert. Emergence of scaling in random networks. *science*, 286(5439):509–512, 1999.

[355] Edgar N Gilbert. Random graphs. *The Annals of Mathematical Statistics*, 30(4):1141–1144, 1959.

[356] Bao Wang and Philippe J Giabbanelli. Identifying informative features to evaluate student knowledge as causal maps. *International Journal of Artificial Intelligence in Education*, pages 1–31, 2023.

[357] Steven Gray, Eleanor J Sterling, Payam Aminpour, et al. Assessing (social-ecological) systems thinking by evaluating cognitive maps. *Sustainability*, 11(20):5753, 2019.

[358] Dominique Engome Tchupo and Gretchen A Macht. Comparing fuzzy cognitive maps: Methods and their applications in team communication. *International Journal of Industrial Ergonomics*, 92:103344, 2022.

[359] Peter Wills and François G Meyer. Metrics for graph comparison: a practitioner's guide. *Plos one*, 15(2):e0228728, 2020.

[360] Ron Milo, Shalev Itzkovitz, Nadav Kashtan, Reuven Levitt, Shai Shen-Orr, Inbal Ayzenshtat, Michal Sheffer, and Uri Alon. Superfamilies of evolved and designed networks. *Science*, 303(5663):1538–1542, 2004.

[361] Diane Felmlee, Cassie McMillan, and Roger Whitaker. Dyads, triads, and tetrads: a multivariate simulation approach to uncovering network motifs in social graphs. *Applied network science*, 6(1):1–26, 2021.

[362] Shalev Itzkovitz, Ron Milo, Nadav Kashtan, Guy Ziv, and Uri Alon. Subgraphs in random networks. *Physical review E*, 68(2):026127, 2003.

[363] Krzysztof Juszczyszyn. Motif analysis. In Reda Alhajj and Jon Rokne, editors, *Encyclopedia of Social Network Analysis and Mining*, pages 1392–1399. Springer New York, New York, NY, 2018.

[364] Dominique Engome Tchupo and Gretchen A. Macht. Comparing fuzzy cognitive maps: Methods and their applications in team communication. *International Journal of Industrial Ergonomics*, 92:103344, 2022.

[365] Philippe Joseph Giabbanelli. Self-improving immunization policies for complex networks. Master's thesis, Simon Fraser University, 2009.

[366] Philippe J Giabbanelli, Ketra L Rice, Michael C Galgoczy, Nisha Nataraj, Margaret M Brown, Christopher R Harper, Minh Duc Nguyen, and Romain Foy. Pathways to suicide or collections of vicious cycles? understanding the complexity of suicide through causal mapping. *Social network analysis and mining*, 12(1):60, 2022.

[367] Amro Alabsi Aljundi, Taha Atahan Akyildiz, and Kamer Kaya. Degree-aware kernels for computing jaccard weights on gpus. In *2022 IEEE International Parallel and Distributed Processing Symposium (IPDPS)*, pages 897–907, 2022.

[368] Mingshu Wang, Zheyan Chen, Lan Mu, and Xuan Zhang. Road network structure and ride-sharing accessibility: A network science perspective. *Computers, Environment and Urban Systems*, 80:101430, 2020.

[369] Alfirna Rizqi Lahitani, Adhistya Erna Permanasari, and Noor Akhmad Setiawan. Cosine similarity to determine similarity measure: Study case in online essay assessment. In *2016 4th International Conference on Cyber and IT Service Management*, pages 1–6, 2016.

[370] Pierre Miasnikof, Alexander Y Shestopaloff, Cristián Bravo, and Yuri Lawryshyn. Statistical network similarity. In *Complex Networks and Their Applications XI: Proceedings of The Eleventh International Conference on Complex Networks and their Applications: COMPLEX NETWORKS 2022—Volume 2*, pages 325–336. Springer, 2023.

[371] Philippe J Giabbanelli, David Bernard, and Sylvain Cussat-Blanc. Fast generation of heterogeneous mental models from longitudinal data by combining genetic algorithms and fuzzy cognitive maps. In *Hawaii International Conference on System Sciences*, pages 1–10, 2022.

[372] Philippe J Giabbanelli, Piper J Jackson, and Diane T Finegood. Modelling the joint effect of social determinants and peers on obesity among canadian adults. In *Theories and simulations of complex social systems*, pages 145–160. Springer, 2014.

[373] CDlib Development Team. CDlib - community discovery algorithms: Chinese whispers. `https://cdlib.readthedocs.io/en/latest/reference/cd_algorithms/algs/cdlib.algorithms.chinesewhispers.html`, n.d. Accessed: March 10, 2023.

[374] CDlib Development Team. CDlib - community discovery algorithms: DER. `https://cdlib.readthedocs.io/en/latest/reference/cd_algorithms/algs/cdlib.algorithms.der.html`, n.d. Accessed: March 10, 2023.

[375] CDlib Development Team. CDlib - community discovery algorithms: Paris. `https://cdlib.readthedocs.io/en/latest/reference/cd_algorithms/algs/cdlib.algorithms.paris.html`, n.d. Accessed: March 10, 2023.

[376] CDlib Development Team. CDlib - community discovery algorithms: Pycombo. `https://cdlib.readthedocs.io/en/latest/reference/cd_algorithms/algs/cdlib.algorithms.pycombo.html`, n.d. Accessed: March 10, 2023.

[377] Philippe J Giabbanelli, Thomas Torsney-Weir, and Diane T Finegood. Building a system dynamics model of individual energy balance related behaviour. *Canadian Journal of Diabetes*, 35(2):201, 2011.

[378] U.S. Census Bureau. U.s. census bureau quickfacts: Boise city city, idaho, July 2021. Available via `https://www.census.gov/quickfacts/boisecitycityidaho`. Accessed March 26, 2023.

[379] U.S. Census Bureau. U.s. census bureau quickfacts: Memphis city, tennessee, July 2021. Available via `https://www.census.gov/quickfacts/memphiscitytennesse`. Accessed March 26, 2023.

[380] Mingbin Feng and Jeremy Staum. Green simulation: Reusing the output of repeated experiments. *ACM Transactions on Modeling and Computer Simulation (TOMACS)*, 27(4):1–28, 2017.

[381] Orpha K Duell and Marlene Schommer-Aikins. Measures of people's beliefs about knowledge and learning. *Educational psychology review*, 13(4):419–449, 2001.

[382] Aarti Singh, Dimple Juneja, and Manisha Malhotra. Autonomous agent based load balancing algorithm in cloud computing. *Procedia Computer Science*, 45:832–841, 2015. International Conference on Advanced Computing Technologies and Applications (ICACTA).

[383] Andrea Schaerf, Yoav Shoham, and Moshe Tennenholtz. Adaptive load balancing: A study in multi-agent learning. *Journal of artificial intelligence research*, 2:475–500, 1994.

[384] Muhammad Ibrahim, Muhammad Azhar Iqbal, Muhammad Aleem, Muhammad Arshad Islam, and Nguyen-Son Vo. Maha: Migration-based adaptive heuristic algorithm for large-scale network simulations. *Cluster Computing*, 23(2):1251–1266, 2020.